STUDY OF THE VARIATION OF AIR-GAP PERMEANCE DUE TO THE DISPLACEMENT OF OPPOSED TEETH WITH SPECIFIC BOUNDARY CONFIGURATIONS.

Submitted to the N.S.W. University of Technology for the award of the Degree of Master in Engineering.

I certify that I have not submitted this work to any other University or Institution for the award of a degree or diploma.

(D. T. Nightingale)
20/11/58

in revised form 12/10/59

Study of the Variation of Air-Gap Permeance Due to the Displacement of Opposed Teeth With Specific Boundary Configurations.

SUMMARY

The thesis contains the results of a study of air-gap permeance when opposed teeth are displaced relative to each other. The study includes the adoption and extension of a substitute angle method invented by Dr. R. Pohl, which is applied to teeth of triangular, trapezoidal and rectangular sections. Various approximations to the circular shape have been examined. Where confirmation was not available from theoretical analysis experimental results were obtained. Though the method is designed for rapid assessment of permeance of any shape with simple equations a selected number of tables have been calculated from the basic empirical equations. A fairly comprehensive bibliography of field problems is included.

CONTENTS.

Appendices.

SECTION 1. REVIEW OF PAST WORK.

1.1 Introduction.

The author was introduced to the study of this particular work by Mr. G. F. Freeman who, in 1925, did an excellent analysis of a phonic motor. [1]

It was originally intended that this study be directed towards the theoretical aspects of a new type of phonic motor, but as usually occurs, many of the problems encountered were not adequately covered by published literature. In addition it was found that there was no collected information on small motors. However a study of the problems common to most small motors (and many large ones) showed that the air gap is the place where most reasoned "guessing" takes place. This, of course, was realised very early in the development of electrical machines and led Mr. F. W. Carter to spend many fruitful years on this subject. Prior to 1900 [2], F. W. Carter presented some remarkable solutions on air gap problems associated with teeth which, having stood the test of time, were republished in the I.E.E. Journal in 1926 [3]. Most present day machine designers use Carter's results in one form or the other and new research results are inevitably compared with his figures.

From the foregoing remarks, it would appear that Carter's results are the only solutions to air gap problems. This is far from true. However it is true to say that Carter's results are expressed in a general form which enable designers to obtain a ready figure for air gap permeance of almost any type of machine. In the case of machines depending on the change of reluctance with position,

Carter's method does not help beyond giving a figure for the mean permeance, but the result can be extended to cater for opposed slots.

The method of solution adopted depends to a large extent on the problem, but for most air gap problems there are three methods of approach :

(a) normal boundary with idealised solution ,
(b) idealised boundary with rigorous solution
or (c) normal boundary with rigorous solution.

Carter's solutions are of the class (b) type, and there have been many others of both class (a) and (b), but only a few of the simpler type of problems have been solved by class (c). In this thesis attention is given to problems solvable by class (a).

To separate the air gap from the rest of the machine is wrong in principle since there are so many other factors which can affect the result. Notable among these is the effect of saturation in the teeth, which in the case of a class (b) solution would invalidate the result by changing the effective shape of the boundary.

Incidentally, the first recorded solution of the problem of an air gap bounded by a continuous equipotential plane and a slotted plane was given by Potier [25] in his study of the electrometer.

1.2 Resumé of Carter's Slot Solution.

The slot considered by Carter was idealised in its boundaries and took the form of an infinitely wide parallel air gap of length "g" and an infinitely deep slot of width "s". The boundaries of this

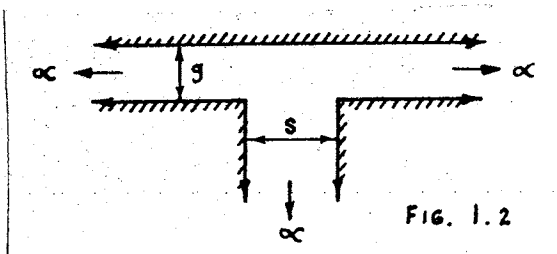

FIG. 1.2

slot are magnetic equipotentials. The results for the permeance of the slot are expressed in the form of $K = f(s/g)$ where K is the fraction of s to be subtracted from the slot width such that the flux distribution over the revised tooth width may be considered uniform. Most textbooks give this function in the form of a graph (a) for open slots and (b) for semi-closed slots. This latter modification was suggested by Professor Miles Walker.

Coe and Taylor [4] have studied independently the effect of a shallow slot on Carter's result for a limited range of values applicable mainly to turbo-alternators and other machines with large air-gaps. They have shown for the cases considered that, provided the depth of slot is made slightly greater than the width of slot, the error involved is small. Apparently Hadamard [4] studied this problem first in 1909 though the author has not read the paper.

In the design of large machines s/g does not usually exceed 12, but for smaller machines, e.g., phonic motors and inductor alternators much larger values are encountered. Values up to and greater than 50 are not uncommon. Physically this figure means that where s would not be much larger than 50-60% of the periphery, g would be extremely small and, consequently, magnitudes of the total reluctance change for opposed slots would be very high. Carter's solution does not take into account the manner in which this reluctance changes and for small values of s/g it is not very important, except in relation to the high frequency fields produced and the consequent tooth losses.

Two examples are given below to show the normal manner of applying Carter's co-efficient to the design of large machines. Additional applications include the shaping and width selection of salient poles to produce a particular distribution of flux in the air gap. This and similar applications are given in most textbooks on machine design.

1.2.1 Application of Carter's Co-efficient to Machine Design[5]. (d.c.)

Consider the two limiting cases of flux distribution :

(a) All flux confined to the teeth. The numeric permeance would then be

$$p = {}^{t}/_{g} \ .$$

(b) Flux uniformly distributed over the tooth and slot. The permeance would then be

$$p = \frac{s + t}{g} \ .$$

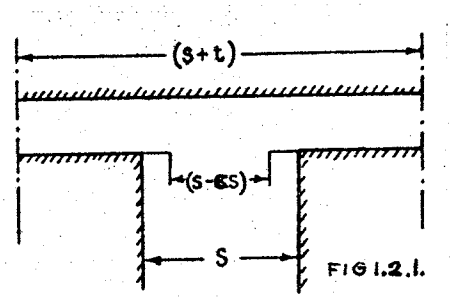

FIG 1.2.1.

Evidently the actual distribution lies somewhere between these extremes and may be represented as :

$$p = \frac{t + cs}{g}$$ where c is Carter's co-efficient.

In the estimation of the increase of reluctance due to slotting in a d.c. machine, it is usual to assume a value for the slotting factor Kg in order to obtain a value for g.

As an example, consider the case of a 750-kW., d.c. generator with dimensions as follows :

$(s+t)$ = 3.19 cm.; s = 1.1 cm.; atg = 5500; no. of ducts n = 6; width of ducts d = 0.9 cm.; core length = 35.3 cm..

For a first estimation of g, assume Kg to be 1.15 which gives g = 0.632 cm. or approximately 0.25" (=0.635 cm.). With this value of g, Kg can now be evaluated and a revised figure for atg obtained.

$$\text{Now, } Kg = \frac{\text{reluctance of slotted gap}}{\text{reluctance of smooth gap}} = Kg' \times Kg''$$

where Kg' is for slots and Kg" for ventilation ducts and are given respectively by :

$$Kg' = \frac{(s+t)}{(s+t) - C's} \quad ; \quad Kg'' = \frac{L}{L - C'' dn}$$

When s/g = 1.1/0635 = 1.73, Carter's co-efficient for slots C' = 0.25 and when d/g = 1.42, C" = 0.24.

Hence,

$$Kg' = \frac{1.1}{3.19 - 0.25 \times 1.1} = 1.095$$

$$Kg'' = \frac{35.3}{35.3 - 0.29 \times 0.9 \times 6} = 1.038$$

Therefore, Kg = 1.135.

This is close to the assumed value and gives the revised value for atg as 5450. An alternative approximation to Kg, which is more accurate is $Kg = Kg_1 + Kg_2 - 1$.

It will be noticed that the total increase in reluctance is approximately 13.5% and though precise analysis is not necessary, must still be considered in the design of a machine of this type.

1.2.2 Application to the Design of an Induction Motor.[6]

In an induction motor both sides of the air gap are slotted and special treatment is necessary in the application of Carter's results. For the purposes of estimation the rotor face is assumed to be an equipotential surface when calculating K_{g1} for the stator. Similarly the stator face is considered to be an equipotential when calculating K_{g2} for the rotor. The resultant value of K_g is then $K_{g1} \times K_{g2}$.

In a particular case of a 5 h.p. motor, $g = 0.45$ mm.; $s = 1$ mm.; $s1 + t1 = 1.612$ cm.; $s_2 + t_2 = 1.523$ cm.; thus -

$$K_{g1} = \frac{1.612}{1.612 - 0.68 \times 0.3} = 1.150$$

$$K_{g2} = \frac{1.523}{1.523 - 0.37 \times 0.3} = 1.025$$

where $C_1 = 0.68$ for s_1/g and $C_2 = 0.37$ for s_2/g, using the curves for semi-closed slots, hence the value of K_g is 1.175.

Corrections for the ducts are as in 1.2.1 except where the stator and rotor slots coincide, in which case the equipotential is assumed to be the centre of the air gap, i.e., the value of C is found for $2s/g$.

1.3 The Lemmas of Forbes.[7]

The lemmas mentioned below formed some of the earliest of simple theorems applicable to varied magnetic circuits. Modifications of these lemmas are used in this paper, so they are mentioned here for both completeness and interest. The theorems assume that the flux follows paths of straight lines and circular arcs.

1.3.1 The First Lemma.

Between two opposed parallel and nearly equal surfaces the permeance in air is equal to the mean of the areas of the two surfaces divided by the distance separating them, viz. -

$$L1 = \frac{1}{2} \frac{AB + CD}{EF} \times a$$

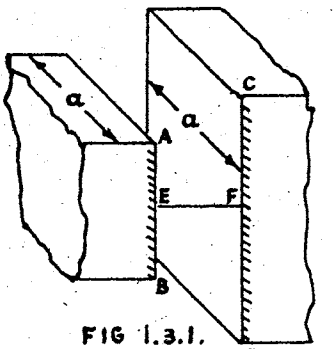

FIG 1.3.1.

In the symbols of this paper EF = g; AB = t_1; CD = t_2 and $\frac{1}{2}(AB + CD) = t$. Hence for a = 1 unit the permeance is t/g.

1.3.2 The Second Lemma.

1.3.2.1 First Case.

If the two surfaces are situated in the same plane and if their distance apart is not greater than a certain value, then :-

$$L2 = \frac{a}{\pi} \log_e \frac{r_2}{r_1},$$

where r_2 = OA and r_1 = OB.

This is easily verified since on considering the cylinder of flux dr, whose path length is πr, the permeance becomes

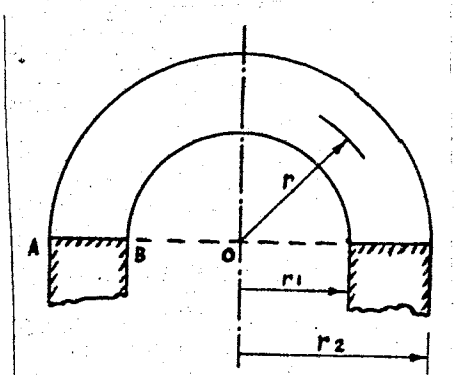

FIG. 1.3.2.1.

$$p = \int_{r_1}^{r_2} \frac{dr}{\pi r} = \frac{1}{\pi} \log_e \frac{r_2}{r_1}$$ for unit length.

1.3.2.2 Second Case.

Where the distance separating the two surfaces is greater than a certain amount

$$L3 = \frac{a}{\pi} \log_e \frac{\pi (AB) + 2(OA)}{2(OA)}$$

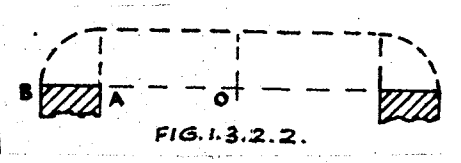

FIG. 1.3.2.2.

The path length, consisting of straight lines and circular arcs, is $2(OA) + \pi r$ and therefore the permeance

$$p = \int_0^{AB} \frac{dr}{2(OA) + \pi r} = \frac{1}{\pi} \log_e \frac{\pi AB + 2(OA)}{2(OA)} \text{ per unit length.}$$

1.3.3. Comments on the Practicability of the Lemmas.

The first lemma assumes that all the flux lines are uniformly spaced, of equal length and normal to the two surfaces. In addition, it is assumed that the side regions do not affect the distribution of flux. Both of these assumptions are entirely incorrect except for cases in which the (mean area)/EF is very large. Cramp and Calderwood have shown [8], using Maxwell's result for a parallel plate capacitor, that instead of Forbe's formula we have for the permeance

$$p = \frac{1}{g}\left(x + \frac{g}{\pi} \right)\left(b + \frac{g}{\pi} \right) .$$

Where $g \ll x$ or b.

In the same paper [8], a revised formula is developed which takes account of the flux linking the vertical faces :

$$p = \frac{1}{g}\left(x + \frac{g}{\pi}(1 - \log_e 2) \right) = \frac{1}{g}\left(x + \frac{0.3069g}{\pi} \right)$$

which is stated to be accurate for $g < x$ or b but inaccurate when $2x/g$ or $2b/g$ approaches unity.

The first case of the second lemma is intended to meet those problems in which the gap between the surfaces is relatively short and the second case for longer gaps. The second case is nothing like the distribution but the first case is nearer the truth when $r_1 \ll r_2$.

1.3.4 Dr. Pohl's Application of Forbe's theorems to Flux Leakage.[9]

Dr. Pohl has applied the lemmas of Forbes to calculate the flux leakage of various pole sections and has expressed the results in a most convenient form for the designer. For square and rectangular poles the second lemma is used without modification. For round poles and pole shoes the flux issuing from the ends is assumed to follow an involute to a circle. The result is arrived at as follows :

The path length -

$$= \frac{s}{2} + \text{arc of involute}$$

$$= \frac{s}{2} + \frac{t}{2} \cdot \frac{\alpha^2}{2}$$

$$= \frac{s}{2} + \frac{2y^2}{t} .$$

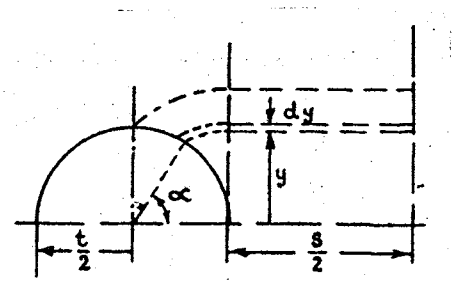

FIG. 1.3.4.

Hence, the permeance

$$p = \int_0^{\frac{\pi t}{4}} \frac{dy}{\frac{s}{2} + \frac{2y^2}{t}} = \sqrt{\frac{2t}{s}} \tan^{-1}\left(\frac{\pi}{4} \cdot \sqrt{\frac{2t}{s}}\right).$$

These results are useful if not very accurate in their original form.

1.3.5. Arnold's Method for Circular Poles.[10]

Arnold replaces the circular pole by a square core of cross-section equal to that of the circular pole. Forbe's first and second lemmas are then applied to the resulting square.

Area of circle = $\frac{\pi . t^2}{4}$.

Area of square = $4b^2$.

Hence, $b = \sqrt{\frac{1}{4} \times \frac{\pi t^2}{4}} = \frac{t}{4}\sqrt{\pi}$.

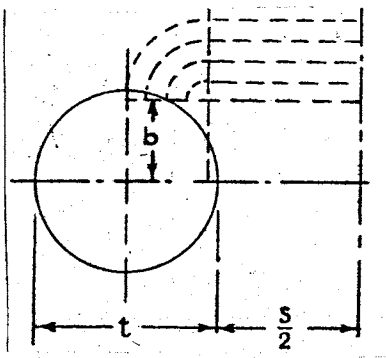

FIG. 1.3.5.

The permeance is then,

$$p = \frac{2b/(s + t)}{1 - 2b/(s + t)} + \frac{2}{\pi} \log_e \left[1 + \frac{\pi\, 2b/(s + t)}{2\,(1 - 2b)/(s + t)} \right].$$

This result has been used in several ways but provides only approximate answers.

1.3.6. The Methods of Douglas.[11]

An early method suggested by Douglas assumed that the flux distribution was sinusoidal. The sine curves were suitably chosen and have since been proved to be very nearly correct.[12]

A later method using conjugate functions in a similar manner to Hague (1.3.7.) gives the permeance for round poles as

$$p = 2\pi . \frac{\cot^2(\pi r/4a) + \coth^2(\pi r/4a)}{\coth^2(\pi r/4a)\log\cot(\pi r/4a) + \cot^2(\pi r/4a)\log\coth(\pi r/4a)} \quad \ldots\ 1.3.6.$$

where $r = t/2$ and $a = (t + s)/2$.

This is an exact result for the leakage permeance of round poles, or move precisely between the pole and its interpolar planes, the planes extending to infinity.

1.3.7. Hague's Method.[12]

Hague has developed a formula for almost circular poles and depending upon the axis of the ellipse, is slightly over or slightly under the exact result. In any case the average of the two methods is exact.

In producing this result Hague drew comparisons between the methods so far mentioned. The following comments by Hague are those appropriate to this work :

(a) Arnold's method gives a better result than Pohl's in this case,

(b) both are particularly in error over the working range of $r/a = t/(t + g)$,

(c) that Douglas' sine method is very nearly correct but involves graphical integration,

and, (d) the average of Hague's two methods is exact.

A comparative table for $r/a = 0.577$ is included below and is taken from Hague's paper.

Table 1.3.7

Method	Perm. for r/a 0.577	Leakage flux Perp. Mlines	approx. flux true
Arnold	6.70	0.391	0.827
Pohl	6.09	0.356	0.753
Pohl 2	8.09	0.472	0.999
Doug.'s sine	7.75	0.482	0.957
Doug.'s exact	8.10	0.473	1.000
Hague	8.80 7.40	0.514 0.432	1.086 0.914

Pohl's method does not show up very well in this comparison, but other factors can be taken into account to give a better agreement. The (Pohl + 2) figure may have some merit in the case of circular pole leakage but it is not much use in proximity cases such as are met with in phonic and similar machines. However Pohl has suggested and investigated a new treatment which is directly applicable to the present study.

1.4 Pohl's treatment of the Pulsating Field Machine.[13]

The part of the paper of interest in connection with this work is the method used to determine the pulsating permeance. The method is called a "substitute angle" method and leads, for a rectangular slot, to equations similar to those developed in Section 2 of this paper for a trapezoidal slot.

The paths of lines of force which are normally curved according to the law of least reluctance are replaced by straight lines and arcs of a circle. This is, of course, a direct application of Forbe's lemmas together with an extension of Pohl's method of leakage calculation. The main difference lies in the estimation of path length.

Consider the case of a rectangular slot and the flux idealised into lines and circular arcs. The permeance/cm. of active length

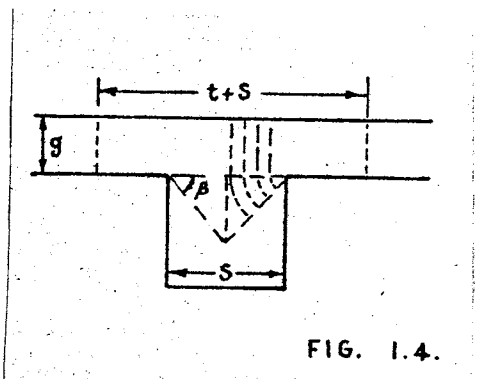

FIG. 1.4.

$$= 2\int_0^{s/2} \frac{dr}{g + \beta r} = \frac{2}{\beta}\log_e \frac{g + \beta s/2}{g}$$

and $$C' = 1 - \frac{(4.6/\beta)\log_{10}(1 + \beta s/2g)}{s/g} \quad \ldots\ldots 1.4.1$$

Here β represents a fictitious length that the lines of flux travel into the slot. The actual value of β to agree with the true result for this type of slot is found by solving 1.4.1 for C' = C where C is Carter's coefficient.

Now expressed in similar terms Carter's coefficient is

$$C = \frac{2}{\pi}\left(\tan^{-1}(s/2g) - \frac{2.3\log_{10}(1 + (s/2g)^2)}{s/g}\right) \quad \ldots\ldots \text{1.4.2}$$

hence to obtain agreement between the two results β was found to vary between 1.0 and 1.1 for 1% accuracy, or more precisely for $s/g \leqslant 10$ $\beta = 1.0$ and s/g between 10 and 100, $\beta = 1.1$. Apparently this accuracy is related to the value of permeance, since the value of C' is not within 1% of C.

It is also stated that when the sides of the slots form with the periphery an angle smaller than 90°, β can be correspondingly reduced for similar accuracy. The comments which occurred to the author when reading this paper were :

(a) the result is compared with Carter's figure in one static case only and it is not known if there is harmonic agreement over the range of movement of the rotor,

(b) the equations produced are very easy to use and enable the permeance to be calculated for any position of the rotor,

(c) no proof or justification is given to support the statement that trapezoidal slots may be treated by the same method,

(d) though the equations enable some deductions to be made on tooth shapes no mention has been made of ideal shapes or even the comparison of various shapes,

and, (e) the result has been determined for the single-sided slot only.

1.5 Flux Pulsations and Tooth Losses.

There is a great deal of literature on this subject which has diverged somewhat from reluctance calculation of air gaps. This is reasonable since on the one hand the interest is centred around the ampere-turns required to establish the air-gap flux, and on the other the effect of the changes in the air-gap permeance on the waveform and tooth losses. The relationship between slotting and the waveform is not so easily separated into the pure effect of air-gap permeance change and other effects, e.g., saturation effects in the iron. In many cases author's have stated that the largest factor is not the change in air-gap permeance.

However since this subject is not exactly compatible with the subject of pulsating field machines where a large change for a given mean is required, only those aspects relative to the air-gap permeance will be commented upon. Additional information may be obtained from the references in Section 7.

1.5.1 Pulsation losses in the teeth are difficult to determine since high frequency pulsations of the flux in any tooth in one member are caused by the relative motion of that tooth with respect to the slot openings in the other member. These pulsations penetrate throughout the whole of the tooth with small magnitude but high frequency. The slot openings are also responsible for a further loss which occurs in a thin layer of the material of the teeth near the air-gap and particularly in the tips of the teeth. This is due to high frequency variations of density, of

wide amplitude, but the depth to which they penetrate is small and the amount of material affected is not great. [14]

In a recent paper by Professor H. Bondi and K. C. Mukherji [15] classical electromagnetic theory is used to investigate the mode of penetration of tooth ripple flux into smooth laminated pole shoes without making any assumption as to the thickness of the laminations employed. It is also shown that only a fraction of the total loss can be called a pole-face loss. However the complete analysis is not of direct interest here since we are not directly concerned with the cause of tooth ripple and not so much its effect. A supporting paper by Professor Greig and Mukherji [14] gives a series of results on practical investigations into this subject.

1.5.2 In making a preliminary study of tooth pulsations Dr. Chapman [16] supposes that if the flux in a stator tooth were $\phi\cos\omega t$ with a smooth rotor and that the effect of rotor slot openings causes a permeance fluctuation of 10% then the flux variation can be expressed by :

$$\phi\cos\omega t \left(1 + \frac{1}{20}\sin 24\omega t\right) = \phi\left(\cos\omega t + \frac{1}{40}(\sin 23\omega t + \sin 25\omega t)\right)$$

Furthermore, if the E.M.F. in a search coil were $2E\sin\omega t$ for a smooth rotor, it would be -

$$2E\left(\sin\omega t + \frac{23}{40}\cos 23\omega t + \frac{25}{40}\cos 25\omega t\right)$$

for a slotted rotor. This would give a ratio of eddy current losses in the tooth as -

$$1 + \left(\frac{23}{40}\right)^2 + \left(\frac{25}{40}\right)^2 = 1.72,$$

i.e., an increase of 72%. It is not clear from Dr. Chapman's writing where this expression was derived from, though it would seem to have

been developed from some practical measurements on machines using search coils and oscillographs.

An analysis of more interest in the present study is Dr. Chapman's determination of tooth pulsations. His basic method is to assume that the effective stator slot width (Cw_o) is projected radially onto the rotor, giving a variable total width of effective rotor slot included within this projection, depending on the relative positions of the two members. In addition, since effective slot widths have been used, it is assumed that the air gap permeance is proportional to the width of the tooth, less the total width of the effective openings.

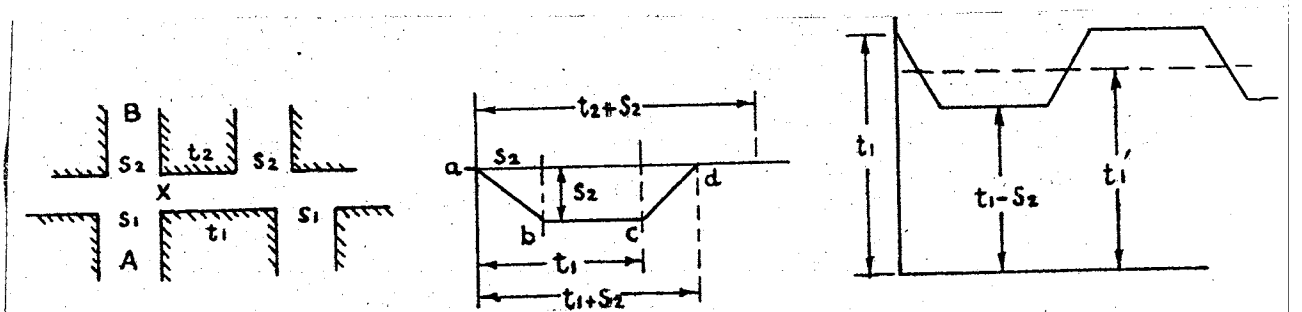

FIG. 1.5.2.1. $t_1 \leqslant t_2$

At the commencement of the passage the rotor slot B is in line with the stator slot A, at x. It increases uniformly until the rotor has moved through a distance s_2, when the slot is entirely under the tooth. This is represented by (ab). Until the leading edge of the tooth comes opposite to the leading edge of the slot there is no further change until the back edge of slot B passes the leading edge of tooth B, when the influence of B on A then ceases. The negative ordinates of (abcd) represent the amount to be added (algebraically) to the width of the tooth, to obtain a length proportional to the permeance in the air-gap

opposite this tooth, for this tooth only. A second slot comes into effect when the rotor has moved a distance of $(s_2 + t_2)$. If $t_1 > t_2$ the effect of a second slot occurs before the first slot is finished.

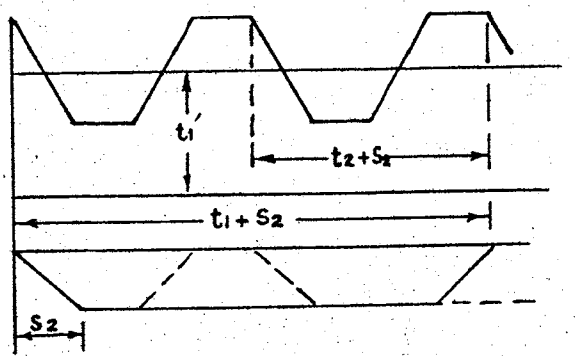

FIG. 1.5.2.2. $t_1 > t_2$

An interesting case is one where $t_1 = t_2 + s_2$ which shows that with the assumptions made there will be no permeance pulsations.

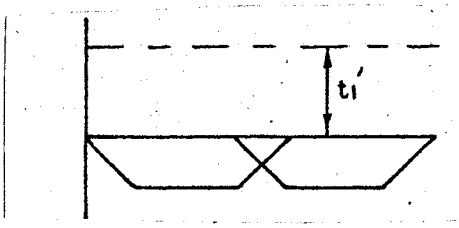

FIG. 1.5.2.3. $t_1 = t_2 + S_2$

This is, of course, fallacious, though since the method is very easy to use and apply results will be compared with other methods in a later section of this work. In all cases, t_1 is the average effective tooth width and is approximately equal to the stator tooth pitch divided by Carter's coefficient C.

1.6 Walker's Method.[17]

In his analysis, Dr. Walker assumes that the iron of the stator and rotor teeth are infinitely permeable, so that the exciting MMF across the air-gap is uniform. Due to the presence of slots, however, the

reluctance of the air-gap is variable being a maximum at the centre of a rotor slot and a minimum at the centre of a rotor tooth. Using Carter's result for rectangular slots[3] he obtains an expression for the flux density in the air-gap as

$$B = B_{max} \frac{K + 1}{\sqrt{\left\{\left[K + \left(\frac{\beta+\gamma}{2}\right)\right]\left[K + \left(\frac{2}{\beta+\gamma}\right)\right]\right\}}} \quad \ldots\ldots 1.6.1.$$

and,

$$\frac{x}{s} = \frac{g}{\pi s}\left[\text{Cosh}^{-1}\left(\frac{2K+\beta}{\gamma}\right) - \text{Cosh}^{-1}\left(\frac{2K^{-1}+\beta}{\gamma}\right)\right] + \frac{1}{\pi}\sin^{-1}\left[\delta\left(\frac{K-1}{K+1}\right)\right] \quad \ldots\ldots 1.6.2.$$

Where s = width of rotor slot, t = width of rotor tooth, g = length of air-gap over rotor tooth,

$$\beta = (s/g)^2 + 2, \qquad \gamma = \pm\frac{s}{g}\sqrt{(s/g)^2 + 4}$$

$$\delta = \pm\frac{s/g}{\sqrt{(s/g)^2 + 4}} \qquad \text{and}$$

K = a parameter corresponding to values of x, where x is a space co-ordinate measured along a rotor slot pitch from the axis of a slot such that $\left[0 \leqslant x \leqslant (s + t)/2\right]$.

For a given value of s/g, a space distribution curve of flux density across a rotor slot pitch can be calculated. Such a curve calculated for the elementary Carter space is reproduced in Fig. 1.6.1.

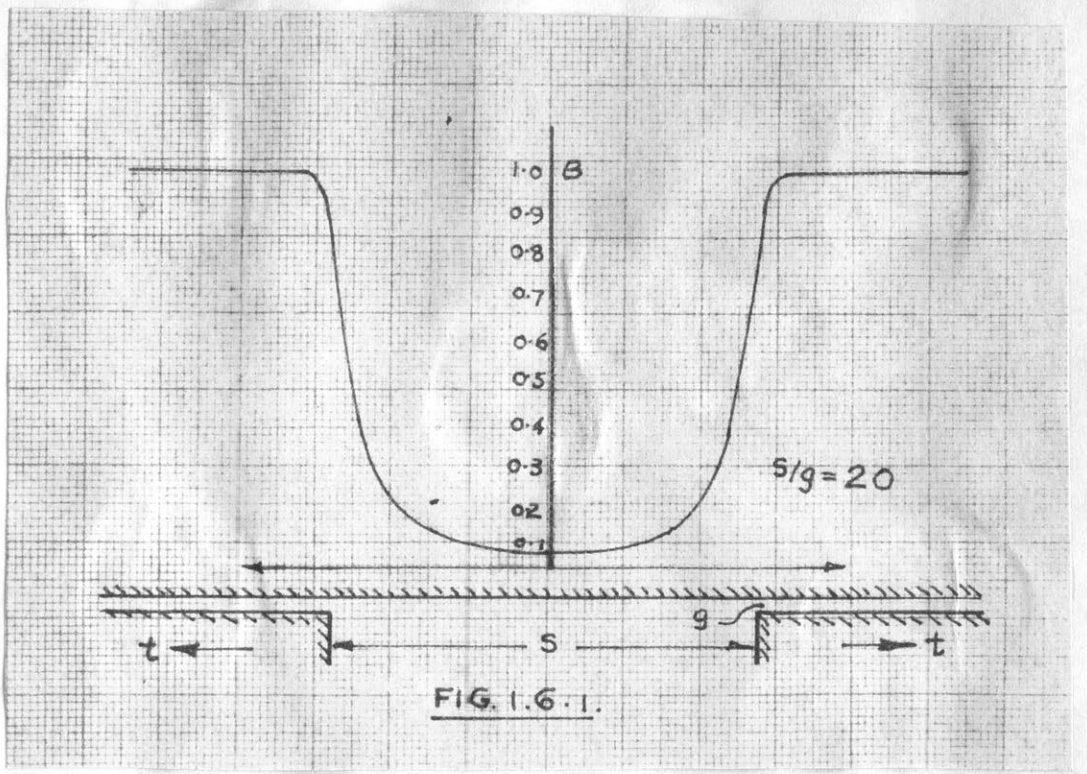

FIG. 1.6.1.

To obtain the variation of alternating flux in time and thence the emf wave shape, it is necessary to take the B ordinates spaced 180° from Fig. 1.6.1 at various points along a rotor slot pitch and plot the values against time or electrical angle as shown in Fig. 1.6.2. This result is difficult to calculate in this form and gives no more information than the Carter result. In applying the method to opposed teeth the same limitations exist as in Carter's method. However for single-sided slots it is possible to obtain a value for the flux distribution over the armature surface and thence the induced e.m.f.

The curve shown in Fig. 1.6.1. represents the conditions which exist in the teeth-out-of-line position of a system slotted on both sides with $t \gg s$.

When the machine is built with the stator slots embedded so that the rotor views a smooth stator, it is necessary to shape the rotor pole faces to produce a sinusoidal flux wave. Hancock[18] and Walker[17]

have produced results for this shaping as follows :

$$B = B_m + B_q \text{ Cos } N_{rs}\theta \quad \ldots\ldots\ldots 1.6.3.$$

where B_q is a constant. The result is achieved by the use of conjugate functions and leads to the shape of the rotor surface given by

$$ny + \lambda' \sinh nynx = ny_o + \lambda' \sinh ny_o \quad \ldots\ldots 1.6.4.$$

where $\lambda' = B_q/B_m$; $n = 2N_{rs}/D$;

y, y_o as given in Fig. 1.6.3.

It is stated in the paper that if for any reasons shapes other than that given in Fig. 1.6.3 are used, the fundamental curve may be obtained by flux plotting.

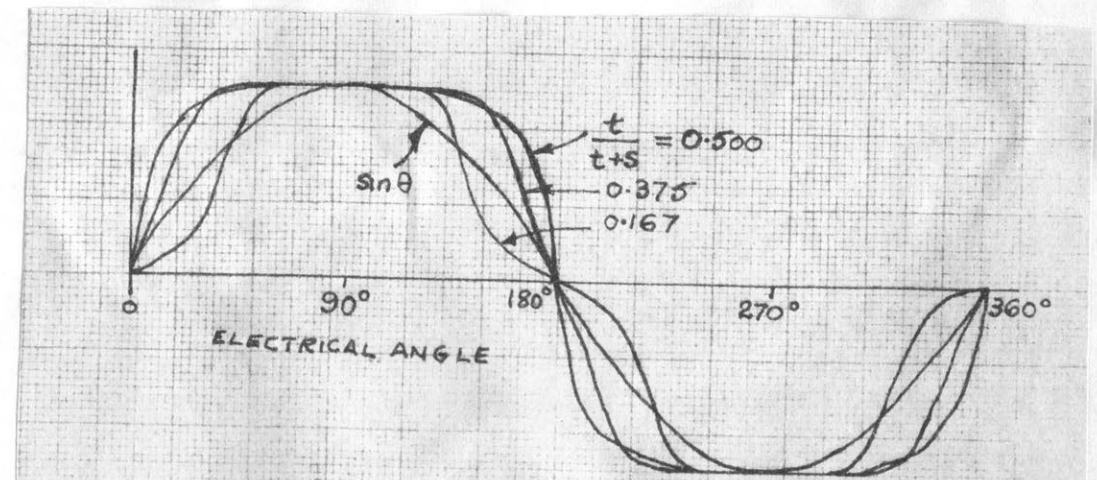

FIG. 1.6.2.

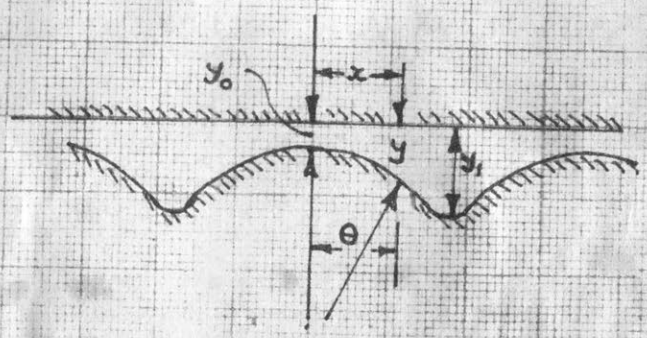

FIG. 1.6.3.

1.7. General Observations.

In the foregoing dissertation selected from a wide range of published literature, it is evident that only a few attempts have been made to analyse slotted systems in a manner of interest to this paper. Dr. Chapman assumes a linear change of permeance with position which produces a trapezoidal permeance wave. As the width of the slots, have been adjusted to agree with Carter's result the accuracy is reasonable throughout a range of $\underline{x}$. However the method of considering both stator and rotor as independent entities is not strictly correct, but it is not important in this instance since extreme accuracy is not intended. The author considers this simple method to be one of the most valuable methods for all types of slotting of rectangular section where an approximate result is required.

Dr. Walker's method is a closer approximation to the truth in the cases where $t \gg s$ but to arrive at a result for a given machine requires a considerable amount of effort and cross plotting. It would appear desirable to have previous results worked out by this method for it to be of practical value, though it is doubtful if the greater accuracy obtainable over the previous method is worth the additional effort.

Both of the former methods are only applicable to rectangular slots since they are based on Carter's result. Hancock's method is only applicable to one specific configuration of rotor tooth designed to produce a sinusoidal wave for a given problem. Evidently, the method of flux plotting is the only other way that the flux distribution for other shapes can be determined.

The method suggested by Dr. Pohl adds considerably to the simple empirical methods of analysing air-gap permeance. As presented by Dr. Pohl, it is based on the same assumption as Dr. Chapman's method, i.e., adjusted to agree with Carter's result in one case only, the point of minimum reluctance and when $t \gg s$. The flux lines having been idealised into straight lines and circular arcs it is necessary to restrict the path length to obtain an accurate result. Dr. Pohl quotes only two values of $\beta(\alpha)$ for the substitute angle applicable to rectangular slots. It is necessary to investigate the accuracy of these statements in relation to the out-of-line position and throughout the motion of the rotor. Since the parameter β is empirical the value to give accurate correspondence of permeance under all conditions will not be constant. However this is no drawback to the method provided for a given configuration and range of movement of the rotor a particular value of β can be used to provide reasonable accuracy.

In the following pages Dr. Pohl's method has been used to develop equations for triangular and trapezoidal teeth, with various other methods, used to determine suitable values for the independent parameter β. Circular teeth have been considered in some detail for a number of reasons:

(a) The rotor shape developed by Hancock and Walker, for the single-sided case is nearly circular and pointed to the fact that a circular shape may be best for sinusoidal (or nearly) flux distribution.

(b) An exact result for circular poles is available in several forms which enables a direct comparison to be made of the circular shape and other shapes equivalent to a circle.

Though this exact result is available it is possible to show that the substitute angle method provides an easy accurate means of obtaining the flux leakage between circular poles.

(c) No literature was found referring to the permeance of circular teeth, though considerable attention has been given to the problem of flux leakage.

No literature of any kind has been located on the question of triangular or trapezoidal teeth except the mention by Dr. Pohl that the method could be applied by suitable adjustment of β.

It is to be hoped that the following pages add in some measure to the knowledge of air-gap permeance which has occupied the minds of so many distinguished men during the last eight or more decades.

SECTION 2.

Triangular and Trapezoidal Teeth - Method A.

2.1 Assumptions.

2.1.1. For this investigation the teeth are assumed to be of infinite permeability, i.e, saturation neglected. In the case of triangular teeth this would not be valid since for some relative positions of stator and rotor there would be considerable bunching at the tips, which would be equivalent to the trapezoidal tooth with small t. However a truly sharp triangular tooth would not be obtained in practice but would be slightly rounded.

2.1.2. All cases considered in this section will neglect the effect of end leakage, but for a reasonable ratio of core length to slot pitch the effect is fairly constant and contributes little to the oscillating permeance. Where short cores are concerned, as in the case of phonic and similar type motors, the end effect is of importance. This effect will be treated briefly in Section 4.

2.1.3. The flux lines will be assumed to follow simple geometric shapes for the sake of simplicity of solution. The equations will be developed such that there is a uniform flux throughout the air-gap.

2.2 Triangular Section Slots.

The basic geometric constants used in this investigation are as follows :

g = length of air-gap.

α_p= angle of elevation of slot side to the plane of the gap;

α_E the exact substitute angle; α the approximate substitute angle.

s = total gap opening at the plane of the gap. For circular teeth s is taken to mean the width at the base of the tooth (see Section 3).

x = relative displacement of (say) the lower member with respect to the upper. Hence for $x = s/2$, $\theta = \pi$ for triangular teeth and for $x = (s + t)/2$ $\theta = \pi$ for trapezoidal teeth.

t = width of tooth at plane of gap.

P_x = the geometric permeance per unit length at x.

Where other constants are used they are explained as they occur in the text.

2.2.1. Teeth in Line.

The flux path consists of a straight portion crossing the air-gap plus two circular arcs. Hence the magnetic path length = $g + 2\alpha r$ with an area of dr per unit length of core.

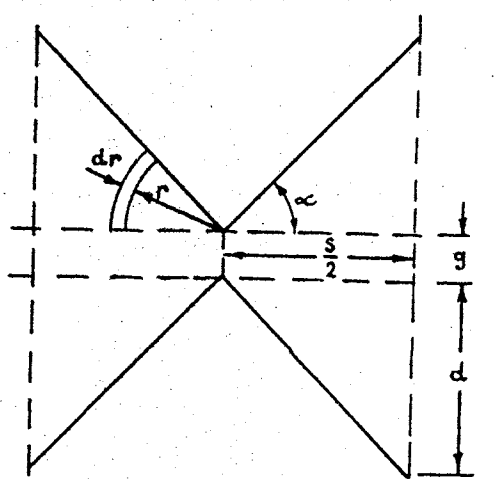

FIG. 2.2.1.

$$\therefore \quad dp = \frac{dr}{g + 2\alpha r}$$

$$\text{and} \quad p = 2\int \frac{dr}{g + 2\alpha r}$$

$$= \frac{1}{\alpha} \log_e(g + 2\alpha r) .$$

Where 2 is for both identical halves; thus with limits $s/2$ and 0 and $x = o$,

$$p_o = \frac{1}{\alpha} \log_e\left(1 + \frac{\alpha s}{g}\right) \qquad \text{--------- 2.2.1.}$$

As $g \rightarrow o$ $p_o \rightarrow \infty$, hence the expression may not be used for the rectangles formed by $g = o$, but $p_o \rightarrow s/g$ as $\alpha \rightarrow o$.

2.2.2. Teeth Out of Line.

For this condition the path length

$$\ell = g + \frac{s}{2}\alpha$$

and, hence

$$p_{s/2} = 2\int_0^{s/2} \frac{dr}{g + \alpha\, s/2}$$

$$= \frac{s/g}{1 + \alpha\, s/2g} \qquad \text{-------- 2.2.2.}$$

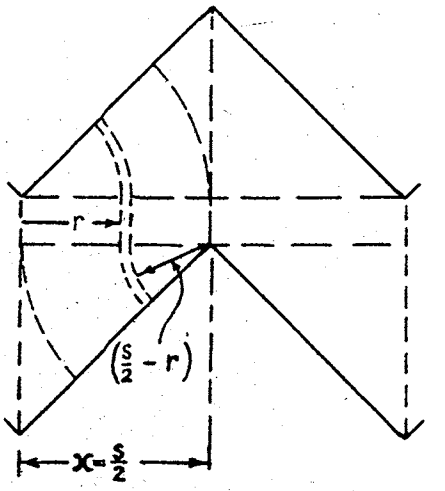

FIG. 2.2.2.

2.2.3. General Position x.

For this case three kinds of flux path occur, each of which have three sections as before. As the plot is symmetrical beyond $s/2$ i.e., $p(x < s/2)$ is mirrored for $x > s/2$, only one equation is required.

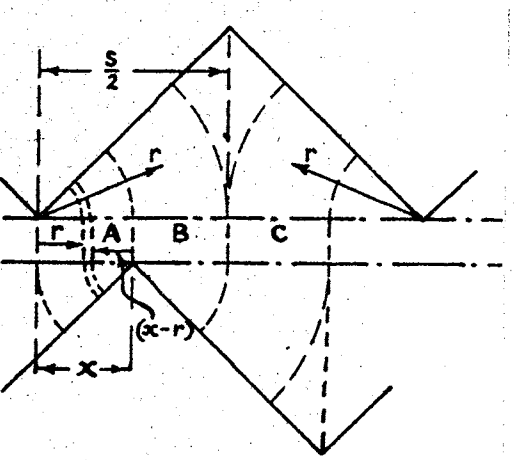

FIG. 2.2.3.

2.2.3.1. Area A.

The path length being $(g + \alpha x)$ gives

$$p_{ax} = \int_0^x \frac{dr}{g + \alpha x} = \frac{x}{g + \alpha x} \qquad \text{------- 2.2.3.1.}$$

2.2.3.2. Area B.

The path length = $(g + 2\alpha r - \alpha x)$ resulting in

$$p_{bx} = 2\int_x^{s/2} \frac{dr}{g + 2\alpha r - \alpha x}$$

$$= \frac{1}{\alpha} \log_e \frac{(1 + \alpha(s-x)/g)}{(1 + \alpha x/g)} \qquad \text{-------- 2.2.3.2.}$$

for both areas.

2.2.3.3. Area C.

The path length = $g + \alpha(s-x)$.

$$\therefore \text{pox} = \int_{s/2}^{s/2 + x} \frac{dr}{g + \alpha(s-x)} = \frac{x}{g + \alpha(s-x)} \qquad \text{---- 2.2.3.3.}$$

2.2.3.4. Combined General Case.

Combining the three areas, the total permeance for x where $o \leqslant x \leqslant s/2$ we obtain

$$p_x = \frac{x}{g + \alpha x} + \frac{x}{g + \alpha(s-x)} + \frac{1}{\alpha} \log_e \frac{g + \alpha(s-x)}{g + \alpha x} \qquad \text{--- 2.2.3.}$$

To check, put x = o and $s/2$ in 2.2.3. and p reduces to 2.2.1. and 2.2.2. respectively. This equation is seen to be homogeneous in s and g where x is expressed as a fraction of s. This expression may be differentiated to obtain the differential permeance, a function much used.

2.3. Trapezoidal Teeth.

The treatment for trapezoidal teeth is precisely the same as for the triangular shape where

$$t_{2\tau} = t_{1\tau} = t \ ,$$

$$t_{1\rho} = t_{2\rho} = o \ .$$

Where $t_{1\rho}$ and $t_{2\rho}$ are the root widths of the stator and rotor teeth respectively. However where either or both members have $t_{1\rho}$ and/or $t_{2\rho} \neq o$ the equations developed herein will still apply provided $t_{1\rho}$ or $t_{2\rho} \not> S(1-\cos\alpha)$, but it may be necessary to use a different value of α .

2.3.1. Teeth in Line.

The permeance here differs from 2.2.1. only by the addition of t/g hence

$$p_o = \frac{t}{g} + \frac{1}{\alpha} \log_e\left(1 + \frac{\alpha s}{g}\right) \quad \text{---- 2.3.1.}$$

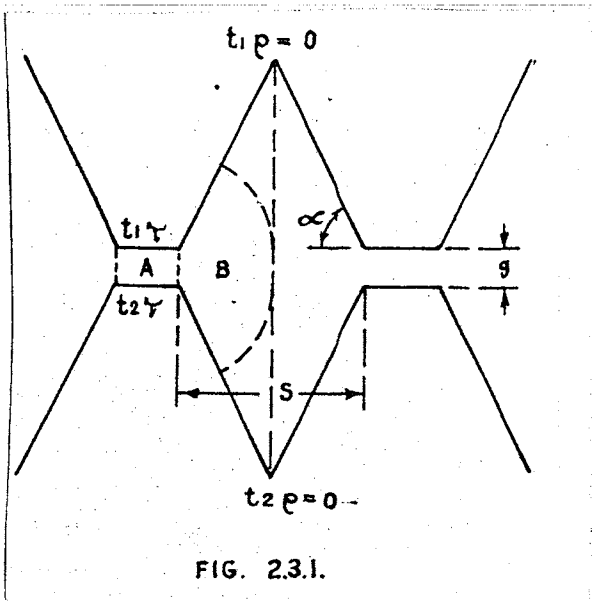

FIG. 2.3.1.

2.3.2. Teeth Out of Line.

For the two areas in this position,

$$p_a = 4 \int_0^{t/2} \frac{dr}{g + \alpha(s/2 - r)}$$

$$= \frac{4}{\alpha} \log_e \frac{1 + \alpha\, {}^{s}/_{2g}}{1 + \alpha\,(s-t)/2g}$$

and,

$$p_b = 2 \int_{t/2}^{s/2} \frac{dr}{g + (\alpha/2)(s-t)} = \frac{(s-t)/g}{1 + \alpha(s-t)/2g}$$

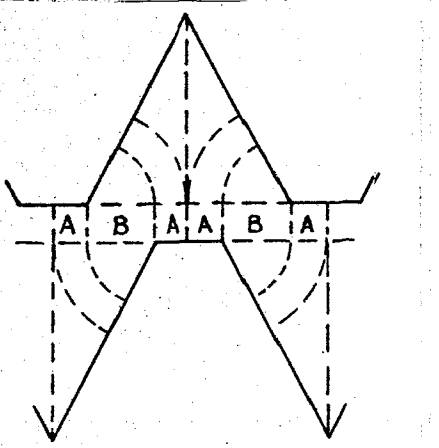

FIG. 2.3.2.

resulting in,

$$p_{s/2} = \frac{2(s-t)}{2g + \alpha(s-t)} + \frac{4}{\alpha} \log_e \frac{2g + \alpha s}{2g + \alpha(s-t)} \quad \text{----- 2.3.2.}$$

In 2.3.2. as $t \rightarrow o$ $p_{s/2} \rightarrow$ 2.2.2. which is correct.

By inspection 2.3.2. will be seen to be valid for $t \leqslant s$.

2.3.3. General Position x ($t \leqslant s/2$).

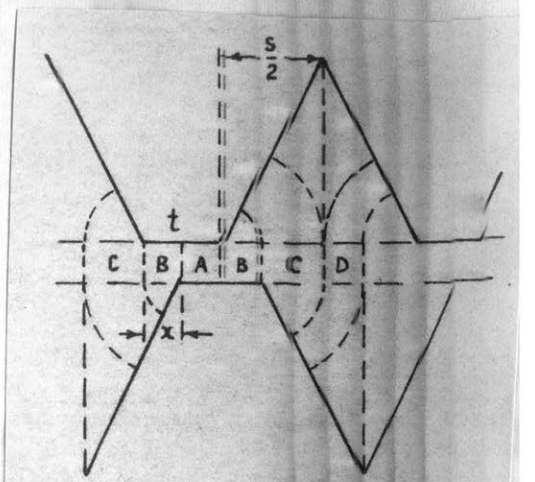

FIG. 2.3.3.

Examination of Figure 2.3.3. reveals that several sets of equations are required, depending on the ratio t/s. Furthermore for a given t/s, several equations are required to specify a complete half cycle. The three categories of the ratio t/s are

(i) $o \leqslant t \leqslant s/2$,

(ii) $s/2 \leqslant t \leqslant s$, and

(iii) $t \geqslant s$.

Category (i) is treated here, (ii) and (iii) in subsequent paragraphs.

2.3.3.1. p_x for $o \leqslant x \leqslant t$.

By the method of 2.2. the four areas produce permeance equations as follows :

$$p_{xa} = \frac{t-x}{g} \quad ;$$

$$p_{xb} = 2\int_{o}^{x} \frac{dr}{g + \alpha r} = \frac{2}{\alpha} \log_e(1 + \alpha x/g) \quad ;$$

$$p_{xc} = 2\int_{x + t/2}^{\frac{s+t}{2}} \frac{dr}{g+2\alpha r- \alpha(x+t)} = \frac{1}{\alpha} \log_e \frac{1 + \alpha(s-x)/g}{1 + \alpha x/g} \quad ;$$

$$p_{xd} = \int_{\frac{s+t}{2}}^{\frac{s+t}{2} + x} \frac{dr}{g + \alpha(s+t/2 - r) + \alpha(r-x+t/2)} \quad ;$$

$$= \frac{x/g}{1 + \alpha(s-x)/g} \cdot$$

Combining these we obtain for $o \leqslant x \leqslant s/2$

$$p_x = \frac{t-x}{g} + \frac{2}{\alpha} \log_e \frac{(1+\alpha x)}{g} + \frac{1}{\alpha} \log_e \frac{g + \alpha(s-x)}{g + \alpha x}$$

$$+ \frac{x}{g + \alpha(s-x)} \cdot \quad \text{----- 2.3.3.1.}$$

When $t = x = o$, p_x (2.3.3.1.) $\longrightarrow$ 2.2.1; when $x = o$ $p_x \longrightarrow$ 2.3.1., which is correct.

2.3.3.2. <u>p_x for $t \leqslant x \leqslant s/2$.</u>

The four areas for this case are shown in Figure 2.3.3.2. and produce permeance as follows :

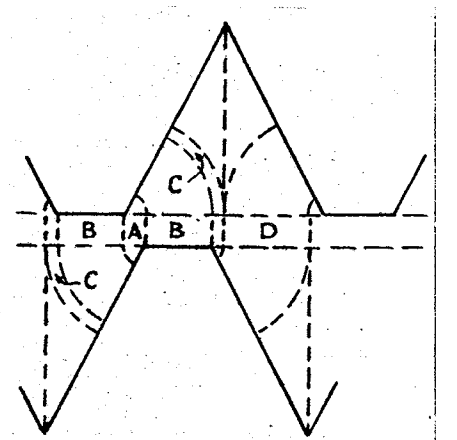

FIG. 2.3.3.2.

$$p_{xa} = \int_t^x \frac{dr}{g + \alpha(x-t)} = \frac{(x-t)}{g + \alpha(x-t)} ;$$

$$p_{xb} = 2\int_x^{x+t} \frac{dr}{g + \alpha(r-t)} = \frac{2}{\alpha} \log_e \frac{g + \alpha x}{g + \alpha(x-t)} ;$$

$$p_{xc} = \int_x^{s/2} \frac{dr}{g + 2r\alpha - \alpha x} = \frac{1}{\alpha} \log_e \frac{g + \alpha(s-x)}{g + \alpha x} ;$$

and,

$$p_{xd} = \int_{s/2}^{\frac{s+t}{2}} \frac{dr}{g + \alpha(s/2 - x)} = \frac{x}{g + \alpha(s-x)} ,$$

which on combining give for $t \leqslant x \leqslant s/2$

$$p_x = \frac{2}{\alpha} \log_e \frac{g + \alpha x}{g + \alpha(x-t)} + \frac{(x-t)}{g + \alpha(x-t)} + \frac{x}{g + \alpha(s-x)}$$

$$+ \frac{1}{\alpha} \log_e \frac{g + \alpha(s-x)}{g + \alpha x} . \quad \text{----- 2.3.3.2.}$$

At the point of discontinuity where $x = t$,

p_t (2.3.3.2.) = p_t (2.3.3.1.).

2.3.3.3. p_x for $s/2 \leqslant x \leqslant s/2 + t$.

The limit in this case need only be taken to $\frac{s+t}{2}$ as the curve is symmetrical up to $(s/2 + t)$. The four areas produce permeance as follows :

$$p_{xa} = 2 \int_x^{t+s/2} \frac{dr}{g + \alpha(r-t)}$$

$$= \frac{2}{\alpha} \log_e \frac{g + \alpha(s/2)}{g + \alpha(x-t)},$$

$$p_{xb} = 2 \int_{t+s/2}^{x+t} \frac{dr}{g + \alpha(s+t-r)}$$

$$= \frac{2}{\alpha} \log_e \frac{g + \alpha s/2}{g + \alpha(s-x)},$$

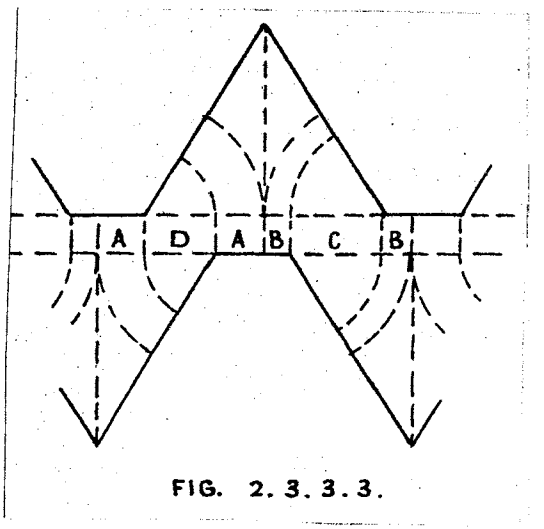

FIG. 2.3.3.3.

$$p_{xc} = \int_x^s \frac{dr}{g + \alpha(s-x)} = \frac{x-t}{g + \alpha(s-x)}$$

and

$$p_{xd} = \int_t^x \frac{dr}{g + \alpha(x-t)} = \frac{x-t}{g + \alpha(x-t)} .$$

The result for $s/2 \leqslant x \leqslant (s/2 + t)$ is therefore

$$p_x = \frac{2}{\alpha} \log_e \frac{g + \alpha s/2}{g + \alpha(x-t)} + \frac{2}{\alpha} \log_e \frac{g + \alpha s/2}{g + \alpha(s-x)} + \frac{s-x}{g + \alpha(s-x)} + \frac{(x-t)}{g + \alpha(x-t)} \quad \text{----- 2.3.3.3.}$$

$p_{s/2}$ (2.3.3.3.) $\longrightarrow$ $p_{s/2}$ (2.3.3.1.).

$p_{\frac{s+t}{2}}$ (2.3.3.3.) $\longrightarrow$ $p_{s/2}$ (2.3.2.) .

2.3.4. General Position x ($s/2 \leqslant t \leqslant s$).

For the in line or maximum permeance 2.3.1. applies. Equation 2.3.2. only applies to cases where $t \leqslant s$ but needs modification beyond this region. Examination of Figure 2.3.4.1. reveals that 2.3.3.1. applies for $o \leqslant x \leqslant s/2$. Beyond this a separate set is required. If $t \geqslant s$ the first discontinuity occurs at $x = s/2$, the second at $x = s$.

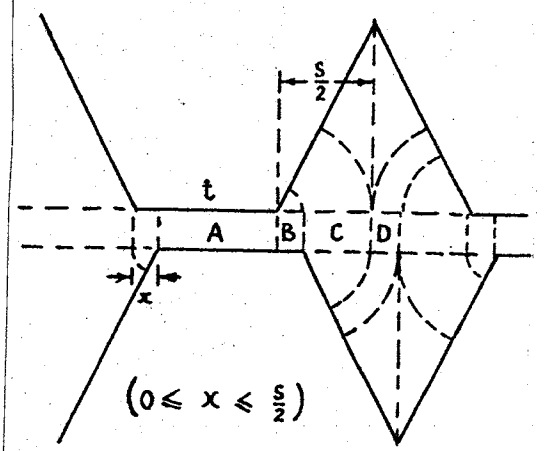

FIG 2.3.4.1.

2.3.4.1. p_x for $s/2 \leqslant x \leqslant t$.

Four areas in this region produce permeances as follows :

$$p_{xa} = \frac{t-x}{g} ,$$

$$p_{xb} = \frac{2}{\alpha} \log_e \left(1 + \frac{\alpha s}{2g}\right) ,$$

$$p_{xc} = \frac{2}{\alpha} \log_e \frac{1 + \alpha s/2g}{1 + \alpha(s-x)/g}$$

and,

$$p_{xd} = \frac{(s-x)}{g + \alpha(s-x)} .$$

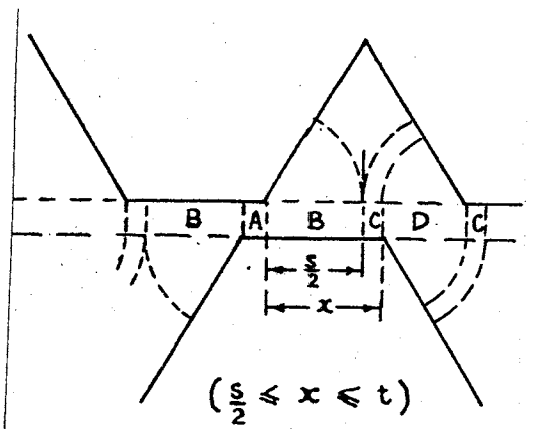

FIG. 2.3.4.2.

The combined permeance for $s/2 \leqslant x \leqslant t$

is thus

$$p_x = \frac{t-g}{g} + \frac{2}{\alpha}\log_e(1 + \alpha s/2g) + \frac{2}{\alpha}\log_e\frac{(1 + \alpha s/2g)}{1 + \alpha(s-x)/g}$$

$$+ \frac{(s-x)}{g + \alpha(s-x)} \qquad \text{------ 2.3.4.1.}$$

which agrees with 2.3.3.1. at $x = s/2$.

2.3.5. General Position x ($t \geqslant s$).

As mentioned previously 2.3.1. applies to the poles in line position, 2.3.3.1. up to $x = s/2$ and 2.3.4.1. up to $x = s$. Beyond this a new equation is required. However this is seen to be constant as follows :

$$p_{xa} = \frac{t-x}{g}, \quad p_{xb} = \frac{2}{\alpha}\log_e(1 + \frac{\alpha s}{2g}),$$

$$p_{xc} = \frac{2}{\alpha}\log_e\left\{\frac{(1 + \alpha s/2g}{1 + \alpha(s-x)/g}\right\}, \quad p_{xd} = \frac{(s-x)/g}{1 + \alpha(s-x)/g},$$

which on combining give :

$$p_x = \frac{4}{\alpha}\log_e(1 + \frac{\alpha s/2g)}{2g} + \frac{(t-s)}{g} \qquad \text{------ 2.3.5.1.}$$

which is constant and equal to 2.3.4.1. when $x = s$.

2.4. Summary.

The equations developed in this section have been given in full for the various configurations for convenience. These are summarised in the following and nominated with their original equation number.

2.4.1. Triangular Teeth.

$$p_x = \frac{x}{g + \alpha x} + \frac{x}{g + \alpha(s-x)} + \frac{1}{\alpha}\log_e\frac{g + \alpha(s-x)}{g + \alpha x} \qquad \text{----- 2.2.3.}$$

for $o \leqslant x \leqslant s/2$.

2.4.2. Trapezoidal Teeth.

(i) $o \leqslant t \leqslant s/2$

$$p_x = \frac{t-x}{g} + \frac{2}{\alpha}\log_e \frac{g + \alpha x}{g} + \frac{1}{\alpha}\log_e \frac{g + \alpha(s-x)}{g + \alpha x} + \frac{x}{g + \alpha(s-x)}$$

for $o \leqslant x \leqslant s/2$. ------ 2.3.3.1.

$$p_x = \frac{2}{\alpha}\log_e \frac{g + \alpha x}{g + \alpha(x-t)} + \frac{(x-t)}{g + \alpha(x-t)} + \frac{x}{g + \alpha(s-x)} + \frac{1}{\alpha}\log_e \frac{g + \alpha(s-x)}{g + \alpha x}$$

------ 2.3.3.2.

for $t \leqslant x \leqslant s/2$.

$$p_x = \frac{2}{\alpha}\log_e \frac{g + \alpha s/2}{g + \alpha(x-t)} + \frac{2}{\alpha}\log_e \frac{g + \alpha s/2}{g + \alpha(s-x)} + \frac{(s-x)}{g + \alpha(s-x)} + \frac{(x-t)}{g + \alpha(x-t)}$$

------ 2.3.3.3.

for $s/2 \leqslant x \leqslant (s/2 + t)$.

(ii) $\underline{s/2 \leqslant t \leqslant s}$.

$$p_x = \frac{t-x}{g} + \frac{2}{\alpha}\log_e \frac{g + \alpha x}{g} + \frac{1}{\alpha}\log_e \frac{g + \alpha(s-x)}{g + \alpha x} + \frac{x}{g + \alpha(s-x)}$$

------ 2.3.3.1.

for $o \leqslant x \leqslant s/2$.

$$p_x = \frac{t-x}{g} + \frac{2}{\alpha}\log_e \left(1 + \frac{\alpha s}{2g}\right) + \frac{2}{\alpha}\log_e \left(\frac{1 + \alpha s/2g}{1 + \alpha(s-x)/g}\right) + \frac{(s-x)}{g + \alpha(s-x)}$$

------ 2.3.4.1.

for $s/2 \leqslant x \leqslant (t+s)/2$.

(iii) $\underline{t \geqslant s}$.

$$p_x = \frac{t-x}{g} + \frac{2}{\alpha}\log_e \frac{g + \alpha x}{g} + \frac{1}{\alpha}\log_e \frac{g + \alpha(s-x)}{g + \alpha x} + \frac{x}{g + \alpha(s-x)}$$

------ 2.3.3.1.

for $o \leqslant x \leqslant s/2$.

$$p_x = \frac{t-x}{g} + \frac{2}{\alpha}\log_e \left(1 + \frac{\alpha s}{2g}\right) + \frac{2}{\alpha}\log_e \left(\frac{1 + \alpha s/2g}{1 + \alpha(s-x)/g}\right) + \frac{(s-x)}{g + \alpha(s-x)}$$

------ 2.3.4.1.

for $s/2 \leqslant x \leqslant s$.

$$p_x = \frac{4}{\alpha}\log_e \left(1 + \frac{\alpha s}{2g}\right) + \frac{t-s}{g}$$ ---------- 2.3.5.1.

for $s \leqslant x \leqslant (s+t)/2$.

2.4.3. Permeance Tables.

A number of tables have been calculated from the foregoing equations for values of s and t given in the following table. The value of g is taken as unity and the numbers represent the table numbers in Appendix 3.

s \ t	0	1	2	3	4	6	8	9	10	12	15	20
5	1	8	13	24	-	-	-	-	-	-	-	-
10	2	9	14	18	19	25	-	-	-	-	-	-
15	-	-	-	-	-	-	-	26	-	-	-	-
20	3	10	15	-	20	21	22	-	23	27	-	-
30	4	11	16	-	-	-	-	-	-	-	28	-
40	-	-	-	-	-	-	-	-	-	-	-	29
50	5	12	17	-	-	-	-	-	-	-	-	-
75	6	-	-	-	-	-	-	-	-	-	-	-
100	7	-	-	-	-	-	-	-	-	-	-	-

The tables are given in two sections with the same number. The first section (A.3.1) gives the value of p_x calculated directly from the foregoing equations appropriate to the ratio t/s. It will be appreciated that though several different equations may be required to specify the permeance between x = o and (s+t)/2 they are continuous surves. Hence, to use the ourves, it is not necessary to refer to the equations, unless extensions beyond the range covered are required.

Consider, for example, an air-gap slotted on both sides, with rectangular slots arranged such that s/g = 20 and t/g = 10. From the chart it is evident that table 23 gives the permeance variation, with position. Assuming that the substitute angle is α = 1.0 for this shape of slot, then we obtain

x	o	0.1(s+t)	0.2(s+t)	0.3(s+t)	0.4(s+t)	0.5(s+t)
p_x	13.0445	11.4433	9.0540	6.5375	4.5555	4.0912

where x is the displacement of one tooth with respect to the other, as a fraction of the slot pitch (s+t). Hence, at x = o, p_x = 13.0445 is the maximum or in-line permeance and x = 0.5(s+t) is the minimum or out-of-line permeance.

To calculate these values independently we see first that t = s/2, so that we may use equations 2.4.2.(i) or 2.4.2.(ii).

In all cases the curves are symmetrical, i.e., the second half of the wave between 0.5(s+t) and (s+t) is the mirror image of the first half between 0 and 0.5(s+t). To obtain an analysis of this permeance wave, any number of methods may be used, a typical standard method being given in Appendix 1. However, for convenience the second half of table 23 (A.3.2) contains an analysis of this permeance wave as follows :

a_o	b_1	b_2	b_3	b_4	b_5
8.0316	4.3307	0.3592	0.1249	0.1770	0.0210

Hence for this particular slotting arrangement the permeance variation with position may be represented by :

$$p_x = 8.0316 + 4.3307 \cos\theta + 0.3592 \cos 2\theta + 0.1249 \cos 3\theta + 0.1770 \cos 4\theta + 0.0210 \cos 5\theta \text{ ---}$$

The differential permeance is then simply :

$$\frac{d\,p_x}{d\,\theta} = 4.3307 \sin\theta + 0.7184 \sin 2\theta + 0.3747 \sin 3\theta + 0.7080 \sin 4\theta + 0.1050 \sin 5\theta \text{ ----}$$

Where θ may be equal to wt.

It must be remembered that in all cases considered in this work the permeance p_x referred to is the geometric permeance and that when using this figure for magnetic calculations it must be multiplied by $\mu_o = 4\pi \times 10^{-7}$ (for rationalised MKS units).

It will be appreciated that it is not possible to specify a unique substitute angle for all configurations as α will vary with all parameters. It will be shown however, that a reasonable approximation to the permeance variation can be obtained by using a constant value of α for a particular configuration.

SECTION 3.

CONSIDERATION OF CIRCULAR AND OTHER TEETH.

3.1. General.

In the following paragraphs methods are given for :

(a) External Circular Teeth,

(b) Internal " "

(c) Elliptic Teeth.

The preferred methods used will be based on and related to the equations in Section 2. Other methods for comparative purposes are given where such are feasible.

3.2. External Circular Teeth.

Four methods are given here, the first of which is an extension of Dr. Arnold's equivalent square applied in two ways, (i) with equations developed in Section 2 and (ii) applied to Dr. Chapman's method. The second method, an equivalent trapezoid applied directly to the equations in Section 2. Finally, an extension of Dr. Pohl's involute method is included for academic interest only.

3.2.1. Equivalent Square.

Consider a circle diameter t and a square of side 2b, then from 1.3.5.

$$\text{Area of circle} = \frac{\pi t^2}{4}$$

$$\text{Area of square} = 4b^2$$

which on equating gives $b = \frac{t}{4}\sqrt{\pi} = \frac{t'}{2}$. This value of t' together with a revised value of s' may be applied to the equations in Section 2 or to the method of Dr. Chapman from Section 1.

3.2.1.1. Method 1.

From 3.2.1. the original tooth pitch

$(s + t) = (s' + t')$

where $t' = t' \times \sqrt{\pi\tau}\ /2$. Hence

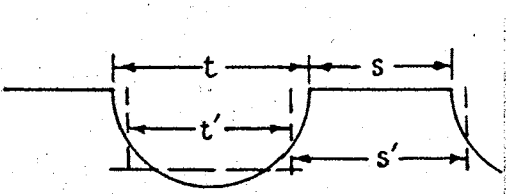

FIG. 3.2.1.1.

from 2.3.1. for the poles-in-line position

$$p_o = \frac{t'}{g} + \frac{1}{\alpha} \log_e \left(1 + \frac{\alpha s'}{g'}\right) \qquad \text{---} \quad 3.2.1.1.$$

Here α is to be adjusted as for rectangular slots in Section 5. The revised value of the air gap g' is $g + (t' - t)$.

For the poles out of line 2.3.2. applies where $t' \leqslant s'$ and 2.3.5.1. for $t' \geqslant s'$. The equations for displacement are chosen from Section 2 according to the ratio t'/s'.

3.2.1.2. Method 2.

For a particular ratio of s'/g' from 3.2.1. a revised value of t', t'' ($t'' > t'$) is obtained from Figure A.3.1. in Appendix 3. The final constants are then t'', s'' ($s'' = (s'+t') - t'' = (s+t) - s''$) and g'.

The in-line permeance is given by t''/g', decreasing linearly to the out-of-line permeance of $\frac{t'' - s''}{g'}$.

3.2.2. Equivalent Trapezoid.

A trapezoid may be fitted more accurately to the circular shape than the square of Arnold. The trapezoid may be fitted to the semi-circle in two ways, (i) by sitting the trapezoid on t and taking equal areas, or (ii) taking the average of the incribing and circumscribing hexagons.

3.2.2.1. Method 1.

With the air-gap length g preserved

Area of semi-circle = $\frac{\pi}{8} t^2$ =

$$\frac{t + t'}{2} \cdot \frac{t}{2} ,$$

from which $t' = t(\frac{\pi}{2} - 1)$. The corresponding value of equivalent physical $\propto$ $(\propto_P)$

$$= \tan^{-1} \frac{t/2}{(t-t'/2)} = 1.66^c.$$

The value of s' is, as before - (s+t-t'), hence the equations in Section 2 may now be applied directly.

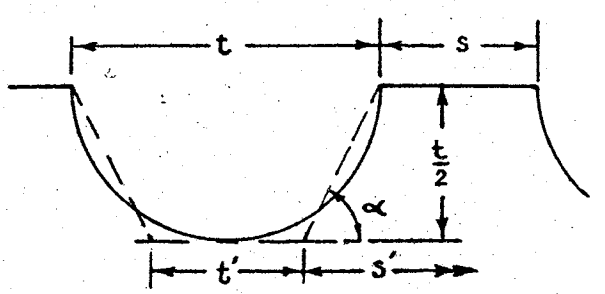

FIG. 3.2.2.1.

3.2.2.2. Method 2.

From Figure 3.2.2.2.

$$OB = \frac{t}{2} \sec \theta ,$$

$$BC = \frac{t}{2} \sec \theta \sin \theta ,$$

$$AF = \frac{t}{2} \sin \theta .$$

Hence,

$$\frac{t'}{2} = \frac{\frac{t}{2} \sin \theta + \frac{t}{2} \sec \theta \sin \theta}{2}$$

$$= \frac{t}{8} (1 + \frac{2}{\sqrt{3}}) = 0.539 (\frac{t}{2}) .$$

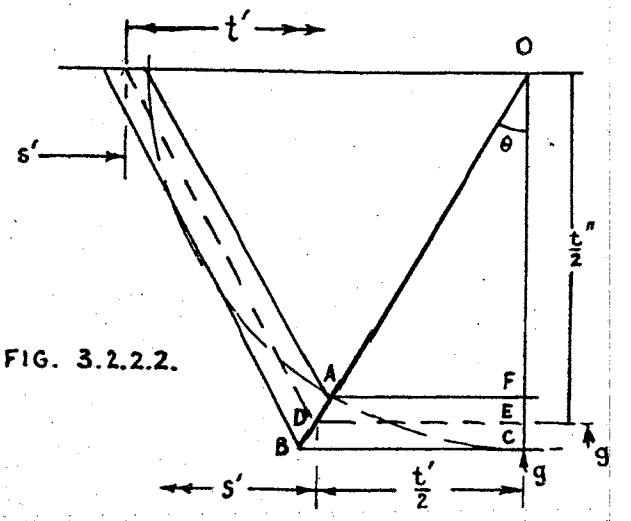

FIG. 3.2.2.2.

In method 1, t' is 0.571t thus method 2 gives a reduction in t' of nearly 6%. From Figure 3.2.2.2., $t'' = \sqrt{3}t'$ which gives $g' = (t + g - t'')$. The equations in Section 2 may now be applied with t', g', $s' = (s + t - t')$ and α_p (equivalent) $= \pi/3$.

3.2.3. Involute Method.

This method is based on that of Dr. Pohl who applied it to the leakage permeance between circular poles. The flux path is assumed to consist of straight portions crossing the gap plus arcs of involutes to the tooth profile. As will be seen, the result is fairly simple for a single calculation of the in-line position, but where a displacement is involved the equation becomes untidy, with awkward terms. As an empirical solution, it is therefore not recommended for general use. Moreover, when t/s is other than a fixed ratio special treatment is necessary.

3.2.3.1. Poles in Line.

As a special case consider a tooth whose dimensions are restricted to $s = t\,(\pi/2 - 1)$ this will enable the gap to be completely occupied with flux. Below this ratio the integral can only be taken to $(s + t)/2$, above this ratio the result is dependent on (a) the depth of slot and (b) the depth of straight tooth flank beneath the circular tooth end.

The path length

$$= g + \frac{2t}{2} \cdot \frac{\alpha 2}{2} = g + \frac{2r^2}{t};$$

$$P_o = 2 \int_0^{\frac{s+t}{2}} \frac{dr}{g + \frac{2r^2}{t}}$$

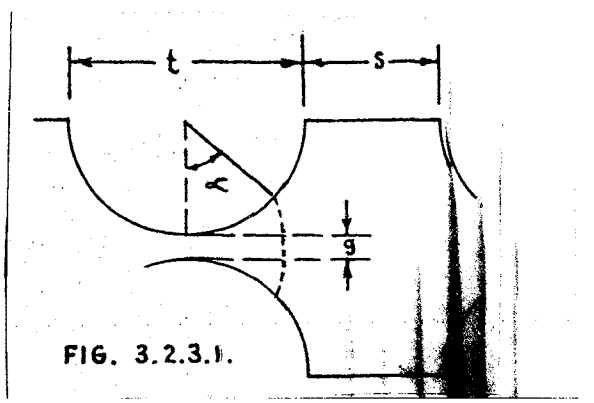

FIG. 3.2.3.1.

when $\frac{2r^2}{t} = x^2$, $x = r/\sqrt{t/2}$, $dx = \frac{dr}{\sqrt{t/2}}$,

and $g = a^2$; then for $(s + t) \leqslant \frac{\pi t}{2}$

$$p_o = 2\sqrt{\frac{t}{2}} \int_0^{\frac{s+t}{2}} \frac{dx}{a^2 + x^2}$$

$$= \frac{2t}{g} \tan^{-1} \frac{(s+t)}{2gt} . \qquad \text{----- 3.2.1. (a)}$$

Also, when $s = t\left(\frac{\pi}{2} - 1\right)$, i.e. $\frac{s+t}{2} = \frac{\pi t}{4}$,

$$p_o = \sqrt{\frac{2t}{g}} \tan^{-1} \frac{\pi}{4}\sqrt{\frac{2t}{g}} . \qquad \text{----- 3.2.1. (b)}$$

3.2.3.2. Poles Out of Line.

The special case of $\frac{s+t}{2} = \frac{\pi t}{4}$ is shown in Figure 3.2.3.2.

The path length

$$= g + \ell_1 + \ell_2$$

$$= g + \frac{t}{2} \cdot \frac{\alpha^2}{2} + \frac{t}{2} \cdot \frac{\beta^2}{2}$$

$$= g + \frac{t}{4}\left(\frac{\pi}{4}\right)^2 + \frac{t}{2}\left(\alpha^2 - \frac{\alpha\pi}{4}\right)$$

$$= \left(g + \left(\frac{\pi}{8}\right)^2 t\right) + \frac{t}{2}\left(\alpha - \frac{\pi}{8}\right)^2 .$$

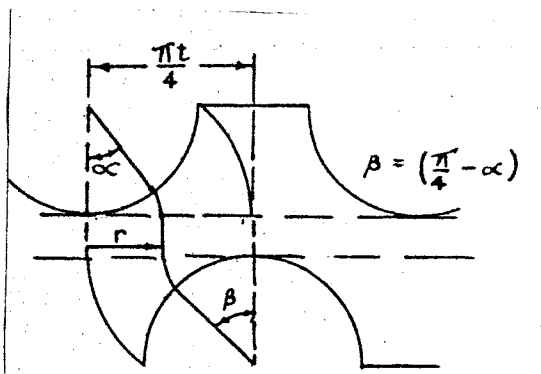

FIG. 3.2.3.2.

Now with $r = \alpha t/2$, then

$$\ell = g + \left(\frac{\pi}{8}\right)^2 2t + \frac{t}{2} \cdot \left(\frac{2}{t} - \frac{\pi}{8}\right)^2 .$$

The permeance is then (for both identical areas) :

$$p_{s/2} = 2 \int_0^{\frac{\pi t}{4}} \frac{dr}{\left(g + \left(\frac{\pi}{8}\right)^2 t\right) + \frac{t}{2}\left(\frac{2r}{t} - \frac{\pi}{8}\right)^2} .$$

Putting $a^2 = \frac{1}{2}\left\{gt + (\frac{\pi t}{8})^2\right\}$ and $\left\{r - \frac{\pi t}{16}\right\} = x^2$,

$$p_{s/2} = t \int \frac{dx}{a^2 + x^2} = \frac{t}{a} \tan^{-1} \frac{x}{a} ,$$

which on reverting to t and inserting the limits

$$p_{s/2} = \theta \left\{\tan^{-1} \frac{3\pi}{16}\theta + \tan^{-1} \frac{\pi}{16}\theta\right\} \qquad \text{—— 3.2.2.}$$

where $\theta = \sqrt{\frac{2t}{g + \left(\frac{\pi}{8}\right)^2 t}}$ and s is implicit.

3.2.3.3. Poles Displaced $0 \leqslant x \leqslant (s+t)/2$ and $s = t\left(\frac{\pi}{2} - 1\right)$.

Three areas are involved here with produce permeances as shown in Fig. 3.2.3.3. Area A is of the previous type which produces :

$$p_{xa} = \sqrt{\frac{2t}{g + \left(\frac{\pi}{8}\right)^2 t}} \tan^{-1} \frac{r - \frac{\pi t}{16}}{\sqrt{\frac{1}{2}(gt + (\frac{\pi t}{8})^2}} \Bigg]_0^x$$

$$= \theta \left[\tan^{-1} (\frac{x}{\partial} - \frac{\pi}{16}\theta) + \tan^{-1} \frac{\pi}{16}\theta\right] ,$$

where $\partial = \sqrt{\frac{1}{2}\left\{gt + (\frac{\pi}{8} t)^2\right\}}$

and, $\theta = \sqrt{\frac{2t}{g + (\frac{\pi}{8})^2 t}}$.

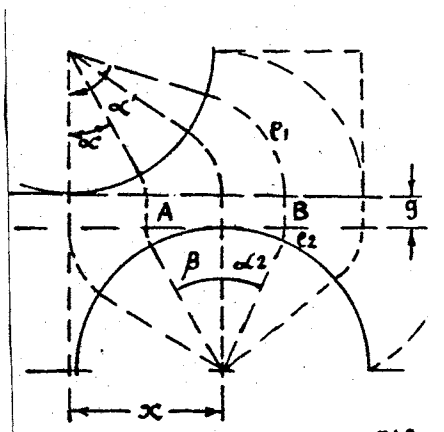

FIG. 3.2.3.3

For area B the path length

$$= g + \ell_1 + \ell_2$$

$$= g + \frac{t}{2} \cdot \frac{\alpha_1^2}{2} + \frac{t}{2} \cdot \frac{\alpha_2^2}{2} .$$

Now $\frac{\alpha_1 t}{2} = r$ and $(r - x) = \frac{t\alpha_2}{2}$,

$\therefore \frac{t\alpha_1}{2} - x = \frac{t\alpha_2}{2}$ and $\alpha_2 = \frac{2}{t}\left(\frac{t\alpha_1}{2} - x\right) = \alpha_1 - \frac{2x}{t}$;

$$\therefore \text{ the path length } = g + \frac{\alpha_1^2 t}{2} + \frac{t}{2}\left(\alpha_1 - \frac{2x}{t}\right)^2$$

$$= g + \frac{t}{2}\left(\frac{2}{t}\right)^2 . r^2 + \frac{t}{2}\left(\frac{2r}{t} - \frac{2x}{t}\right)^2$$

$$= g + \frac{2}{t}\left[x^2 - \frac{(1-2x)^2}{2}\right] + \frac{2}{t}\left(r + \frac{1-2x}{2}\right)^2$$

$$= \frac{2}{t}\left(A^2 + \psi^2\right).$$

Hence

$$p_{xb} = \frac{2t}{A} \tan^{-1} \frac{\psi}{A} \Bigg]_{r=0}^{r=\frac{\pi t}{4}}$$

where $A^2 = \frac{t}{2}\left[\left(x^2 - \left(\frac{1-2x}{2}\right)^2\right)\frac{2}{t} + g\right]$

and $\psi = \left(r + \frac{1-2x}{2}\right)$.

Area C is similar to 3.2.3.2. thus

$$p_{xc} = \theta \tan^{-1}\left(\frac{r}{\partial} - \frac{\pi}{16}\theta\right) \Bigg]_{\left(\frac{\pi t}{4} - x\right)}^{\frac{\pi t}{4}}$$

The resulting permeance is thus

$$p_x = p_{xa} + p_{xb} + p_{xc} \qquad \text{----- 3.2.3.3.}$$

3.3. Internal Circular Teeth.

Where the tooth consists of a straight flank plus a circular end at the root of the tooth the method of Section 2 may be applied directly subject to the limitations of depth and tooth width for rectangular teeth.

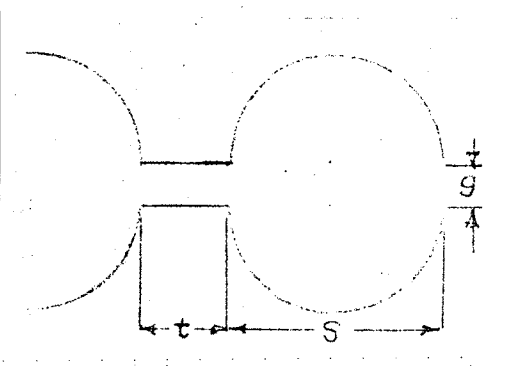

When $s \geqslant d \geqslant o$ any of the methods for external circular teeth may be applied, consider (a) the equivalent square and (b) the equivalent trapezoid. It will be noted that the third method used for external circular teeth would become evolutes when applied to internal teeth. No results will be given for $d < o$ as special treatment is required.

Fig.3.3.

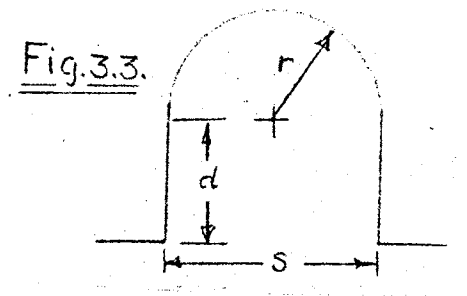

3.3.1. Equivalent Square.

The area of the slot

$= sd + \pi s^2/8$

$= s' (d + s/2)$

i.e., $s' = s \left(\frac{d + \pi s/8}{d + s/2}\right)$

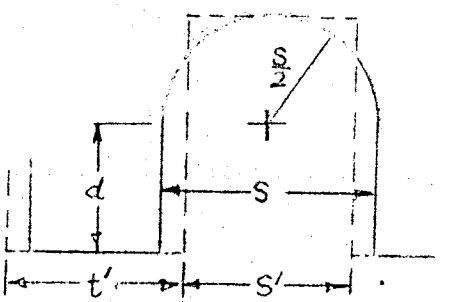

Fig. 3.3.1.

The revised $t' = (s+t) - s'$ and the equations of Section 2 may then be applied directly with the limitation that $(d + s/2) \geqslant s'$, which is not significant. In addition where $d/s > 1$ the value if permeance is almost identical with Carter's result. Alternatively, s'' and t'' may be found from Carter's curves using s'/g, from which the in-line permeance becomes t''/g, decreasing linearly to $(t'' - s'')/g$. Obviously for $s'' \geqslant t''$ this result is not valid. Consideration of the accuracy of this method is given in Section 5.

3.3.2. Equivalent Trapezoid.

The equivalent trapezoid is not much use where any d exists as the shape is too near that of rectangular teeth. Therefore from the reasoning in 3.2.2.2. and Figure 3.3.2. and with d = o,

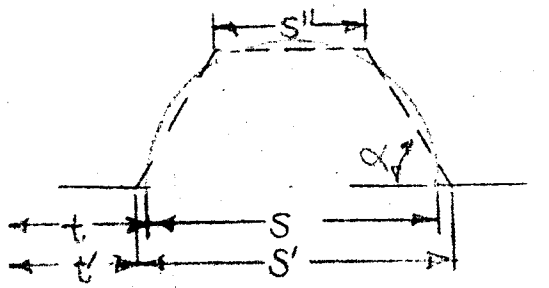

Fig. 3.3.2

$$s'' = \frac{s}{8}\left(1 + \frac{2}{\sqrt{3}}\right) = 0.539S$$

$$s' = \frac{s}{4}\left(1 + \frac{2}{\sqrt{3}}\right) = 1.078S$$

Hence, the equations, in Section 2, may now be applied with t', s', g and $\alpha_p = \pi/3$ as the equivalent physical angle.

3.4. Elliptic and Other Shaped Teeth.

As any shape can be replaced by an equivalent square or equivalent trapezoid, there is no limit to the type of tooth which may be treated by the method of Section 2. However, where more precise results are required resort must be had to the more analytical methods. Where possible, equivalent slots and teeth have been treated analytically so that precise constants could be determined. For the empirical application here internal and external elliptic teeth are treated where the profile is not greater than a semi-axis.

3.4.1. External Elliptic Teeth.

An approximately equivalent trapezoid may be fitted to elliptic teeth as follows :

Draw CD // AB and tangent to the ellipse at P.

Draw EF such that EA is $\frac{3}{4}$ AC.

Hence,

BF = BE = $t'/2$

and $\angle$B AO = α = $\tan^{-1} b/a$.

The value of s' is, as before, equal to (s + t - t'), and by using g the equations may be applied directly from Section 2.

An equivalent rectangle may be fitted by area, e.g.,

area of quadrant

= $\pi/4$ ab

= a' x b'.

Divide a'b' in the ratio

$\frac{a'}{b'} = \frac{a}{b}$

then b' = $\frac{b}{2}\sqrt{\pi}$ and a' = $\frac{a}{2}\sqrt{\pi}$ = $t'/2$.

The revised value of gap length g' is given by (2b + g) - 2b' and the value of s' = (a + s) - a', s', t' and g' may now be applied to the equations in Section 2.

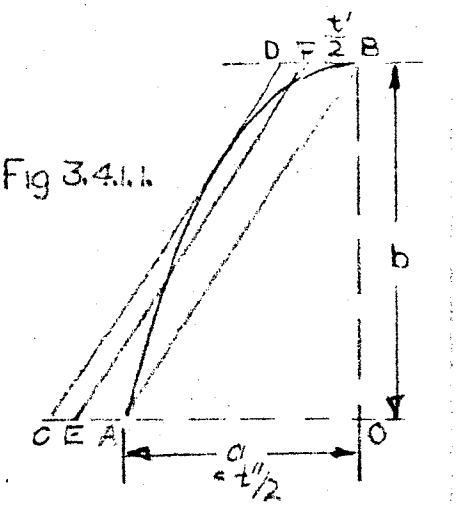

Fig 3.4.1.

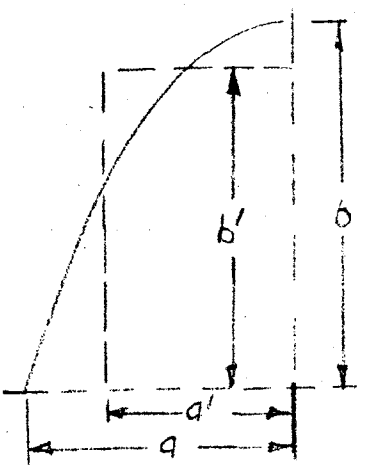

Fig 3.4.2.

3.4.2. Internal Elliptic Teeth.

Where the ratio of the semi-major axis to the minor axis, i.e. $d/s > 1$, it is not worth taking an equivalent shape for the slot, but the equations of Section 2 may be applied

as for rectangular teeth.

If this ratio is < 1, an equivalent square is best fitted as follows -

From 3.4.1. and Figure 3.4.2. $s' = S\sqrt{\pi}$ and $t' = (s + t) - s'$. As g remains the same s', t' and g may now be applied as for rectangular teeth.

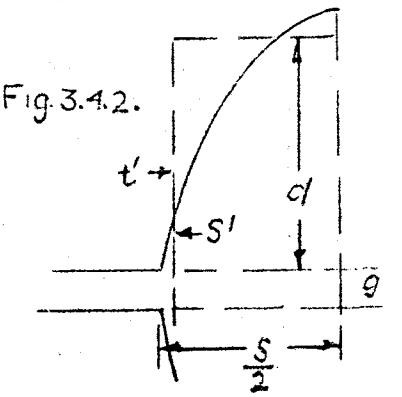

Fig. 3.4.2.

If more correct shaping is required an equivalent trapezoid may be fitted as in 3.4.1..

SECTION 4.

MISCELLANY.

4.1. Method B for Triangular and Trapezoidal Teeth.

In method A the flux is assumed to cross the air-gap at right angles. For the method given here the flux lines are assumed to be circular with a turning point at the centre of the air-gap. Two additional factors P and H will thus appear in the equations and though the results will be simple they are no more simple than method A. Moreover the value of permeance calculated in section 5 will be much lower than method A and requires more correction. The result for triangular teeth and a result for trapezoidal teeth are included here for comparative purposes only. From Fig. 4.1.

$$\tan\alpha = \frac{g}{2p}, \quad P = \frac{g}{2}\cot\alpha,$$

$$\sin\alpha = \frac{g}{2H}, \quad H = \frac{g}{2}\operatorname{cosec}\alpha.$$

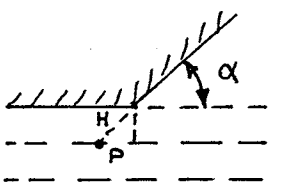

FIG. 4.1.

Hence for triangular teeth in line

$$p_o = \frac{1}{\alpha}\log_e \frac{s/2 + g/2\cot\alpha}{g/2\operatorname{cosec}\alpha}$$

$$= \frac{1}{\alpha}\log_e (\cos\alpha + s/g \sin\alpha) \quad \ldots\ldots 4.1.1.$$

For the out-of-line position

$$p_{s/2} = \frac{1 - 2H}{\alpha K_1} \quad \ldots\ldots 4.1.2.$$

where $K_1 = s/2 + 2P$.

For the general position x, based on three areas

$$p_x = \frac{x + 2(P-H)}{2\alpha(x+2P)} + \frac{1}{\alpha}\log_e \frac{g\cot\alpha + s-x}{g\operatorname{cosec}\alpha + x} + \frac{x}{\alpha(s+2P-x)}.$$

For trapezoidal teeth with $t \leqslant s/2$,

$$p_o = \frac{t}{g} + \frac{1}{\alpha} \log_e (\cos \alpha + s/g \sin \alpha) \quad \ldots\ldots \quad 4.1.4.$$

$$p_{s/2} = \frac{2}{\alpha}\left(1 - \frac{2H}{K2}\right) + \frac{4}{\alpha} \log_e \frac{K3}{K3 - \alpha t} \quad \ldots\ldots \quad 4.1.5.$$

where $K_2 = (s/2 - t + 2P)$ and $K_3 = \alpha(s+2P) + g$.

When $0 \leqslant x \leqslant t$,

$$p_x = \frac{t-x}{g} + \frac{2}{\alpha} \log_e \frac{g + 2\alpha(x+P)}{g + 2\alpha H} + \frac{1}{\alpha} \log_e \frac{s-x+2P}{2H-x} + \frac{x}{\alpha(s-x+2P)} \quad \ldots\ldots \quad 4.1.6.$$

When $t \leqslant x \leqslant s/2$,

$$p_x = \frac{2}{\alpha} \log_e \frac{g + 2\alpha(x+P)}{g + 2\alpha(x+P-t)} + \frac{1}{\alpha} \log_e \frac{s-x+2P}{2H-x} + \frac{x}{\alpha(s-x+2P)} \quad \ldots\ldots \quad 4.1.7.$$

When $s/2 \leqslant x \leqslant \frac{s+t}{2}$,

$$p_x = \frac{(x-t) + 2(P-H)}{\alpha(x-t+2P)} + \frac{2}{\alpha} \log_e \frac{\left(1 + \alpha \frac{s+2P}{g}\right)}{1 + \frac{2\alpha(x-t+P)}{g}} + \frac{2}{\alpha} \log_e \frac{g + \alpha(s+2P)}{g + 2\alpha(s-x+P)} + \frac{s + 2(P-H) - x}{\alpha(s-x+2P)} \quad \ldots\ldots \quad 4.1.8.$$

4.2. Application of Bipolar Transformation to External Circular Teeth.

A suitable transformation for this boundary configuration is the bilinear transformation which converts the Z-plane into a parallel strip in the W-plane.

Consider the function

$$f(Z) = \log_e \frac{(Z-a)}{(Z+a)} \quad \ldots\ldots \quad 4.2.1.1.$$

$$= \log_e (Z-a) - \log_e (Z+a).$$

Let $(Z-a) = r_1 e^{i\theta 1}$ and $(Z+a) = e^{i\theta 2}$ ..... 4.2.1.2.

where r_1 and r_2 are measured from two new origins O_1 and O_2, distant $\pm a$ from the original origin O (Fig. 4.2.1.1.).

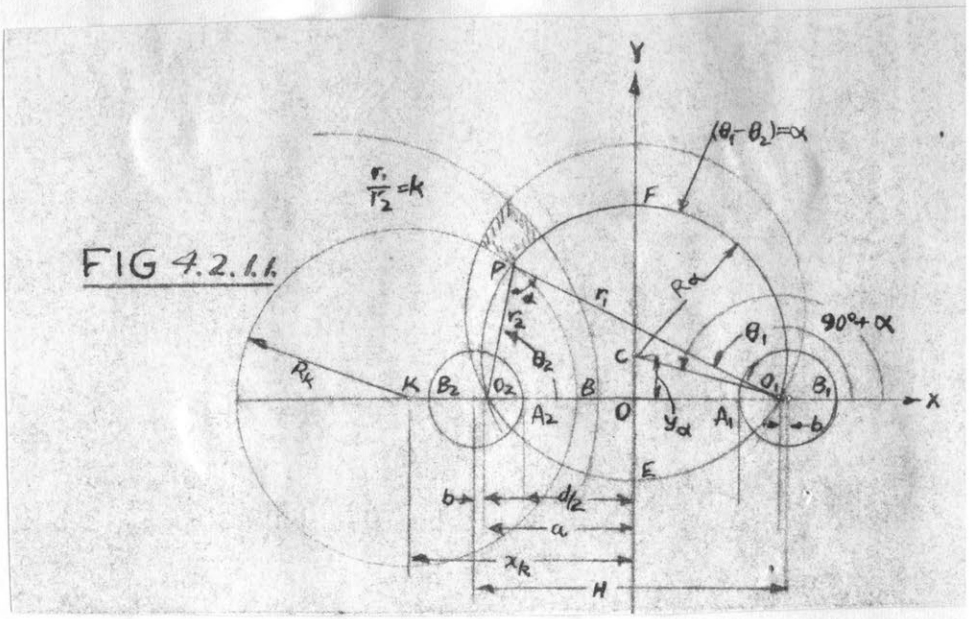

FIG 4.2.1.1.

Hence f(Z) becomes,

$$f(Z) = \log_e \frac{r_1}{r_2} + i\,(\theta_1 - \theta_2) \qquad \ldots\ldots \text{ 4.2.1.3.}$$

The equations for a conformal transformation are therefore

$$\left.\begin{aligned} u &= u(x,y) = \log_e \frac{r_1}{r_2} \\ v &= v(x,y) = (\theta_1 - \theta_2) \end{aligned}\right\} \qquad \ldots\ldots \text{ 4.2.1.4.}$$

which satisfy the Cauchy-Riemann conditions.

When $\frac{r_1}{r_2} = k$, a constant, then u is constant and $r_1^2 = k^2 r_2^2$.

From Fig. 4.2.1.1.

$$r_1^2 = (x - a)^2 + y^2$$

$$r_2^2 = (x + a)^2 + y^2.$$

Hence,

$$(x - a)^2 + y^2 = k^2 (x + a)^2 + y^2)$$

$$x^2 + y^2 + a^2 - \left(\frac{1 + k^2}{1 - k^2}\right) 2ax = 0 \qquad \ldots\ldots \text{ 4.2.1.5.}$$

This is the equation of a circle with centre on the x axis through O_1 O_2. The curves of constant u are thus two families of circles with centres on the x-axis.

Let $f = \frac{1 + k^2}{1 - k^2}$ then,

$$x^2 + y^2 + a^2 - 2a\,fx = o. \qquad \ldots\ldots 4.2.1.6.$$

Therefore at $y = o$,

$x_a = a(f - \sqrt{f^2 - 1}\ )$ and,

$x_b = a(f + \sqrt{f^2 - 1}\ )$

which are the vertical intercepts on the x-axis.

The distance x_k from the origin O to the centre k of the circle becomes,

$$x_k = \tfrac{1}{2}\left[a(f + \sqrt{f^2 - 1}\ ) + a(f - \sqrt{f^2 - 1}\ )\right]$$

$$= af = a\left\{\frac{(1 + k^2)}{(1 - k^2)}\right\}. \qquad \ldots\ldots 4.2.1.7.$$

The corresponding radius R_k of the circle,

$$R_k = \tfrac{1}{2}(x_b - x_a) = a\left\{\frac{2k}{(1 - k^2)}\right\} \qquad \ldots\ldots 4.2.1.8.$$

In addition the locus of points corresponding to constant differences $(\theta_1 - \theta_2) = \alpha$ are portions of circles which pass through the poles O_1 and O_2 and whose centres lie on the y axis, which is the perpendicular bisector of the pole distance O_1O_2. The distance y_α from the origin to the centre C of the circle corresponding to $\theta_1 - \theta_2 = \alpha$ is given by

$$y_\alpha = a \cot\alpha \qquad \ldots\ldots 4.2.1.9.$$

and, $$R_\alpha = a \operatorname{cosec}\alpha\,. \qquad \ldots\ldots 4.2.1.10.$$

The entire xy plane is transformed into a narrow strip 2π units in width and of infinite length, the x-axis being the limiting circles for which $\theta_1 - \theta_2 = \pm\pi$. In the transformed infinite strip, the circle for which α approaches $+\pi$ gives the upper boundary $V = \pi$ and the circle for which α approaches $-\pi$ gives the lower boundary $V = -\pi$.

The y-axis represents the circle whose centre is at infinity on the x-axis. For this circle $r_1/r_2 = 1$ and $u = o$, thus the y-axis is transformed into the V-axis.

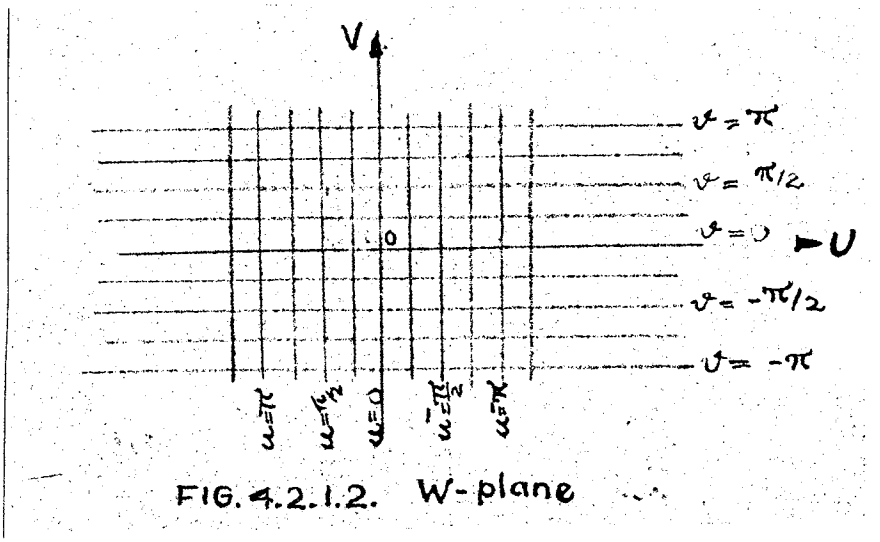

FIG. 4.2.1.2. W-plane

When particular values are inserted in these expressions the transformation in the w-plane becomes long and thin. When g is small and as the y axis is an equipotential, a fairly close approximation to the true result would be obtained by taking a mean length and a uniform distribution.

The same transformation may be used when the teeth are displaced with respect to each other. A revised value of g, g' is used for the V-axis and is given by (Fig. 4.2.1.3.)

$$(t+g') = \sqrt{x^2 + (t+g)^2},$$

where the line of symmetry is now a line perpendicular to the line joining the centres of the two teeth.

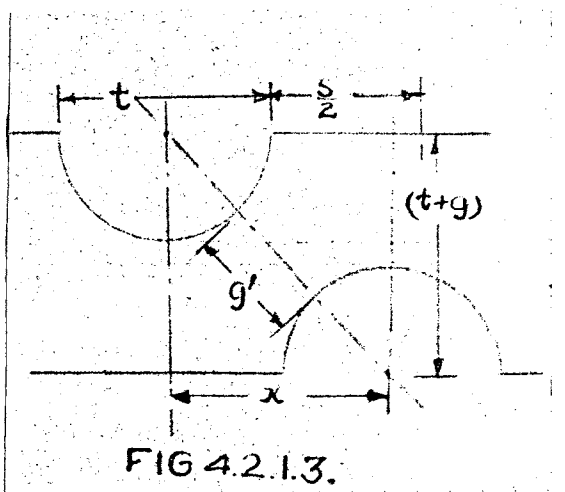

FIG 4.2.1.3.

An alternative method would be a simple logarithmic transformation of one tooth shape but the boundary conditions would be more difficult to meet.

4.3. Extension of Hague's method to Cater for Opposed Circular Teeth.

Consider the flow due to a number of Equal Equidistant Sources along the y-axis. The complex potential w is given by

$$W = C \log_e \sinh \frac{\pi Z}{a} . \qquad \text{----- 4.3.1.}$$

To obtain velocity and stream functions, differentiate 4.3.1. with respect to Z, then,

$$W = \frac{d}{dz}\left(C \log_e \sinh \frac{\pi Z}{a}\right)$$

$$= C' \coth \frac{\pi Z}{a} .$$

This represents a series of doublets located at points (0, 0), (0, $\pm$ a), (0, $\pm$ 2a). Substituting Z = x + iy and separating w into real and imaginery parts ϕ and ψ we obtain,

$$\left.\begin{aligned} \phi &= C' \frac{\sinh 2\pi x/a}{\cosh, 2\pi x/a - \cos 2\pi y/a} \\ \psi &= -C' \frac{\sin 2\pi y/a}{\cosh 2\pi x/a - \cos 2\pi y/a} \end{aligned}\right\} \qquad \text{----- 4.3.2.}$$

Superposing on the flow pattern of 4.3.2. a uniform flow U in the negative x-direction

$$W = Uz; \quad \phi = Ux; \quad \psi = Uy, \text{ then,}$$

$$\left.\begin{aligned} \phi &= Ux + C' \frac{\sinh 2\pi x/a}{\cosh 2\pi x/a - \cos 2\pi y/a} \\ \psi &= Uy - C' \frac{\sin 2\pi y/a}{\cosh 2\pi x/a - \cos 2\pi y/a} \end{aligned}\right\} \qquad \text{----- 4.3.3.}$$

The streamline corresponding to $\psi = 0$ can be shown to be

$$\cosh \frac{2\pi x}{a} - \cos \frac{2\pi y}{a} = \frac{2\pi C'}{aU} - \left(\frac{2\pi}{a}\right)^3 \frac{C'}{U} \frac{y^2}{\lfloor 3} + \cdots ,$$

which is the equation of an oval with origin as centre.

The x-semidiameter is given by $y = o$, viz.,

$$\cosh \frac{2\pi x}{a} - 1 = \frac{2\pi C'}{aU} .$$

The y-semidiameter is obtained by setting $x = o$, thus

$$1 - \cos \frac{2\pi y}{a} = \frac{C'}{Uy} \sin \frac{2\pi y}{a}$$

or,

$$y \tan \frac{\pi y}{a} = \frac{C'}{U} .$$

By putting $C' = \pi b^2 U/a$ and with $b < a$

$$\sinh \frac{\pi x}{a} \rightarrow \frac{\pi x}{a} , \quad \tan \frac{\pi y}{a} \rightarrow \frac{\pi y}{a} ,$$

then both semidiameters can be seen to be approximately equal to b.

4.4. Fourier Method for Triangular Teeth at $g = o$ and $x = o$.

Consider a thin plate bounded by $x = o$, $x = a$, $y = a$ in which the potential field must satisfy :

$$\frac{\partial^2 V}{\partial x^2} + \frac{\partial^2 V}{\partial y^2} = o$$

for which the arbitrary boundary potentials are :

$V = V_1$ @ $y = a$,

$V = V_2$ @ $y = o$,

$V = \eta_1$ @ $x = a$,

and, $V = \eta_2$ @ $x = o$.

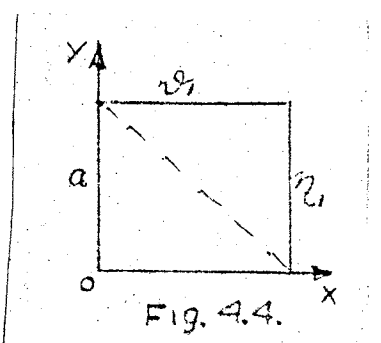

Fig. 4.4.

V and η are functions of y and x respectively. This problem can be solved easily by adding together four solutions corresponding to the four less arbitrary sets of boundary

conditions as follows :

$$\left.\begin{array}{l} V = V_1 \text{ at } y = a \\ V = 0 \text{ at } y = o \\ V = 0 \text{ at } x = a \\ V = 0 \text{ at } x = o \end{array}\right\} \quad (1) \qquad \left.\begin{array}{l} V = 0 \text{ at } y = a \\ V = V_2 \text{ at } y = o \\ V = 0 \text{ at } x = a \\ V = 0 \text{ at } x = o \end{array}\right\} \quad (2)$$

$$\left.\begin{array}{l} V = 0 \text{ at } y = a \\ V = 0 \text{ at } y = o \\ V = \eta_1 \text{ at } y = a \\ V = 0 \text{ at } x = o \end{array}\right\} \quad (3) \qquad \left.\begin{array}{l} V = 0 \text{ at } y = a \\ V = 0 \text{ at } y = o \\ V = 0 \text{ at } x = a \\ V = \eta_2 \text{ at } x = o \end{array}\right\} \quad (4)$$

This is permissable since the differential equation is both homogeneous and linear.

Consider the case represented by (1). Here the primitive product solutions

$$X = C_1 \cos \mu x + C_2 \sin \mu x$$

$$Y = C_3 e^{\mu x} + C_4 e^{-\mu x}$$

apply, and the constants are as follows. Since both X and Y vanish at x = o and a, $C_1 = o$ and $\mu = n\pi/a$, n = 1, 2, 3.

If V is also to vanish at y = o, then $C_3 = - C_4$ and the general solution XY becomes

$$V = \sum_{n=1}^{\infty} C_n \left[e^{\frac{n\pi}{a} y} - e^{\frac{-n\pi}{a} y} \right] \sin \frac{n\pi}{a} x .$$

Finally, for this to satisfy the remaining condition in (1) above, the C_n must be the undetermined amplitudes of the Fourier sine-series expansion

$$V_1 = 2 \sum_{n=1}^{\infty} C_n \sinh n\pi \cdot \sin \frac{n\pi}{a} x,$$

which are given as

$$2C_n \sinh n\pi = \frac{2}{a} \int_o^a V_1 \sin \frac{n\pi}{a} x \, dx .$$

The complete solution corresponding to the particular set of boundary conditions (1) are determined as

$$V_{(1)} = \frac{2}{a} \sum_{n=1}^{\infty} \frac{\sinh (n\pi/a)y}{\sinh n\pi} \sin \frac{n\pi x}{a} \cdot \int_0^a V_1 \sin \frac{n\pi}{a} x \, dx .$$

Alternate solutions for the three remaining sets of boundary conditions 2, 3, and 4 can be written down directly by simply rotating co-ordinates in the above solution. Thus,

$$V_{(2)} = \frac{2}{a} \sum_{n=1}^{\infty} \frac{\sinh n\pi (a-y)/a}{\sinh n\pi} \cdot \sin n\pi x/a \cdot \int_0^a V_2 \sin n\pi x/a \, dx,$$

$$V_{(3)} = \frac{2}{a} \sum_{n=1}^{\infty} \frac{\sinh n\pi y/a}{\sinh n\pi} \cdot \sin n\pi y/a \cdot \int_0^a \eta_1 \sin n\pi y/a \, dy,$$

$$V_{(4)} = \frac{2}{a} \sum_{n=1}^{\infty} \frac{\sinh n\pi (a-x)/a}{\sinh n\pi} \sin n\pi y/a \int_0^a \eta_2 \sin n\pi y/a \, dy.$$

Hence,

$$V = V_{(1)} + V_{(2)} + V_{(3)} + V_{(4)}.$$

For the boundary conditions in this problem $\eta_2 = V_2 = 0$ and $\eta_1 = V_1 = 100$, the problem thus consists of $V_{(1)} + V_{(3)}$ only.

For the integral in $V_{(1)}$ we have :

$$\int_0^a 100 \sin \frac{n\pi}{a} x \, dx = \frac{100a}{n\pi} \left[- \cos \frac{n\pi x}{a} \right]_0^a$$

$= 0$, n even,

$= \frac{200a}{n\pi}$, n odd 1, 3 etc.

Hence we have :

$$V = \frac{400}{\pi} \sum_{1}^{\infty} \frac{\sinh \frac{n\pi y}{a}}{n \sinh n\pi} \sin \frac{n\pi x}{a} + \frac{400}{\pi} \sum_{1}^{\infty} \frac{\sinh \frac{n\pi y}{a}}{n \sinh n\pi} \sin \left(\frac{n\pi y}{a}\right)$$

$$= \frac{800}{\pi} \sum_{1}^{\infty} \frac{\sinh \frac{n\pi y}{a}}{\sinh n\pi} \sin \frac{n\pi}{a}\left(\frac{x+y}{2}\right) \cos \frac{n\pi}{2}\left(\frac{x-y}{2}\right) .$$

This is the complete equation of potential in the square region and since the square is symmetrical also represents the flow. The square being quadrisymmetrical needs potential values in one quadrant only. For a similar method using polar co-ordinates see 4.6.

4.5. Pulsating Permeance for Short Cores.

Beneath the tooth depth some leakage will occur which does not affect the pulsating permeance. If d is large in comparison with s the additional static permeance will not be large and of minor importance. However leakage beyond about 2d could be neglected. A factor of more interest to this work is the effect of leakage over the end of the tooth.

4.5.1. Image Area Method.

Flux is assumed to traverse the space from one tooth to another between the areas which overlap. No movement of flux lines occurs in this method but results in a permeance which is a maximum when the poles are in line and a minimum when the poles are out of line.

4.5.2. Poles in Line.

The area of the flux path is constant and equal to $\frac{1}{2}$ s.d, hence

$$P_o = \frac{\frac{1}{2}\, s.d.}{2\pi \times {}^{2}/_{3}d + 2g}$$

$$\rightarrow 3\, {}^{g}/_{8\pi} \quad \text{where } g \ll d.$$

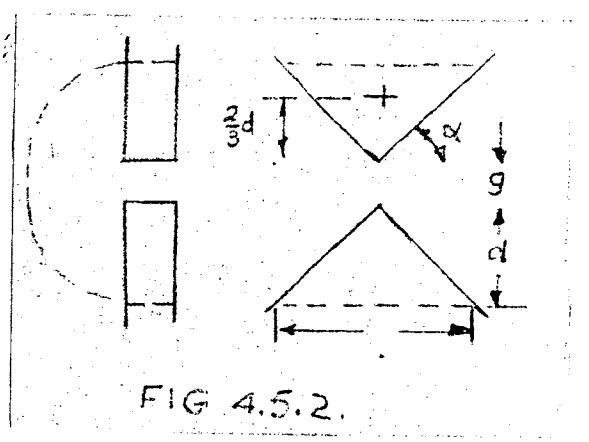

FIG 4.5.2.

4.5.3. Poles Out of Line.

The flux is assumed to leave areas A and A' and settle on areas B and B' respectively.

The area $= \frac{1}{2} \cdot \frac{1}{2} \cdot d \cdot s/2$,

and the permeance

$$= \frac{d \; s/8}{5 \; \frac{\pi d}{3} + 2g} \times 2$$

$$\rightarrow \frac{3s}{20\pi} \quad \text{for } g \ll d.$$

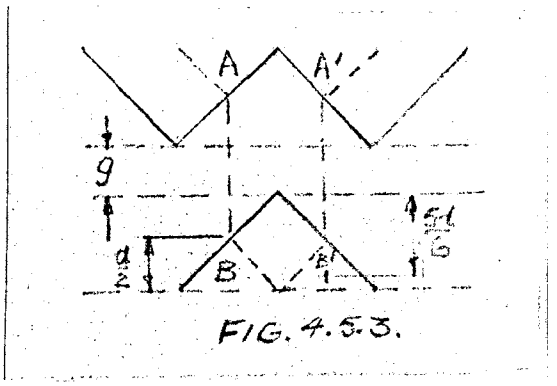

FIG. 4.5.3.

4.5.4. General Position x.

For the LH area,

$$\text{path} = 2\pi \left[\frac{xd}{s} + \frac{2d}{3} - \frac{2x}{3s} \right] + 2g;$$

$$\text{area} = \tfrac{1}{2} (s-x) (d) \left(1 - \frac{x}{s}\right);$$

$$\therefore \; p_{ab} = \frac{d(s-x)^2/2s}{2\pi\left(\frac{xd}{s} + \frac{2d}{3} - \frac{2xd}{3s}\right) + 2g}.$$

For the RH area,

$$\text{path} = 2\pi \left(d - \frac{xd}{s} + \frac{2}{3} \cdot \frac{xd}{s}\right) + 2g;$$

$$\text{area} = x^2 d/2s;$$

$$\therefore \; p_{a'b'} = \frac{x^2 d/2s}{2\pi\left(d - \frac{xd}{s} + 2/3 \, \frac{xd}{s}\right) + 2g}$$

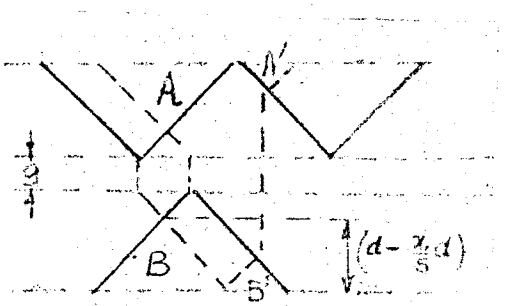

FIG 4.5.4.

The combined permeance is

$$p_x = p_{ab} + p_{a'b'} \qquad \ldots\ldots \; 4.4.1.3.$$

It is easily seen how this method may be extended to trapezoidal teeth, but is slightly more complex for semi-circular teeth. However no further work is intended here on end conditions. Other methods may be developed using the whole of the tooth face, and there is no reason why a substitute angle could not be applied to all end conditions.

4.6. Application of Fourier Method to Internal Circular Teeth at g = o.

This method is adapted directly from Zworykin p.370 (ref. 7.3.82) and is similar to the method used for a square slot 4.3.. The solution

enables plots to be made of the potential distribution in a circle. The permeance can thus be deduced for large values of $^{s}/_{g}$, quite accurately enough for practical purposes.

Separation of variables can be used in the solution of the two-dimensional Laplace Equation in polar co-ordinates. When it is assumed that the potential function can be separated as follows :

$$\phi\,(r,\theta) \;=\; f(r).\;\; g(\theta)$$

then the general solution can be expressed as the summation

$$\phi\,(r,\theta) \;=\; (A_k r^k \;+\; B_k/r^k)\;\; (\sin k\theta \;+\; D_k \cos k\,\theta)$$

where k is the separation parameter.

With the potential distribution on a circular cylinder known the distribution reduces to

$$\phi\,(r,\theta) \;=\; \sum_{n\,=\,o}^{\infty\,\prime} \left(\frac{r}{R}\right)^n (a_n \sin n\theta + b_n \cos_n \theta)$$

where,

$$a_n \;=\; \frac{1}{\pi} \int_o^{2\pi} \phi\,(R,\theta) \sin n\theta \; d\theta,$$

$$b_o \;=\; \frac{1}{2\pi} \int_o^{2\pi} \phi\,(R,\theta)\; d\theta$$

and, $$b_n \;=\; \frac{1}{\pi} \int_o^{2\pi} \phi\,(R,\theta) \cos n\,\theta\; d\,\theta, \quad n \neq o.$$

Hence R is the radius of the cylinder and $\phi\,(R,\theta)$ the potential distribution on the surface of this cylinder.

For the case of two semicylinders of radius R at potentials of V and -V respectively, the co-efficients are :

$$a_n \;=\; \frac{1}{\pi} \int_o^{\pi} V \sin n\,\theta\; d\,\theta \;+\; \frac{1}{\pi} \int_{\pi}^{2\pi} (-V) \;\; \sin n\,\theta\; d\,\theta$$

$$= \frac{4V}{n\pi} \quad (n \text{ odd}), \qquad = 0 \quad (n \text{ even})$$

$$\text{and, } b_n = \frac{1}{\pi}\int_0^{\pi} V \cos n\theta \, d\theta + \frac{1}{\pi}\int_{\pi}^{2\pi} (-V) \cos n\theta \, d\theta = 0.$$

The solution becomes therefore,

$$(\phi r, \theta) = \frac{4V}{\pi} \sum_{k=1}^{\infty} \frac{1}{2k-1} \left(\frac{r}{R}\right)^{2k-1} \sin (2^{k-1})\theta \quad \ldots\ldots \quad 4.6.1.$$

A plot of this potential distribution is given in Fig. 4.6.1.

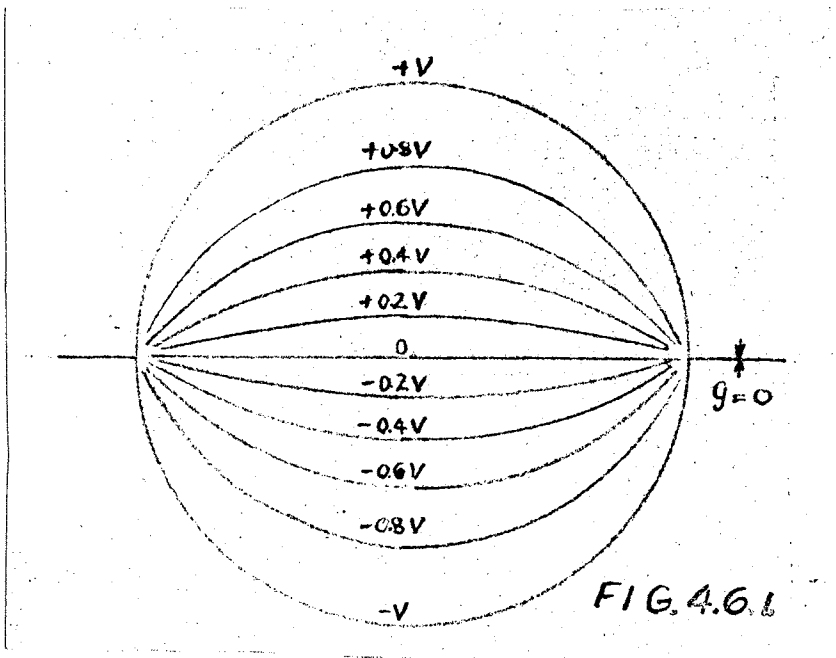

FIG. 4.6.1

4.7. Application of Schwarz - Christoffel Transformation to Trapezoidal Teeth.

Conformal transformation of tooth shapes with $\alpha \neq 90^{\circ}$ prove to be almost unworkable in the forms required for trapezoidal teeth and will not be attempted in this work. Carter[3] encountered this problem on several occasions in his air-gap calculations. His approach was to choose an equipotential line which most nearly fitted the shape of the pole shoe, where the equipotential lines resulted from the distribution

between rectilinear planes.

A similar method may be applied to trapezoidal teeth using a transformation given by Schofield [21] in a heat flow problem.

The Z-plane area to be transformed to the W-plane area via an intermediate t-plane is shown in Fig. 4.7.1. where the dimensions ℓ, m and n are restricted to $o \leqslant m \leqslant \ell$ and $n/\ell = \infty$.

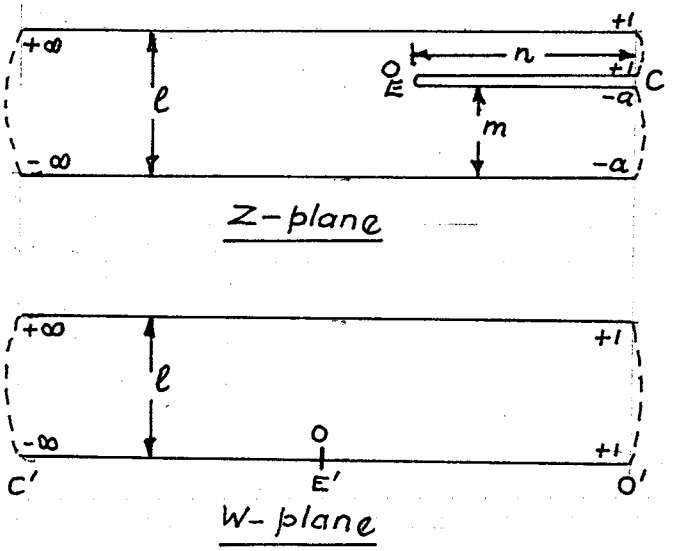

Fig. 4.7.1.

For the transformation to the t-plane from the Z and W planes we have :

$$\frac{dz}{dt} = Pt\,(t-1)^{-1}(t+a)^{-1} \qquad \ldots\ldots \text{ 4.7.1.}$$

$$\frac{dw}{dt} = Q\,(t-1)^{-1} \qquad \ldots\ldots \text{ 4.7.2.}$$

If E, E' and OC, O'C' are the respective origins and real axes we have on integration and evaluation of the constants :

$$W = \frac{\ell}{\pi}\log_e(1-t) \qquad \ldots\ldots \text{ 4.7.3.}$$

$$Z = \frac{\ell-m}{\pi}\log_e(1-t) + \frac{m}{\pi}\log_e\left(1+\frac{t}{a}\right) \qquad \ldots\ldots \text{ 4.7.4.}$$

where $a = m/(\ell - m)$.

Hence,

$$EO = -\frac{\ell - m}{\pi}\left[\log_e(1-t)\right]_{t=1} - \frac{m}{\pi}\log_e\left(\frac{1+a}{a}\right), \quad \ldots\ldots 4.7.5.$$

$$EC = \frac{\ell}{\pi}\left[\log_e t\right]_{t=\infty} - \frac{m}{\pi}\log_e a, \quad \ldots\ldots 4.7.6.$$

$$E'O' = -\frac{\ell}{\pi}\left[\log_e(1-t)\right]_{t=1}, \quad \ldots\ldots 4.7.7.$$

$$E'C' = \frac{\ell}{\pi}\left[\log_e t\right]_{t=\infty} \quad \ldots\ldots 4.7.8.$$

$$\therefore x = O'E' + E'C' - EC - EO\left[\ell/(\ell - m)\right]$$

$$= \frac{\ell m}{(\ell - m)\pi} \cdot \log_e \frac{\ell}{m} + \frac{m}{\pi}\log_e\left(\frac{m}{\ell - m}\right)$$

and, $$\frac{x}{\ell} = \frac{1}{\pi}\left\{\frac{m}{\ell - m} \cdot \log_e \frac{\ell}{m} + \frac{m}{\ell} \cdot \log_e \frac{m}{\ell - m}\right\}. \quad \ldots\ldots 4.7.9.$$

For calculating the complete distribution t must be eliminated from equations 4.7.3. and 4.7.4., so that the co-ordinates $(x+iy)$ of the Z-plane may be obtained in terms of those $(u+iv)$ of the w-plane.

Now from 4.7.3.

$$t = 1 - e^{u\pi/\ell}\left\{\cos(v\pi/\ell) + i\sin(v\pi/\ell)\right\} \quad \ldots\ldots 4.7.10.$$

While from 4.7.3. and 4.7.4.

$$(x + iy) = \frac{\ell - m}{\ell}(u + iv)$$

$$+ \frac{m}{\pi}\log_e\left[1 + \frac{(\ell - m)\left\{1 - e^{\frac{n\pi}{\ell}}\left(\cos\frac{v\pi}{\ell} + i\sin\frac{v\pi}{\ell}\right)\right\}}{m}\right]$$

$\ldots\ldots 4.7.11.$

Hence,

$$x = \frac{\ell - m}{\ell} \cdot u + \frac{m}{2\pi}\log_e\left[A^2 + B^2\right] \quad \ldots\ldots 4.7.12.$$

$$y = \frac{\ell - m}{\ell} \cdot v + \frac{m}{\pi}\tan^{-1}(B/A) \quad \ldots\ldots 4.7.13.$$

where

$$A = \frac{\ell-(\ell-m)e^{u\pi/\ell}\cos(v\pi/\ell)}{m} \qquad \ldots\ldots 4.7.14.$$

and, $$B = \frac{-(\ell-m)e^{u\pi/\ell}\sin(v\pi/\ell)}{m} \qquad \ldots\ldots 4.7.15.$$

From equations 4.7.12 to 4.7.15 the co-ordinates of the points of intersection of the equipotentials with the flow lines may be calculated. The nearest equipotential lines to the trapezoidal shapes may be used to determine the permeance for a given physical α .

SECTION 5.

PRACTICAL CONSIDERATIONS - RECTANGULAR TRIANGULAR AND TRAPEZOIDAL TEETH.

5.1. Rectangular Slots.

In a recent paper by Dr. Liebmann[16] some practical results on rectangular slots were given. These results were obtained by considering the slot as a resistance network and solving for permeance by an analogue method.

The terminology is somewhat different from that used in this paper, but it must be noted that his generalisations lead to fewer diagrams for a given range of values. Dr. Liebmann's dimensions are shown in brackets, his useful generalisations are

$$\delta = \frac{s}{g} = \left(\frac{d}{g}\right)$$

$$\tau = \frac{s + t}{g} = \left(\frac{t}{g}\right)$$

$$\Sigma_0 = \frac{x}{g} = \left(\frac{x}{g}\right)$$

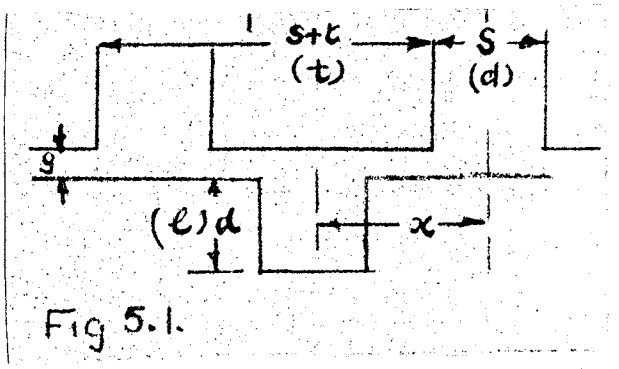

Fig 5.1.

5.1.1. Description of the Method.

The expressions δ, τ, Σ_0 are chosen as relative dimensions of width, pitch and displacement.

The change of air-gap flux is assumed to be independent of the relative slot pitch τ, provided that $\tau \geqslant 2(\delta + 2)$. This is confirmed to some extent by his experimental results. To interpret this in the terms of the present paper

$$\tau \geqslant 2(\delta + 2)$$

i.e.,

$$\frac{s + t}{g} \geqslant 2\left(\frac{s}{g} + 2\right)$$

or $s + t \geqslant 2s + 4g$

or $t \geqslant (s + 4g)$.

It is not clear where this limit was derived from but $t = (s + 4g)$ represents the minimum value of t for which Carter's result for a deep slot is valid. However equations have been developed to cover these conditions so a full comparison will be possible.

Models were established for various Σ and for different δ. It was then necessary to measure the total resistance R between the two conductors outlining the shapes of the model since $P(\Lambda) \propto 1/R$

Values of $dp/d\Sigma$ were obtained by numerical differentiation.

5.1.2. Abstracted Results.

g \ Σ	0	0.5	1.0	2.0	3.0	4.0	4.5	5.0	6.0
5	0.835	0.832	0.824	0.802	0.782	0.762	0.755	0.754	0.754
4	0.877	0.867	0.850	0.834	0.825	0.825	0.8246	0.8246	0.8246
3.5	0.898	0.894	0.888	0.876	0.864	0.858	0.858		
3	0.917	0.914	0.909	0.897	0.89	0.8895	0.8895		
2.5	0.935	0.933	0.929	0.919	0.917	0.916	0.916		
2.0	0.945	0.922	0.903	0.903					
1.0	0.98	0.975	0.913	0.973					
0	1.0								

These results were scaled from a graph in the IEE Journal. The values of Λ quoted is for a value of $\tau = 20$, which is readily convertible to any other value of τ, subject to the earlier mentioned restriction that $\tau \geqslant 2(\delta + 2)$. In the terms of this paper the conversion to other τ is

$$p_\tau = (1 - 20 \frac{g}{s + t}) \quad (1 - p_{20}).$$

It will be noted that this expression remains positive only for

$$20\,\frac{g}{s+t} = 1, \quad \text{i.e., for } \frac{s+t}{g} = 20$$

which is the limiting maximum.

5.1.3. Comparison of Methods.

In the following, comparisons are made between the results of Dr. Liebmann and the other methods so far suggested.

The methods to be compared are as follows :

1. Method A.

   Exactly as derived in Section 2.

2. Method P.

   Method of Pohl with α adjusted to agree with Carter.

3. Method B.

   As derived in Section 4.

4. Method BP.

   Method B with α adjusted, as in 2.

5. Method C.

   Dr. Chapman's result from Section 1.

Comparisons will be made for each method at the maximum and the minimum permeance position and then over a range of x for the case of $\tau = 20$; $g = 1$; $s = 5$, so that $t = 20-5 = 15 > 5 + 4$.

5.1.3.1. Comparison of Maximum and Minimum Permance Values.

Maximum Permeance.

For method A from 2.3.1. we have with $\alpha = \pi/2$.

$$p_o = \frac{t}{g} + \frac{2}{\pi}\log_e\left(1 + \pi s/2g\right) \qquad \ldots\ldots \text{A.}$$

The equation for method B is obtained from 4.1.4.1. with $\alpha = \pi/2$

$$p_o = \frac{t}{g} + \frac{2}{\pi}\log_e(s/g) \qquad \ldots\ldots \text{B.}$$

In the case of method P, $\alpha = 1.0$ in 2.3.1., that is

$$p_o = \frac{t}{g} + \log_e\left(1 + s/g\right) \qquad \ldots\ldots \text{P.}$$

Method BP requires a special value of α to obtain conformity with Carter's result. It is sufficient here to adjust α to agree with P at the in-line position. A value of $\alpha = 0.8$ agrees with P for $\alpha = 1.0$ within 0.12%, thus

$$p_o = \frac{t}{g} + \frac{1}{0.8}\log_e\left(\cos 0.8^\circ + \frac{s}{g}\sin 0.8^\circ\right) \quad \ldots\ldots \text{BP.}$$

It is necessary to use Carter's results for method C, hence, for convenience a plot of this is included in Appendix 2. For this case $\frac{s+t}{g} = 20$; therefore from Fig. A.2.1. curve B for $s/g = 10$ C = 0.67. Hence t = 15 + 0.33 x 5 = 16.65, s' = 3.35, and the relative permeance = $16.65/20 = 0.8325$. This figure is the exact value for this type of slotting.

Minimum Permeance.

From 2.3.5.1. with $\alpha = \pi/2$ and 1.0 respectively we have

$$p_{s/2} = \frac{t-s}{g} + \frac{8}{\pi}\log_e\left(1 + \frac{\pi S}{4g}\right) \quad \ldots\ldots \text{A.}$$

$$p_{s/2} = \frac{t-s}{g} + 4\log_e\left(1 + \frac{S}{2g}\right) \quad \ldots\ldots \text{P.}$$

For methods B and BP the permeance is given by :

$$p_{s/2} = \frac{t-s}{g} + \frac{2}{\alpha}\log_e\frac{G/2 + \alpha(s/2 + P)}{g/2 + H}$$

where for method B, $\alpha = \pi/2$; P = 0 and H = g/2. For method BP, $\alpha = 0.8$; P = g/2 cosec 0.8°.

With Dr. Chapman's method it is only necessary to determine the amount of overlap. For this case the overlap is 16.65 - 3.35 = 13.30 and the relative permeance 13.30/20 = 0.665.

Table 5.1.3.1.1.

	MAXIMUM PERMEANCE					
Method	A	B	P	BP	C	L
Rel.Perm.	0.819	0.801	0.840	0.842	0.8325	0.835
% Diff.	-1.92	-4.08	+0.6	+0.84	-0.3	-

Table 5.1.3.1.1. (Contd.)

MINIMUM PERMEANCE						
Method	A	B	P	BP	C	L
Rel. Perm.	0.703	0.5805	0.751	0.6250	0.665	0.754
% Diff. from L	-6.75	-23.1	-0.4	-17.1	-12%	-

Points of interest in this comparison are :

(a) Method P is very powerful and maintains the accuracy claimed by the author, for the conditions of this problem.

(b) Method A accuracy is quite good but the method is only useful in its relation to method P.

(c) The slope of methods B and BP are far too different from that of method L to be of any use in the present application. It must be noted that the permeance is reduced mainly by the reduction of flux penetration into the slot and even though α is varied, the slope is still not sufficiently improved. No further mention will be made of these methods.

(d) Most surprising is the accuracy and simplicity of method C, the only drawback is that Carter's curve must be referred to, before it is applied; though this is no deterrent since the curve is so well known.

5.1.3.2. Comparison of Permeance with Displacement of Rotor.

Methods A and P are calculated from equations in 2.3.5. with $\alpha = \pi/2$ and 1.0 respectively. For Dr. Chapman's method the permeance decreases linearly to the minimum value at $x = s'$, where s' is the reduced value of the slot opening.

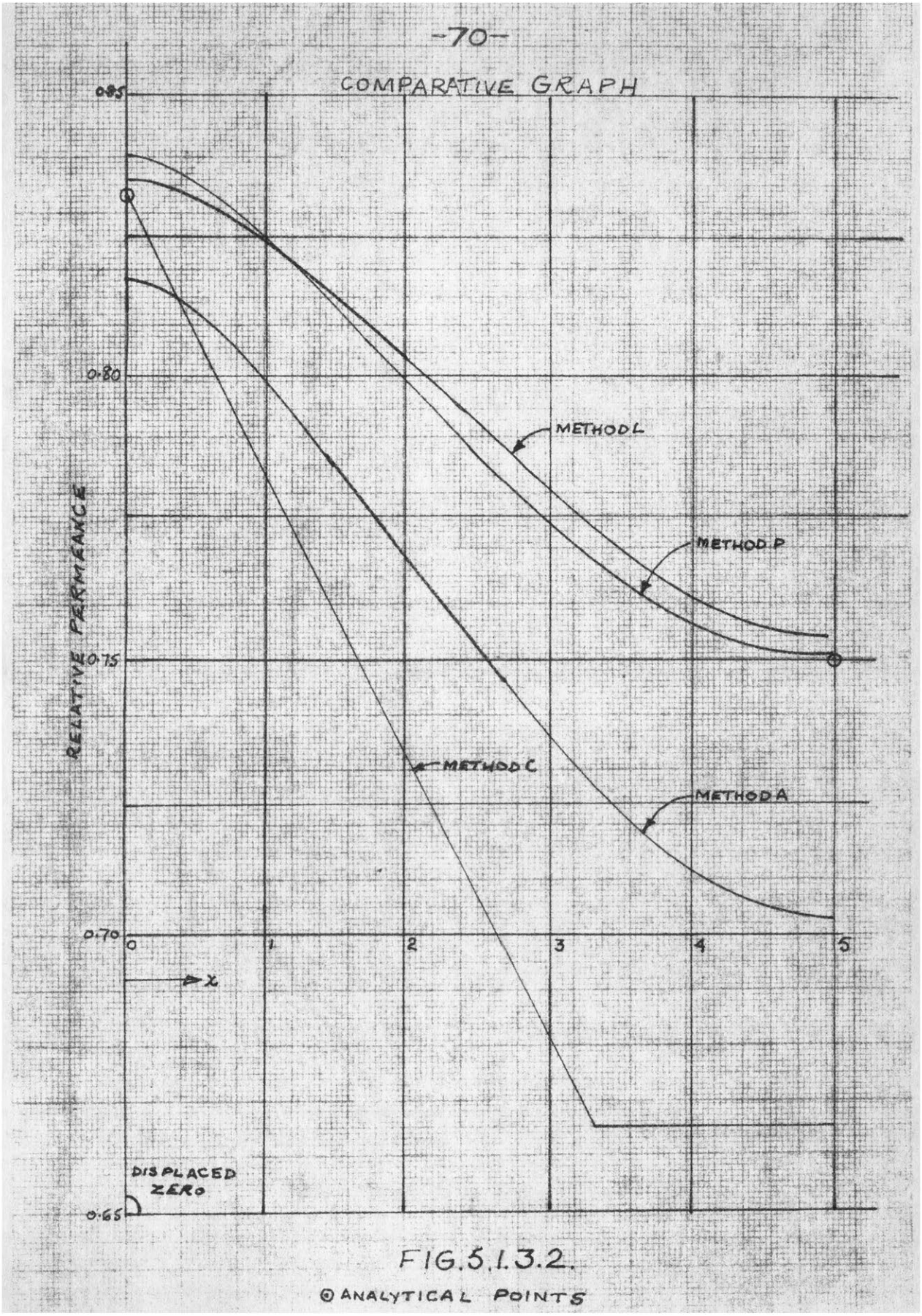

FIG. 5.1.3.2.

⊙ ANALYTICAL POINTS

Table 5.1.3.2.

τ = 20;	δ = 5;	g = 1;	s = 5;	t = 15.				
X	0	0.5	1.0	2.0	3.0	4.0	4.5	5.0
A	0.819	0.813	0.800	0.768	0.737	0.712	0.705	0.703
P	0.840	0.835	0.825	0.799	0.774	0.756	0.752	0.751
L	0.835	0.832	0.824	0.802	0.782	0.762	0.755	0.754
% Diff. P to L	0.6	0.36	0.12	0.37	1.02	0.79	1.0	0.4

The above figures are plotted in Fig. 5.1.3.2. and show the accuracy which is maintained by method P over the whole range.

5.1.4. Comparison of Carter's Result with Method P.

In previous paragraphs some practical results have verified the overall accuracy of method P in a practical case where $t/s = 3.0$. Furthermore this accuracy is maintained throughout the range of movement of the rotor. Though a nominal value of $\alpha = 1.0$ was used in the calculations it does not follow that it is the correct value to use in all cases, nor indeed in the case studied. The value of α is not very critical in this problem since the contribution to the permeance by the term involving α is only a small fraction of the total. Dr. Liebmann shows that his results are lower than the figures obtained by an independent calculation due to a systematic error in the method of measurement.

In using Carter's result, it is assumed that enough t exists for the flux distribution to be uniform in the t-region when the slots are either remote or opposed. This departure from linearity and the slot fringing flux is taken care of in the coefficient C. In the following paragraphs a value α_E is calculated for exact correspondence between Carter's coefficient C and an equivalent coefficient C from

method P. This is not an original calculation but is given as a check on the constant's suggested by Dr. Pohl. It would appear from Dr. Pohl's writing that no account has been taken of the variation of C either when the slots are opposed or when they are of finite depth. In induction motors and similar type machines with rectangular slots, the ratio s/d is much smaller than unity, in which case C is not very much different to the normal value of C for $s/d = 0$, but for inductor and phonic machines s/d may approach unity, suggesting a reduction in the value of α for a given αp.

5.1.4.1. Minimum Permeance for the Single-Sided Slot.

From equation 1.4.2. Carter's coefficient

$$C = \frac{2}{\pi}\left[\tan^{-1}\left(\frac{S}{2g}\right) - \frac{1}{s/g}\log_e\left\{1 + \left(\frac{S}{2g}\right)^2\right\}\right] \quad \ldots\ldots \quad 5.1.4.1.1.$$

which enables the permeance to be calculated for the out-of-line position when t/s is large enough for the distribution to be considered uniform in the t-region. Similarly from Fig. 1.4. and equation 1.4.1. the equivalent coefficient C' for method P is

$$C' = 1 - \frac{1}{s/2g} \cdot \log_e\left(1 + \frac{S}{2g}\right) \quad \ldots\ldots \quad 5.1.4.1.2.$$

In the two groups $0 \leqslant s/g \leqslant 10$ and $10 \leqslant s/g \leqslant 100$, Dr. Pohl states that the values of α required to obtain agreement between C and C' within an accuracy of 1% are 1.0 and 1.1, respectively. Calculations for these values are given in table 5.1.4.1.1. together with a value that gives exact agreement for a range of s/g up to 90.

It is evident that for $0 \leqslant s/g \leqslant 10$, $\alpha = 1.0$ is not within the 1% stated by Dr. Pohl but varies between +26% at $s/g = 1.0$ to -3.6% at $s/g = 10$. However due to the large value of t necessary, $\alpha = 1.0$

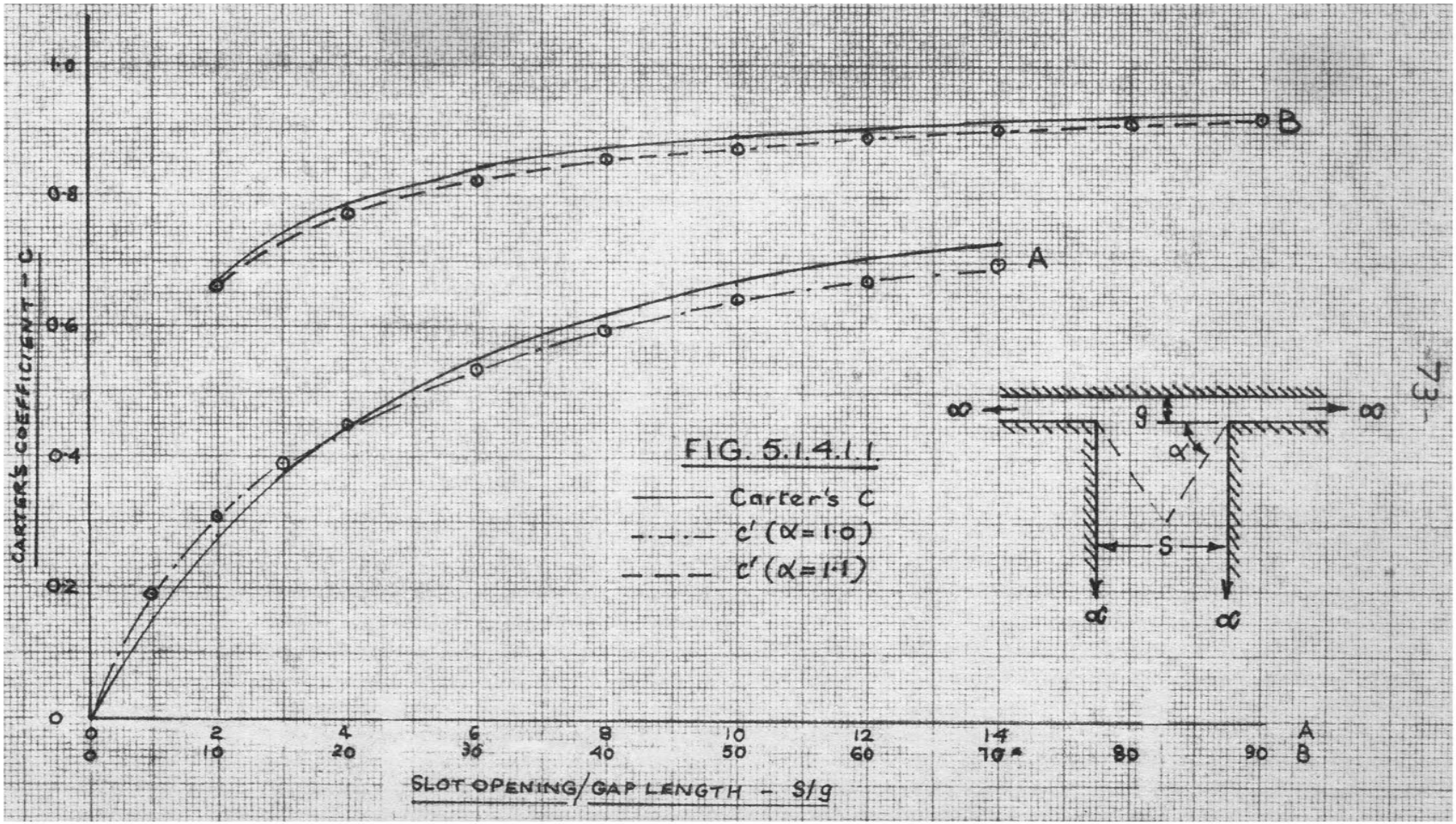

FIG. 5.1.4.1

——— Carter's C

-·-·-·- C' (α = 1·0)

– – – C' (α = 1·1)

will almost certainly give a value of p within 1%. For the higher range of s/g the value of $\alpha = 1.1$ is not nearly good enough.

Table 5.1.4.1.1.

s/g	1	2	3	4	6	8	10	12	14
C	0.153	0.279	0.371	0.449	0.551	0.619	0.666	0.703	0.733
C' α = 1.0	0.189	0.307	0.389	0.450	0.538	0.598	0.642	0.676	0.704
α_E	0.750	0.85	0.92	1.0	1.06	1.10	1.13	1.17	1.20
s/g	10	20	30	40	50	60	70	80	90
C	0.666	0.789	0.843	0.874	0.892	0.906	0.917	0.925	0.931
C' α = 1.0	0.642	0.760	0.815	0.848	0.870	0.885	0.898	0.907	0.915
C' α = 1.1	0. 660	0.774	0.827	0.858	0.878	0.893	0.903	0.914	0.921
C' α = 1.2	0.676	0.786	0.836	0.866	0.886	0.900	0.911	0.919	0.926
α_E	1.13	1.22	1.27	1.31	1.31	1.31	1.32	1.32	1.32

A plot of C verous s/g is given in Fig. 5.1.4.1.1. with the approximations suggested by the author and by Dr. Pohl indicated. A plot of α_E versus s/g is given in Fig. 5.1.4.1.2. The limit of accuracy of the results given here is dependent on the ratio t/s which will be discussed in later paragraphs.

5.1.4.2. Maximum Permeance or Opposed Slots.

When both members of the machine are slotted and opposing, Carter shows[3] that the amount of periphery w to be annulled to allow for the slots is

$$W = \frac{2}{\pi}\left\{\frac{S_1+S_2}{2}\tan^{-1}\frac{S_1+S_2}{g} + \frac{S_1-S_2}{g}\tan^{-1}\frac{S_1-S_2}{g} - \frac{g}{2}\log_e\left[1+\left(\frac{S_1+S_2}{2g}\right)^2\right]\left[1+\left(\frac{S_1-S_2}{2g}\right)^2\right]\right\} \quad \ldots\ldots \quad 5.1.4.2.1.$$

Where S_1 and S_2 are the respective widths of the slot openings. The amounts to be annulled, W_1 and W_2, for each slot, are given by equation 5.1.4.2.1. with S_2 and S_1 put zero in turn. When the slots are remote

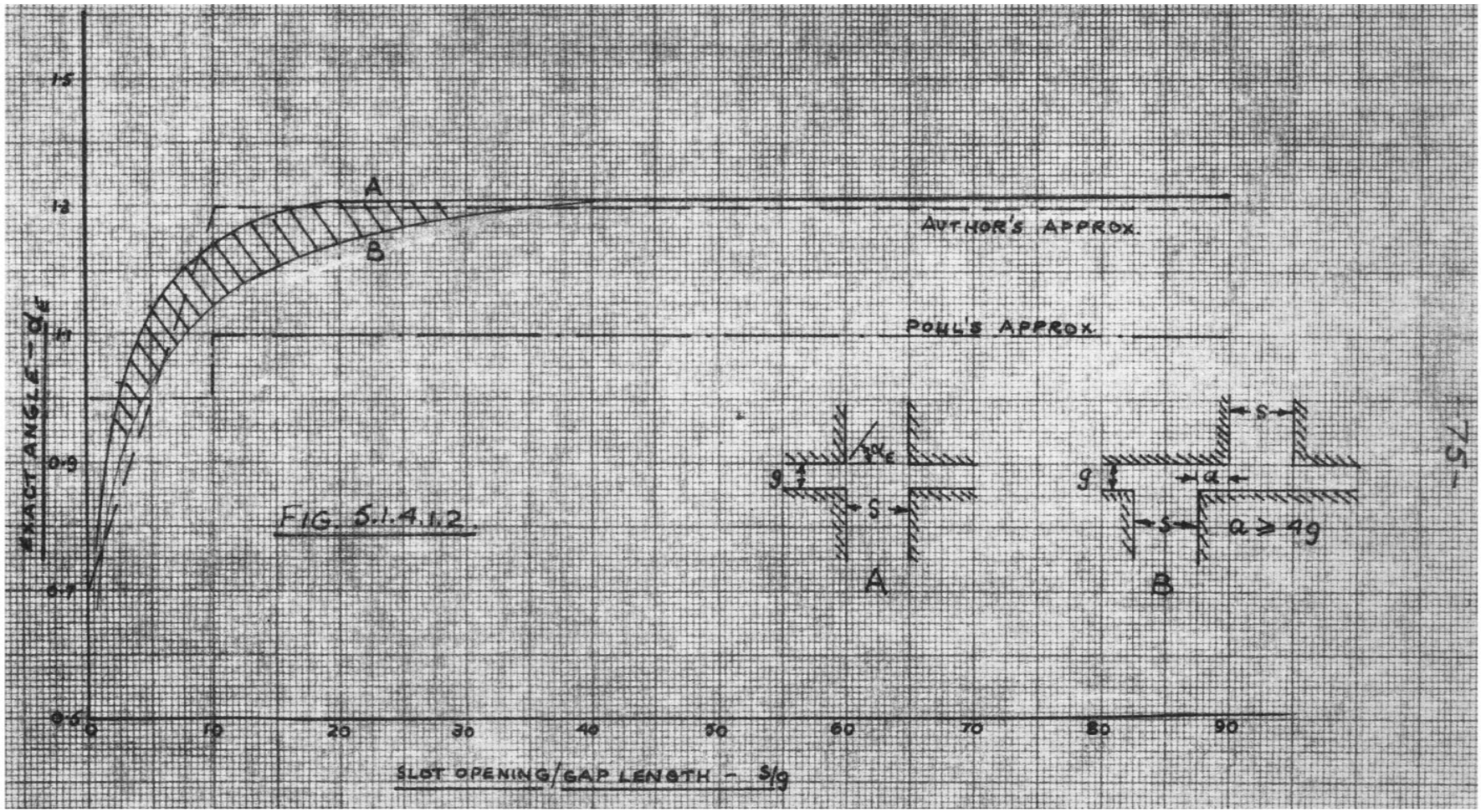
1·5
1·2
1·1
0·9
0·7
0·6
EXACT ANGLE - θ'
A
B
AUTHOR'S APPROX.
POLL'S APPROX.
0
10
20
30
40
50
60
70
80
90
SLOT OPENING/GAP LENGTH - S/g
g
S
A
a
a ≥ 4g
B

FIG. 5.1.4.1.2

from each other (as in 5.1.4.1.) $W_1 + W_2$ is the amount that must be annulled. Hence equation 5.1.4.1.1. is obtained by putting $S_1 = S$ and $S_2 = 0$. For our case, where $S_1 = S_2$, we obtain

$$C = \frac{2}{\pi}\left\{\tan^{-1}\frac{s}{g} - \frac{1}{2^{s}/g} \cdot \log_e\left[1 + \left(\frac{s}{g}\right)^2\right]\right\} \quad \ldots\ldots \quad 5.1.4.2.2.$$

Most designers use one of the approximations suggested by Carter to determine the air-gap permeance, viz., $k = k_1 \times k_2$ (as in 1.2.2.) or more accurately $k = k_1 + k_2 - 1$. We are not concerned with these approximations but with the best value of α for the in-line condition.

Since equations 5.1.4.2.2. and 5.1.4.1.1. are both homogeneous in (s/g) the value of α required to satisfy 5.1.4.2.2. is given by that satisfying 5.1.4.1.1. in $2^{s}/g$. The values of α_E are plotted in Fig. 5.1.4.1.2. and show the further inaccuracy of the constants suggested by Dr. Pohl.

The values suggested by the author for a ratio $s/t = 0$ are for $0 \leqslant s/g \leqslant 10$ that $\alpha = 0.70 + 0.06\ s/g$ and for $10 \leqslant s/g \leqslant 100$, $\alpha = 1.30$. As mentioned previously these figures will apply to some values of $s/t > 0$ which will be studied separately.

5.1.4.3. Minimum Ratio t/g for Successive Slots.

In a few cases plotted by the author and from the plots given by Dr. Liebmann [19] a reasonable approximation to the minimum value of t/g that can be sustained without modification of C is

$t \geqslant g$, provided that the slots are on one side of the air-gap only. If slots are on both sides of the air-gap this approximation is only valid for the in-line position. For the out-of-line position the approximation would be $t \geqslant (s + 2g)$ with both members slotted.

In a calculation by Gibbs [24] agreement to 3 significant figures is obtained when $g/s = 0.18$ and $t/s = 0.78$, from which $t/g = 4.329$. This is by no means the minimum limit to this ratio, as a calculation given by Carter [3] shows that for $2g/s = 1.0$ and $t/s = 1.0$, i.e., $t/g = 2.0$ the value of C is 0.279, whilst from the transformation with $s/t = 0$, $C = 0.276$. This indicates that $t/g = 2.0$ is almost the limiting ratio, though the error in the estimation of C is seen to be about 1% which when converted into p would be considerably less.

Coe and Taylor [4] have taken this problem further and calculated gap coefficients for values of s/g up to 3.0 for various ratios of s/t between 0.25 and infinity. They state that the gap coefficient given by Carter is less than 0.5% (negative) in error for values of $s/t < 3$ and $s/g < 2.5$ with somewhat larger errors for larger ratios. Examining the limiting values of this statement in some detail we find the gap coefficient Kg to be 1.397 for $s/g = 3.0$ and $s/t = 3.0$ which results in a

coefficient C of 0.380, the Carter coefficient, from table 5.1.4. for $^{s}/t = 0$, being 0.371. Evidently the author's approximation lies between the other two and would provide quite good accuracy. It would be useful to extend Coe and Taylor's results to values of $^{s}/t \leqslant 0.5$ and $^{s}/g \leqslant 100$, to cover the complete range of interest to this work, but it is sufficient here to have established the limit of accuracy of Carter's result in relation to the substitute angle method. Further comments for t = 0 will be given in 5.1.4.5.

5.1.4.4. Slots of Finite Depth.

As mentioned in 1.2., provided the slot depth is not less than the slot width Carter's result is not materially affected by finite depths. For completeness, a comparison is made here of the variation of C with $^{d}/s$ for values of $^{s}/g = 2.5$ and 5.0 as calculated from Coe and Taylor's results.

Table 5.1.4.4.1.

$^{s}/g$	$^{d}/s$	0.1	0.2	0.3	0.5	0.6	0.75	∞
2.5	C	0.169	0.252	0.291	0.315	0.329	0.339	0.343
	α_E	0.35	0.59	0.74	0.84	0.90	0.94	0.96
5.0	C	0.288	0.404	0.455	0.479	0.494	0.501	0.508
	α_E	0.36	0.64	0.81	0.91	0.98	1.01	1.04

A value of the exact substitute angle α_E is calculated and recorded in table 5.1.4.4.1.. Some care has been taken to scale the above results from Coe and Taylor's paper but they cannot be relied upon beyond the first two digits, which is sufficient for the comparison made here. Due to the limited range of these figures it is not possible to

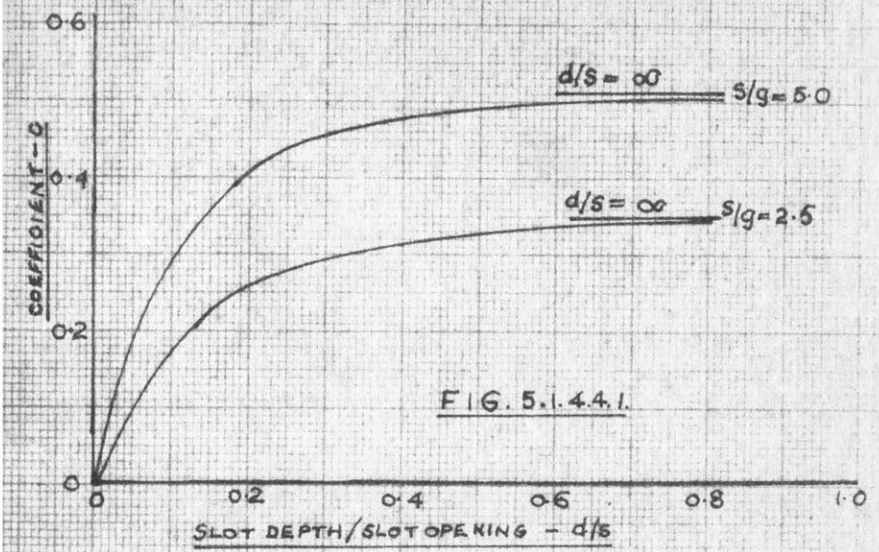

FIG. 5.1.4.4.1.

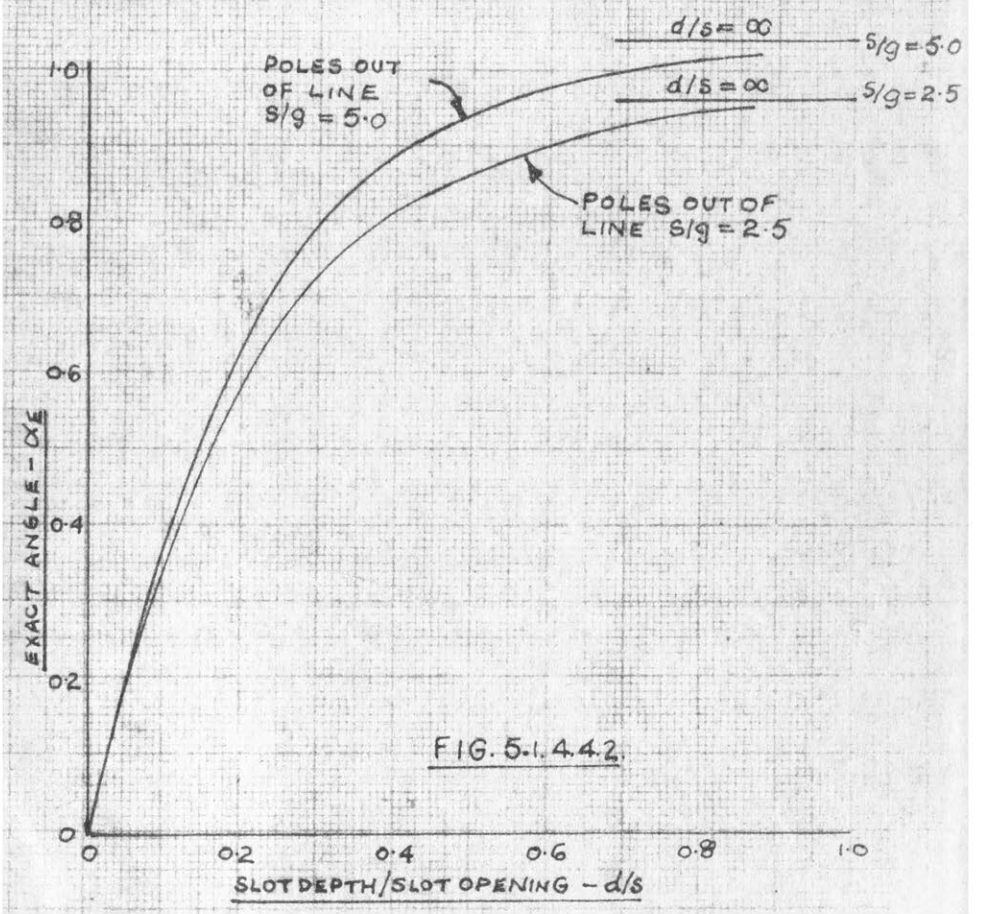

FIG. 5.1.4.4.2.

make concrete deductions. However the values of α for $^{d}/_{s} \geq 1.0$ are not materially different from those given when $^{d}/_{s} = \infty$.

5.1.4.5. Special Case of t = o.

In previous paragraphs an approximate limit has been determined for the ratio $^{t}/_{g}$ and $^{s}/_{g}$ where the Carter method may be applied. If the tooth width is infinitely thin the problem becomes the limiting case for (a) slots of rectangular section varying t and (b) slots of triangular section varying α. If Carter's result is applied directly to a problem with a slot infinitely deep but with enough t for the slot flux to become uniform, then the permeance variation becomes a linear function of t, down to the limit of proportionality discussed in 5.1.4.3.

It can be shown by an elliptic transformation that when the medium between two parallel planes distance ℓ apart, is disturbed by the addition of a tooth, infinitely thin and of length $(\ell - g)$, perpendicular to and at the same potential as one plane, that the resulting distribution is equivalent to adding a length 2X to the original dimensions for each tooth, where

$$X = \frac{2\ell}{\pi} \log_e \operatorname{cosec}\left(\frac{g\pi}{2\ell}\right) \qquad \ldots\ldots \text{ 5.1.4.5.1.}$$

This result is true for one tooth in an infinitely long air-gap whereas for successive teeth is less than 1% in error when the semi-tooth pitch is slightly more than ℓ, where ℓ = d (the slot depth) + g.

For a comparison here, consider the ratio $^{s}/_{d} = 1.0$ so that (a) the effect of slot depth does not materially affect C and (b) the slot width is wide enough for 5.1.4.5.1. to be accurate. The comparison will be made for a slot on one side of the air-gap only, but from previous work the method of accounting for opposed slots will be the same.

In table 5.1.4.5. a comparison is made of C, p_o, and C', p_o' where C is the Carter coefficient and p_o, the corresponding permeance, assuming that t = o. The values of C' and p_o' are obtained from the following :

$$C' = (1 - p_o'/s/g), \quad p_o' = \frac{2x + s}{\ell} \qquad \text{-----} \qquad 5.1.4.5.2.$$

Consider as an example the case of $s/g = 10$, i.e., s = d = 10 and $\ell = (d + g) = 11.0$. From equation 5.1.4.5.1.,

$$X = \frac{2 \times 11}{\pi} \log_e \operatorname{cosec} \frac{\pi}{22} = \frac{2 \times 11 \times 1.9495}{\pi}$$

$$= 13.652.$$

Hence, $$p_o' = \frac{2 \times 13.652 + 10}{11.0} = 3.391.$$

$$C_o' = (1 - \frac{3.391}{10}) = 0.6609$$

From table 5.1.4.11. we have for $s/g = 10$, C = 0.666, and the corresponding $p_o = s/g(1 - C') = 3.34$. It is surprising that such accuracy is given by Carter's result but evidently while any t exists the result is only approximate and in the absence of t the fringe rearranges itself and improves the accuracy, the differences being 0.76% in C and 1.47% in p_o. These figures are considered in the same range as for table 5.1.4.1.1. To return to the original work of the thesis we now require the value of α_E corresponding to p_o' which is calculated (for the single slot) from equation 1.4.1. and gives for $s/g = 10$, $\alpha_E' = 1.11$ which differs by 1.8% from α_E associated with p_o.

Table 5.1.4.5.

s/g	4	10	20	40	60	80	100
C	0.449	0.666	0.789	0.874	0.906	0.925	0.931
C'	0.426	0.661	0.783	0.870	0.906	0.925	0.937
p_o	2.20	3.34	4.22	5.04	5.64	6.00	6.90
p_d	2.30	3.39	4.35	5.21	5.64	6.00	6.30
α_E	1.00	1.13	1.22	1.31	1.31	1.32	1.32
α_E	0.89	1.11	1.17	1.25	1.31	1.32	1.34

These results are plotted in Fig. 5.1.5.4.1. and show that there is almost no difference between the result for deep slots and large t and shallow slots with no t. The case plotted here for no t was with $s/d = 1.0$ which is outside the specified range of accuracy of equation 5.1.4.5.1., but it can be shown that the variation is not significant; e.g., $s/g = 20$, $s = 20$, $g = 1$, $\ell = 11$ gives $p_o' = 4.30$ and $C' = 0.785$ which differ by $\frac{1}{4}\%$ in C' and 1% in p_o' from those in table 5.1.4.5.. That these results are not conclusive would be because the separate effects of fringing in the t-region and slot depth are self compensating. From table 5.1.4.4.1. for $d/s = \infty$ and $s/g = 2.5$ and 5.0, C is 0.343 and 0.508 respectively when $t = o$. These are plotted in Fig. 5.1.5.4.1. and lie a little above the curve for $s/t = o$, but the difference could reduce for higher values of s/g, though this needs to be proved.

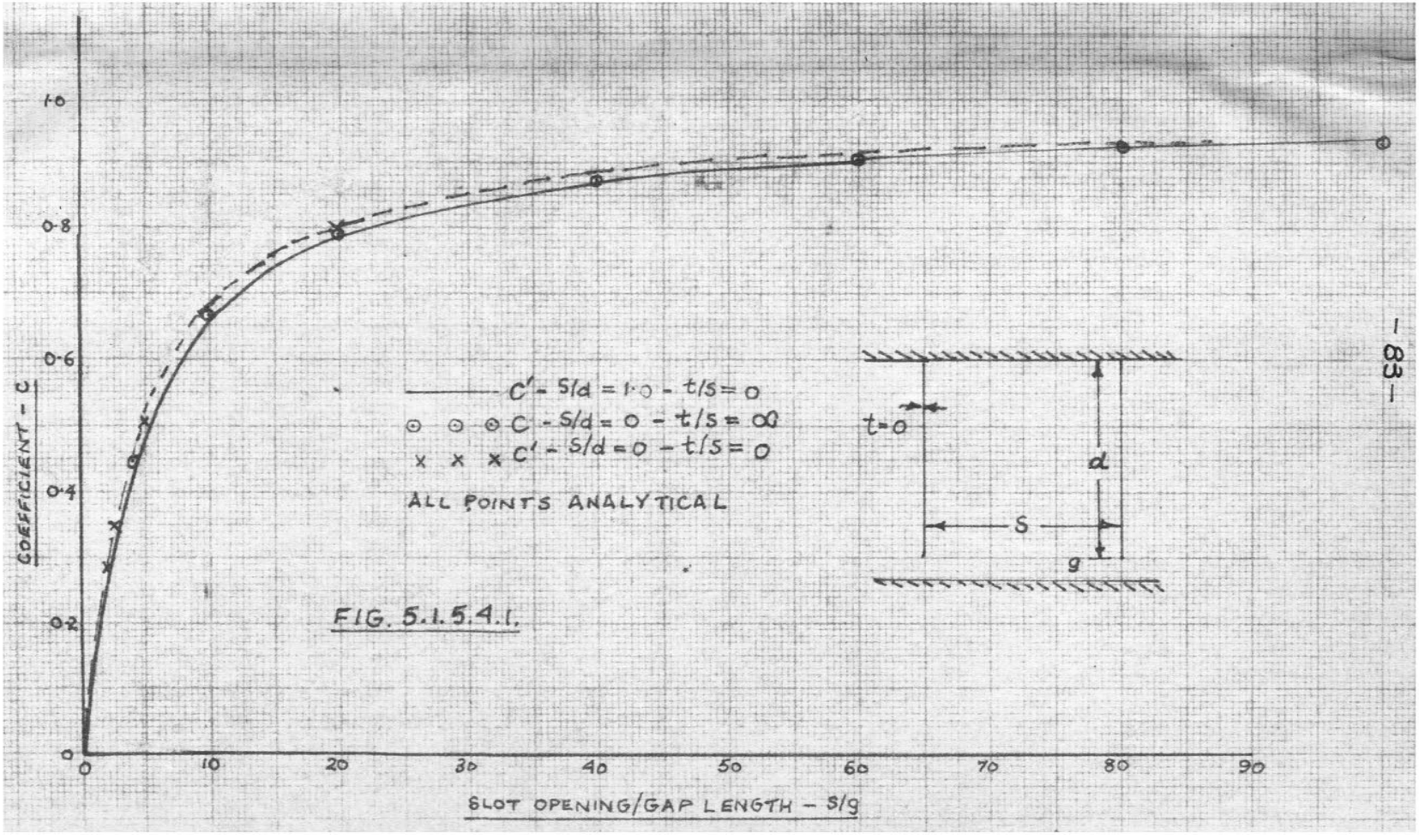
COEFFICIENT - C
1·0
0·8
0·6
0·4
0·2
0
0
10
20
30
40
50
60
70
80
90
SLOT OPENING/GAP LENGTH - S/g
C' - S/d = 1·0 - t/s = 0
C - S/d = 0 - t/s = ∞
C' - S/d = 0 - t/s = 0
ALL POINTS ANALYTICAL
t=0
d
S
g

FIG. 5.1.5.4.1.

To check this last statement we will take the case of $s/g = 20$, $t/s = 0$ and $s/d = 0$. From Coe and Taylor's[4] paper the gap coefficient

$$K_g = \frac{g'}{g} = \frac{\phi_o}{g} \times \frac{1}{B_m}$$

where

$$B_m = \frac{\phi_o}{g} \times \frac{2g}{S} \cdot \frac{K_1'}{K_1} \qquad \text{----- 5.1.5.4.3.}$$

and K_1 is the first complete elliptic integral to modulus

$$k_1 = \operatorname{sn}\alpha = \tanh \frac{g\pi}{S} \qquad \text{----- 5.1.5.4.4.}$$

From these we obtain $K_g = s/2g \cdot K_1/K'_1$ and since $K_g = 1/(1-C)$, $C = (K_g - 1)/K_g$.

Without access to tables of elliptic functions K may be computed from k' as K' from k by the following :

Let, $-\pi \frac{K}{K'}$,

$$e = q' = \frac{1}{2}\frac{1-\sqrt{k}}{1+\sqrt{k}} + \frac{2}{2^5}\left(\frac{1-\sqrt{k}}{1+\sqrt{k}}\right)^5 + \ldots\ldots,$$

$$\log_e q \cdot \log_e q' = \pi^2,$$

$$\sqrt{\frac{2K'}{\pi}} = \theta(0,q') = 1 + 2q' + 2q'^4 + \ldots\ldots,$$

$$K = -\frac{K'}{\pi} \cdot \log q'.$$

5.1.5.4.5.

Now either k or k' is greater than 0.7, and hence either q or q' may be obtained to five places with only one term in its expansion and with a relative error of only about 0.01%. Moreover either q or q' will be less than 1/20 and a single term 1+2q or 1+2q' gives K or K' to four places.

First let us check the method by a known result. With $^{s}/_{g} = 5.0$, $\tanh {}^{g\pi}/_{s} = 0.556895 = k_1$; $\sqrt{k_1} = 0.746257$ and $q' = 0.0726504$. Hence $K'_1 = 2.06047$ and $K_1 = 1.71576$. Now $K_1/K'_1 = 0.83275$ and $({}^{s}/_{2g}) \times (K_1/K'_1) = 2.08187 = Kg$, and therefore $C = 0.51967$. This agrees with the value obtained by Coe and Taylor[4] by another method for $^{d}/_{s} = \infty$ and $^{s}/_{g} = 5.0$, so we will now use it to extend the range to $^{s}/_{g} = 20$.

For our example ${}^{g\pi}/_{s} = 0.157079$ from which $k_1 = \tanh {}^{g\pi}/_{s} = 0.155801$ and $k'_1 = \sqrt{1-k_1^2} = 0.9877884$, also $\sqrt{k_1} = 0.3947164$, giving

$$q' = \frac{1}{2} \cdot \frac{0.6052836}{1.3947164} + \frac{2}{2^5} \cdot \left(\frac{0.6052836}{1.3947164}\right)^5 + \quad \ldots.$$

$$= \frac{1}{2}(0.4339823) + \frac{1}{2^4}(0.4339823)^5 + \quad \ldots..$$

$$= 0.2169911 + 0.0009621437 + \quad \ldots....$$

$$= 0.2179532.$$

Hence,

$$\sqrt{\frac{2K'_1}{\pi}} = 1 + 2(0.2179532) + 2(0.2179532)^4 + \ldots$$

$$= 1.4359064 + 0.004513186 + \quad \ldots..$$

$$= 1.4404196,$$

from which

$$\frac{K'_1}{\pi} = 1.037404 \text{ and } K'_1 = 3.25910.$$

Therefore $K_1 = -\frac{K'_1}{\pi} \cdot \log_e q'$

$$= -(1.037404)\ (-1.523719)$$

$$= 1.580712,$$

and $\frac{K_1}{K'_1}, = \frac{1.580712}{3.25910} = 0.485015.$

Hence $K_g = 4.85015$ and $C = 0.793816$. This value of C is a little higher than the value for a shallow slot and verifies the statement made previously.

It is possible to develop an approximate formula from the above treatment as follows :

$$k_1 = \tanh \frac{g\pi}{s} \doteq \frac{g\pi}{s}$$

for $s/g > 10$

$$\therefore \quad q' \doteq \frac{1}{2} \cdot \frac{1 - \sqrt{g\pi/s}}{1 + \sqrt{g\pi/s}},$$

$$\sqrt{\frac{2K'_1}{\pi}} = 1 + \frac{1 - \sqrt{g\pi/s}}{1 + \sqrt{g\pi/s}},$$

$$K'_1 = \frac{2}{(1 + \sqrt{g\pi/s})^2}$$

and

$$K_1 = \frac{2}{(1 + \sqrt{g\pi/s})^2} \cdot \log_e \frac{1}{2} \cdot \frac{1 - \sqrt{g\pi/s}}{1 + \sqrt{g\pi/s}} .$$

Hence $$\frac{K_1}{K'_1} = \frac{1}{\pi} \left[\log_e(1 + \sqrt{g\pi/s}) - \log_e(1 - \sqrt{g\pi/s}) \right],$$

giving

$$Kg = \frac{1}{2\pi} \cdot s/g \left[\log_e(1 + \sqrt{g\pi/s}) - \log_e(1 - \sqrt{g\pi/s}) \right] .$$

... 5.1.4.5.6.

Tracing this approximation through for the previous case of $s/g = 20$ we obtain the following results, with the exact figures in brackets :

$k_1 = 0.157079$ (0.155801),

$q' = 0.216127$ (0.217953),

$K'_1/\pi = 1.03740$ (1.03740),

$K_1 = 1.58918$ (1.58071),

$Kg = 4.87614$ (4.85015),

and $C = 0.79492$ (0.793816).

5.1.4.6. Out-of-Line Permeance t = o.

A useful extension of these results would be to obtain the value of $\alpha_{E'}$ when the teeth are out-of-line. The author does not intend to pursue this aspect on an analytical basis, but a transformation could be used similar to that given by Moulton (Proc. Lond. Math. Soc. Vol. III, p.104) for the resistance of plane sheets.

The basic result in equation 5.1.4.5.1. applies to a single slot in a semi-infinite plane, hence provided opposed teeth out-of-line are positioned such that the effect of one on the other is negligible, then we have a result for the limiting case of out-of-line permeance. Consider, for example, the case of $^{s}/_{g} = 20$, g = 1.0 which gives $\ell = 9$ when $s = 2(\ell + g)$, (say). From equation 5.1.4.5.1. we obtain

$$X = \frac{2 \times 9}{\pi} \log_e \operatorname{cosec} \frac{5 \times \pi}{2 \times 9} = 1.527.$$

The permeance per tooth is then 2.561 or 5.122 for the two teeth. For the in-line condition, we obtain X = 13.98 and p = 5.329, i.e., a change of 0.207. The in-line permeance is not the same as in table 5.1.4.5. due to the difference in the ratio $^{d}/_{s}$; it will be appreciated though, that if $^{d}/_{s}$ had been the same then we would obtain the permeance for $2^{s}/_{g}$ (i.e. 40) from table 5.1.4.5. The values of α_E for these two conditions are obtained from equations 2.2.1. and 2.2.2. for the in-line and out-of-line positions respectively. As has been mentioned previously the results in this section represent the limiting conditions for triangular and trapezoidal teeth.

5.2. Triangular Teeth.

No published results are available for triangular teeth and the only analytical solutions obtained are those for $\alpha_p = \pi/2$ as discussed in 5.1. Hence with the limits established for $\alpha_p = \pi/2$ the values for $\alpha_p < \pi/2$ are here determined by other methods. No doubt the best method to use is relaxation, but the few plots calculated by the author proved very tedious. Douglas [11] had considerable success with the method of potential distribution using a thin metal plate and Moore [26] had similar success using graphical flux plotting. The author uses the method of resistance measurement on Teledeltos paper as described in 6.4 for teeth out-of-line and a graphical method for the in-line condition.

5.2.1. The Single Sided Slot.

Using the method of curvilinear squares a number of permeance values have been obtained for a single tooth opposite an equipotential plane for various values of the parameter α_p. Several plots were used for each permeance value as an independent check, one of which is reproduced in Fig. 5.2.1.3. for $\alpha_p = \pi/4$ and $s/g = 20$. The permeance values are recorded in table 5.2.1.1. and Fig. 5.2.1.1. In this table α_p is the angle that the slot side makes with the plane of the air-gap and p_o' is the permeance for one complete slot, g being the distance between the tooth and the equipotential plane.

Two values of p_o' are available as the extreme limits, when $\alpha = o$ and $\pi/2$. The plots mentioned above provide values of p_o' between these extremes. Obviously when $\alpha_p = o$, $p_o' = s/g$, and when $\alpha_p = \pi/2$, p_o' is approximately as given in table 5.1.4.5. For precise accuracy at the limiting condition, $s/d = o$, equations 5.1.5.4.3 - 5

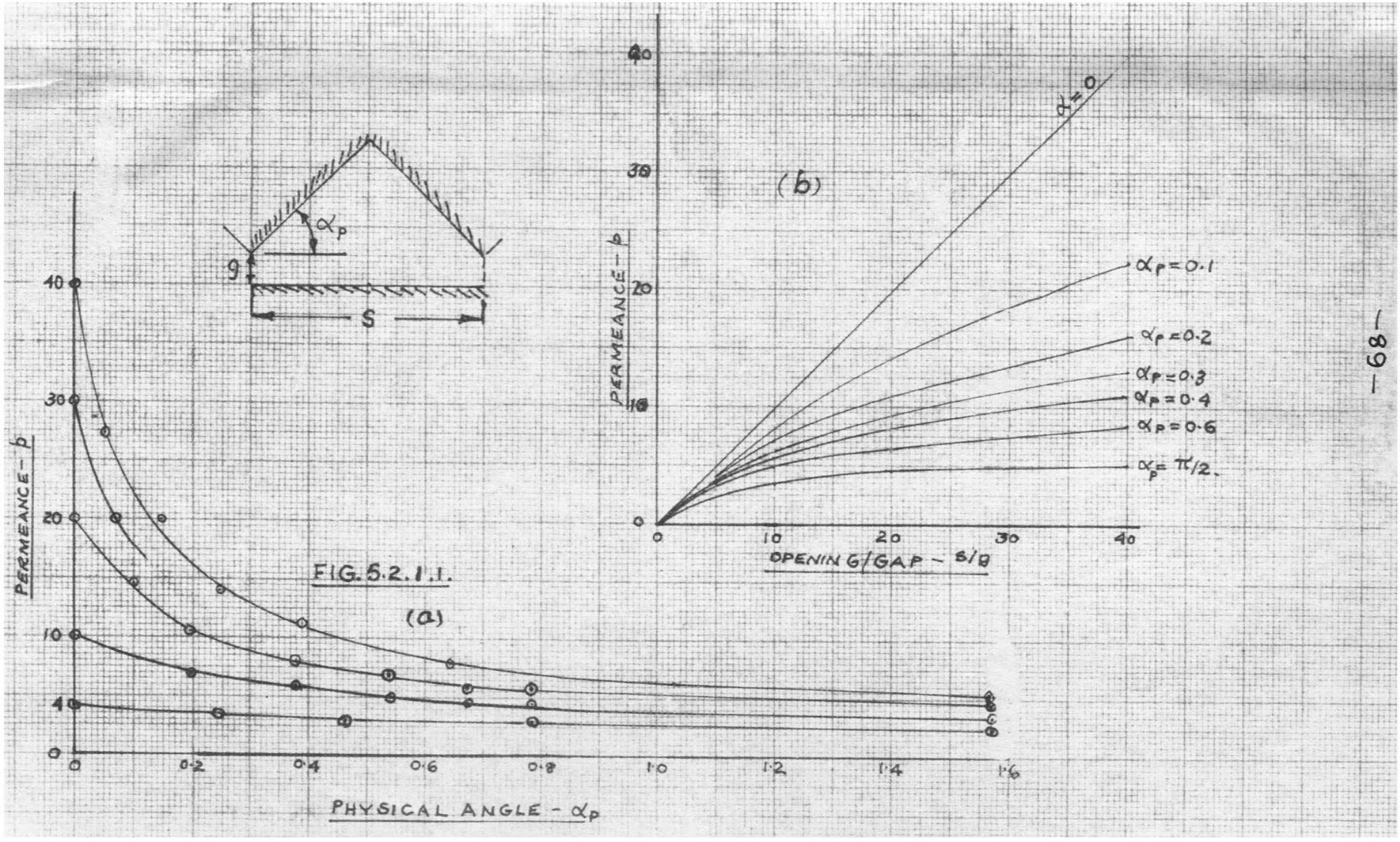
PERMEANCE - b
40
30
20
10
0
0
0·2
0·4
0·6
0·8
1·0
1·2
1·4
1·6
PHYSICAL ANGLE - α_p
α_p
g
S
(a)
(b)
$\alpha = 0$
$\alpha_p = 0.1$
$\alpha_p = 0.2$
$\alpha_p = 0.3$
$\alpha_p = 0.4$
$\alpha_p = 0.6$
$\alpha_p = \pi/2$
PERMEANCE - b
40
30
20
10
0
10
20
30
40
OPENING/GAP - S/g

FIG. 5.2.1.1.

are required, but for results within 0.1%, equation 5.1.5.4.1. is satisfactory.

An equivalent Carter coefficient C' has been calculated as before where $C' = 1 - p_o' (s/g)$ and an exact value of α , $\alpha E'$, to obtain agreement between the permeance p_o' in table 5.2.1.1. and that obtained from equation 1.4.1.

In Fig. 5.2.1.1.(a), p_o' is plotted against αp for various values of s/g and it is evident that when $\alpha p > \pi/4$ the values are nearly equal to those for $\alpha p = \pi/2$. The above values have been replotted against s/g for constant values of αp in Fig. 5.2.1.1.(b).

Table 5.2.2.1.

s/g = 4.0							
αp	0	0.245	0.464	0.785	-	-	$\pi/2$
$\alpha E'$	0	0.147	0.365	0.365	-	-	0.89
p_o'	4.0	3.5	3.0	3.0	-	-	2.3
C'	0	0.125	0.25	0.25	-	-	0.426
s/g = 10.0							
αp	0	0.197	0.380	0.540	0.675	0.785	$\pi/2$
$\alpha E'$	0	0.194	0.310	0.500	0.637	0.637	1.11
p_o'	10.0	7.0	6.0	5.0	4.5	4.5	3.4
C'	0	0.30	0.40	0.50	0.55	0.55	0.661
s/g = 20.0							
αp	0	0.100	0.197	0.380	0.540	0.675	$\pi/2$
$\alpha E'$	0	0.085	0.22	0.40	0.52	0.60	1.17
p_o'	20.0	14.5	10.5	8.0	7.0	6.5	4.4
C'	0	0.275	0.475	0.600	0.650	0.675	0.783
s/g = 40.0							
αp	0	0.05	0.148	0.245	0.390	0.643	$\pi/2$
$\alpha E'$	0	0.053	0.125	0.260	0.380	0.654	1.25
p_o'	40.0	27.3	20.0	14.0	11.3	7.9	5.2
C'	0	0.317	0.500	0.650	0.718	0.803	0.870

Values of $\alpha_{E'}$ are plotted in Fig. 5.2.1.2. for the several values of $^{s}/_{g}$ in table 5.2.1.1. and in each case these values lie slightly above the line between the α = o and $\alpha = \pi/2$ points. With flux plotting of the nature used here the permeance would, if anything, be underestimated, so that the values of α_E would be slightly higher than the true values. It is not possible to give a maximum error because a number of different scales and equipotential lines were used to check each plot. However consider one case for $\alpha_p = \pi/4$ and $^{s}/_{g} = 20$.

The gap space (Fig. 5.2.1.3.) was separated into four layers by three equipotential lines, providing 12 tubes for the half slot. The estimated maximum error from this plot is half a tube. The limits of p_o for the whole slot would therefore be 6.0 to 6.25. When p = 6.0, $\alpha_E = 0.69$ and when p = 6.25, $\alpha_E = 0.64$. This latter figure is closer to the straight line approximation ($\alpha = 2\,\alpha_p\,\alpha_E/\pi$) but in all cases it will be noted that they lie above this line. Hence an approximation for α, more consistent with the results obtained, is

$$\alpha = 1.5\,\alpha_E\,(1 - {}^{-1.9\alpha_p/\pi}) \quad \ldots\ldots \quad 5.2.1.1.$$

For the example above $\alpha_p = \pi/4$ and from table 5.1.4.5. $\alpha_E = 1.17$, yielding $\alpha = 0.66$.

5.2.2. Opposed Teeth in Line.

The case of single slots has been treated in 5.2.1. and shows that an approximate substitute angle α may be determined from equation 5.2.1.1.. For opposed teeth the value of α_E is obtained from table 5.1.4.5. or equation 5.1.4.5.6. for $2^{s}/_{g}$ as before. When $^{s}/_{g} > 20$, $\alpha_E = 1.31$ will suffice.

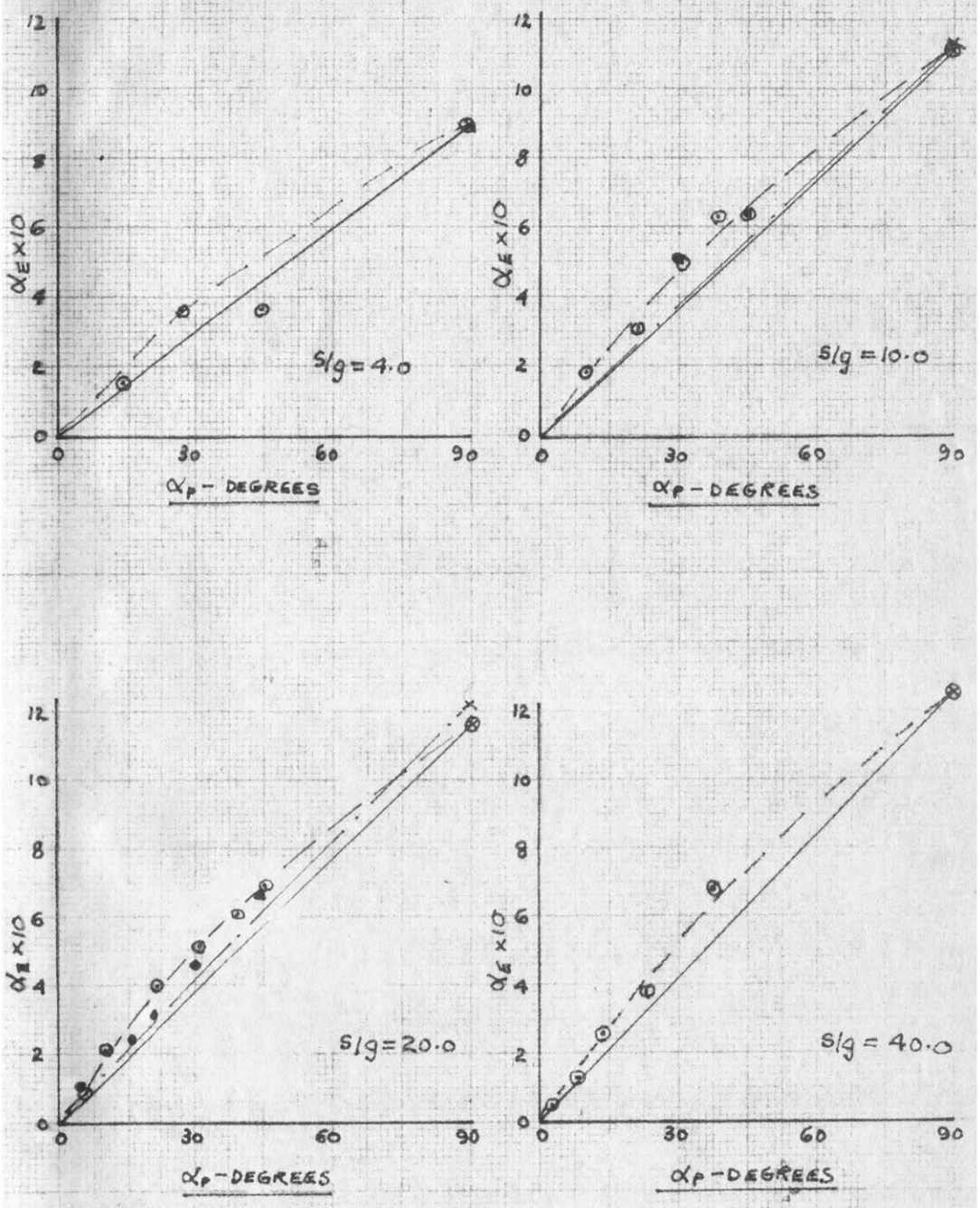

× ⊗ ANALYTICAL POINTS

• ⊙ EXPERIMENTAL POINTS

FIG. 5.2.1.2.

⊗ ⊙ TRIANGULAR TEETH t/s = 0

× • TRAPEZOIDAL TEETH S/t = 0

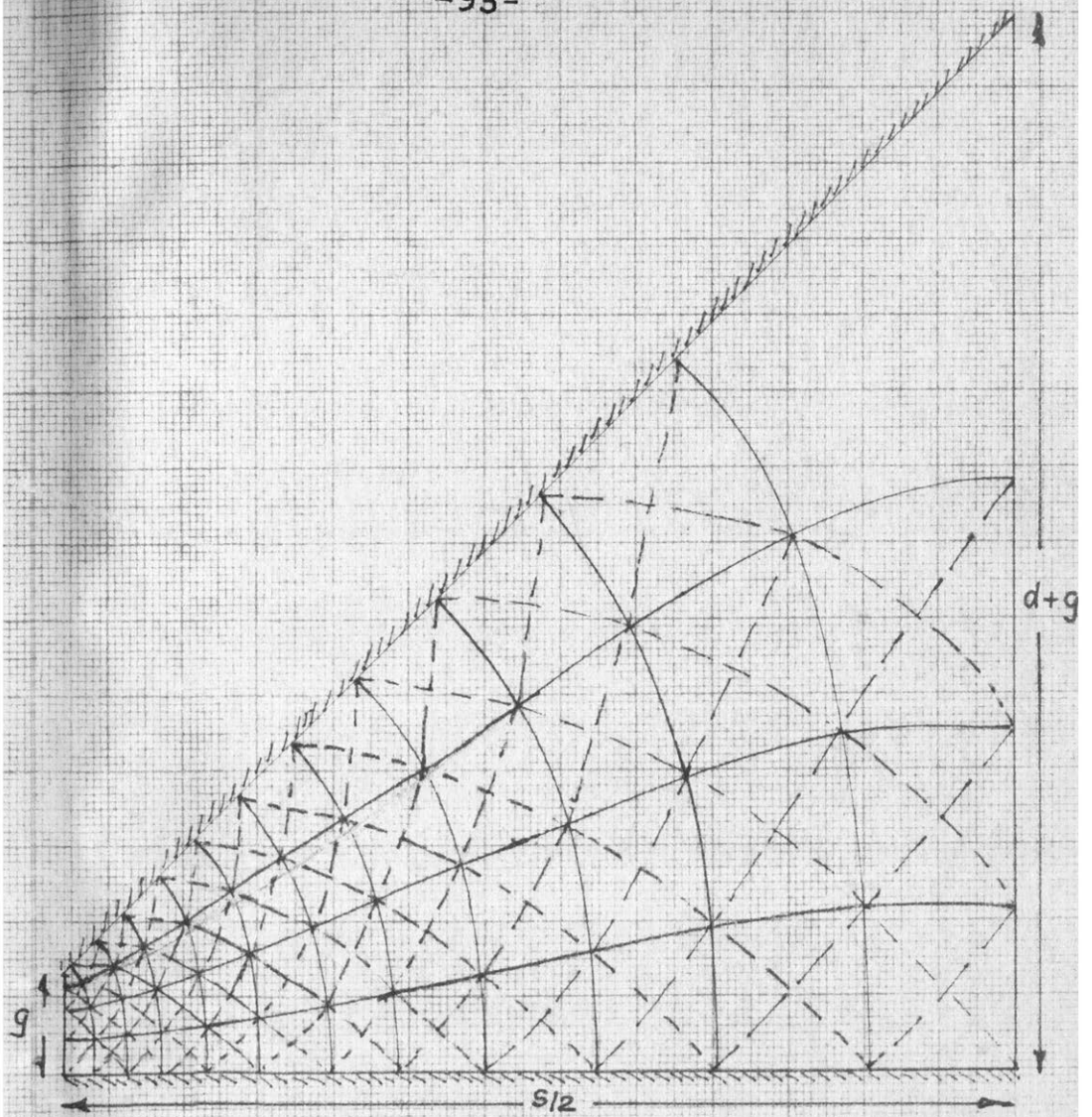

TRIANGULAR TOOTH

$S = 20$; $g = 1.0$; $\alpha_p = \pi/4$;

No OF TUBES = 24.0;

PERMEANCE = 24/4 = 6.0.

FIG. 5.2.1.3.

The values of α determined from the above are applicable to equation 2.2.1. Before accepting the remaining equations for various values of x it is necessary to study the permeance for $x = s/2$.

5.2.3. Opposed Teeth Out-of-Line.

Using the method described in 6.4 a number of permeance values have been obtained for $\alpha_p = \pi/4$. The results are given in table 5.2.3.1. in terms of R the actual measured resistance. The teledeltos paper used was 6" wide with a specific resistance of 319 ohm/inch/6" with a measured thermal resistance of 300 ohm (see Fig. 6.4.1.). The permeance p is for the whole slot pitch and is plotted in terms of g in Fig. 5.2.3.1.(a) and s/g in Fig. 5.2.3.1.(b). Consider example 3 in table 5.2.3.1.,

Table 5.2.3.1.

g"	s/g	α_E	R	p	g	R	p
0	∞	0.704	1650	2.84	-0.5	1580	2.99
0.5	24	0.743	1880	2.42	-1.0	1460	3.30
1.0	12	0.747	2045	2.19	-1.5	1360	3.61
1.5	8	0.770	2250	1.96	-2.0	1200	4.26
2.0	6	0.782	2435	1.79	-3.0	835	7.15
2.5	4.8	0.800	2635	1.64	-3.5	740	8.70
3.0	4	0.800	2780	1.54	-4.0	660	11.6
3.5	3.4	0.810	2965	1.44	-4.5	535	16.3
4.0	3	0.810	3100	1.37	-5.0	420	31.9

$S = 2 \times 6 = 12.0$, $g = 1.0$ and $s/g = 12.0$. The measured resistance is 2045 ohms and the equivalent resistance for the half slot 2045 - 300 = 1745 ohms and the permeance $p = 2 \times 319 \times 6/1745 = 2.19$ for the whole slot. From equation 2.2.2. when $s/g = 12$ and $p = 2.19$, $\alpha_E = (s/g - p)/p\ s/2g = 0.747$. From Fig. 5.2.1.1. values of α_E for the in-line

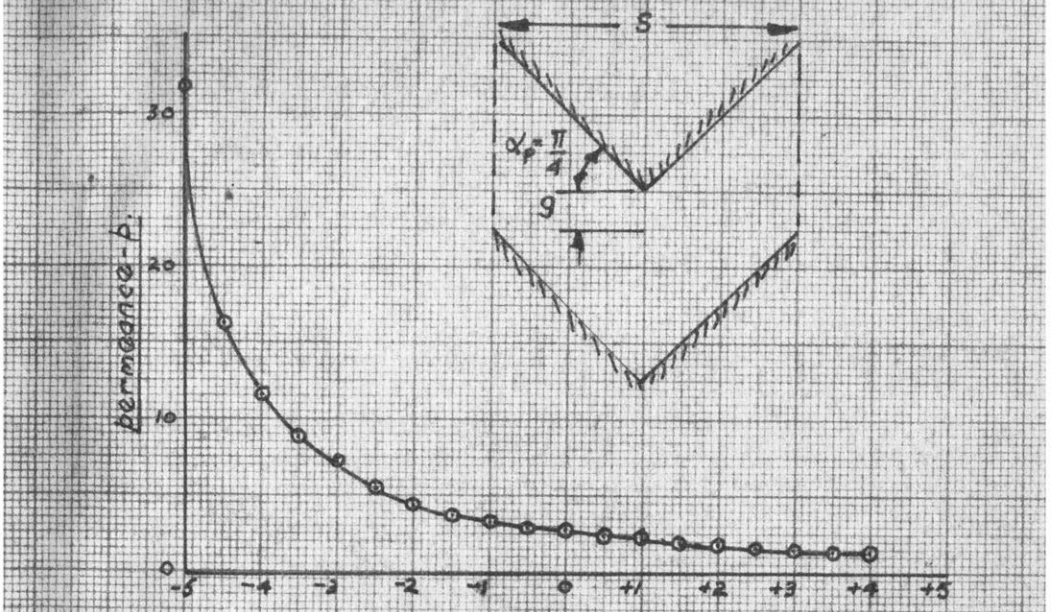

Fig. 5.2.3.1. (a)

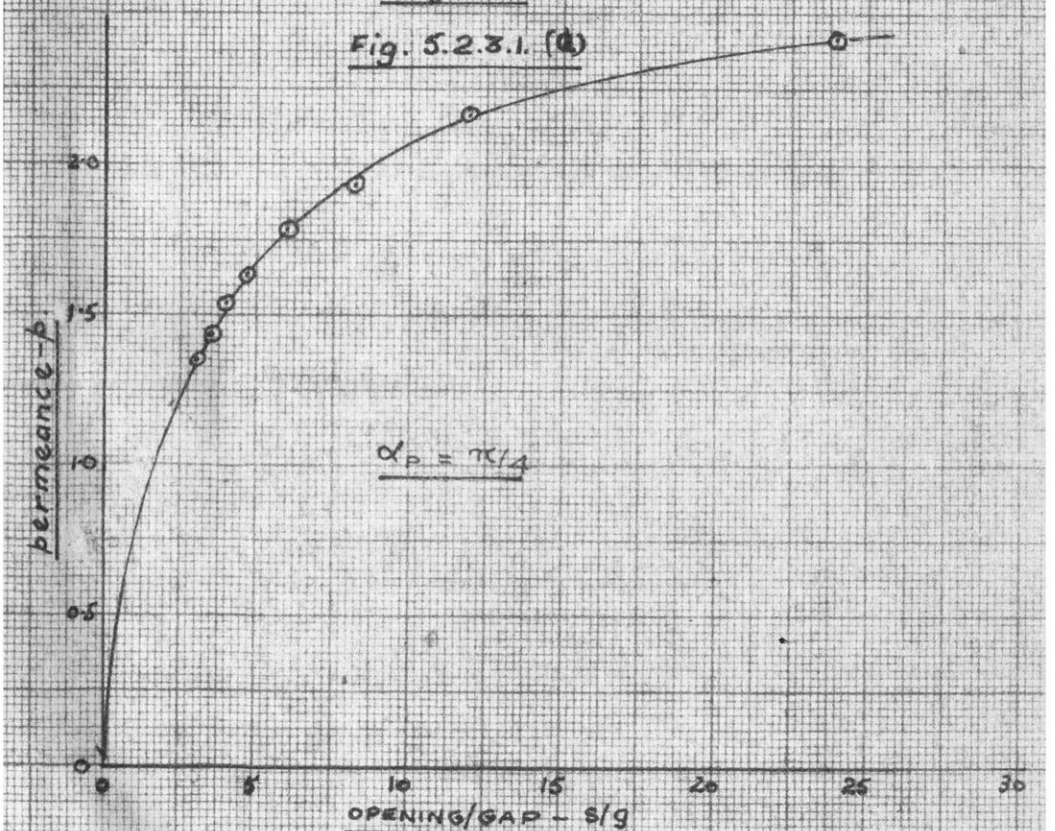

Fig. 5.2.3.1. (b)

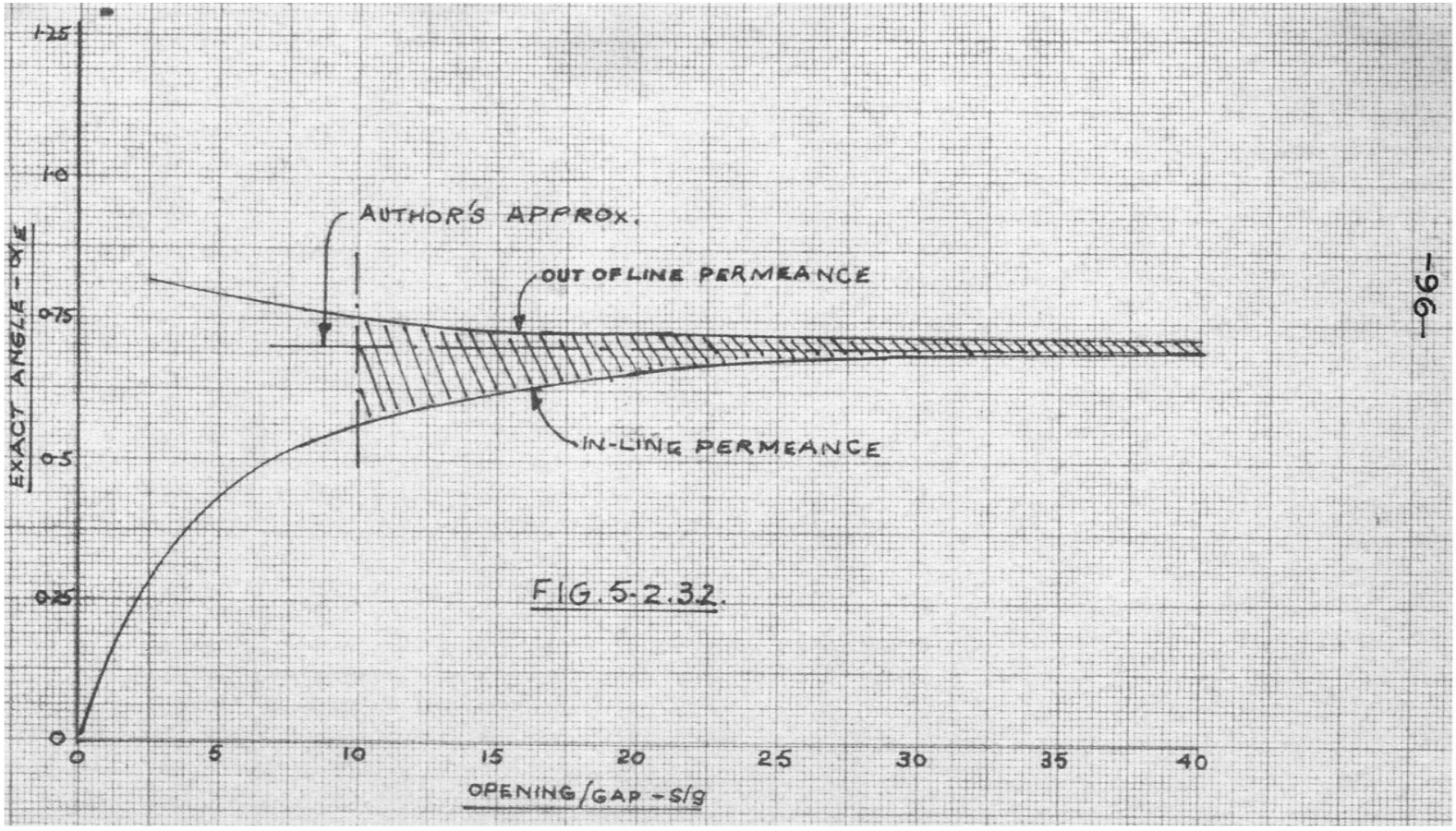
1·25
1·0
0·75
0·5
0·25
0
EXACT ANGLE - Ψ/E
AUTHOR'S APPROX.
OUT OF LINE PERMEANCE
IN-LINE PERMEANCE
0
5
10
15
20
25
30
35
40
OPENING/GAP - S/g

FIG. 5-2.32.

position are obtained and are plotted, together with those from table 5.2.3.1., in Fig. 5.2.3.2.. It will be noticed that there is some divergence between the in and out-of-line values though the divergence is not serious above $s/g = 10$. The best value of α for use with equation 2.2.3 is approximately as given by equation 5.2.1.1. but a better value for the exponent is $1.8 \alpha p/\pi$ so that for $\alpha p = \pi/4$, $\alpha = 0.7$ as shown in Fig. 5.2.3.2..

In dealing with trapezoidal teeth the value of α becomes less critical as t increases.

5.3. Trapezoidal Teeth.

It is evident that results for trapezoidal teeth will be intermediate between those for rectangular and triangular teeth for the same ratios s/d and s/g. There are two limiting conditions for trapezoidal teeth, one for $\alpha p = o$ and the other for $\alpha p = \pi/2$. Obviously when $\alpha p = o$, $2.2.1 \rightarrow (t+s)/g$ (by differentiation of numerator and denominator) and when $\alpha p = \pi/2$, $\alpha E = (0.70 + 0.06\ s/g)$ for $s/g < 10$ and 1.30 for $s/g > 10$. Hence αE will decrease from the $\pi/2$ value to zero in some manner as $\alpha p \rightarrow o$. A study is made in the following to determine the best value of α for use with the equations of section 2.

5.3.1. Practical Determination of Permeance.

As mentioned previously we have two check points, one for $\alpha p = o$ and the other for $\alpha p = \pi/2$. Assuming that $t \geq (s+4g)$ for the single-sided slot and $s/d \rightarrow o$, then the value of C from Fig. 5.1.4.1.1 applies to $\alpha p = \pi/2$ and when $\alpha p = o$, $p = (s+t)/g$. Intermediate values have been determined by graphical flux plotting for three values of s/g. In each case the air-space has been divided by three equipotential lines. The estimated error is +0.5 flux tube for the half-

Table 5.3.1.1.

s/g	t/s = 0.20						
10	p_o	12.0	4.0	8.0	7.0	6.5	-	5.34
	α_p	0.0	0.197	0.380	0.540	$\pi/4$	-	$\pi/2$
20	p_o	24.0	17.5	16.0	14.0	13.0	11.5	8.22
	α_p	0.0	0.100	0.197	0.291	0.380	0.54	$\pi/2$
32	p_o	38.4	21.70	17.50	15.90	14.64	12.91	11.28
	α_p	0.0	0.124	0.303	0.464	0.602	0.752	$\pi/2$

section, or +0.25 in terms of permeance. Table 5.3.1.2. has been calculated similar to and for comparison with the results for triangular teeth.

Table 5.3.1.2.

s/g	α_p	0	0.1	0.197	0.291	0.380	0.540	0.7854	1.571
20	p_s	20.0	13.5	12.0	10.0	9.0	7.5	6.0	4.22
20	C'	0.0	0.325	0.400	0.500	0.550	0.625	0.700	0.789
20	α_E	0.0	0.110	0.159	0.251	0.318	0.459	0.689	1.22
10	p_s	10.0	-	7.0	-	6.0	5.0	4.5	3.34
10	C'	0.0	-	0.300	-	0.400	0.500	0.550	0.666
10	α_E	0.0	-	0.190	-	0.310	0.502	0.635	1.13

Comparing the values in table 5.3.1.2. with those in table 5.2.2.1. it is evident that any differences in α_E and C' are within the limits of experimental error for the method used. Hence it is not possible to specify a separate theory for triangular and trapezoidal teeth. The values of α_E from table 5.3.1.2. are plotted in Fig. 5.2.1.2. and show that the linear approximation is better due mainly to the higher value of α_E when $\alpha_p = \pi/2$. As in the case of rectangular slots the result is accurate provided $t \geqslant (s+4g)$ for successive teeth and d(the slot depth) $>$ s. The slot depth does not need to be considered separately since the infinite depth slot is the natural limit as $\alpha_p \rightarrow \pi/2$.

5.3.2. Opposed Teeth.

When the teeth are opposed and in-line the value for α_E is obtained from table 5.1.4.1.1. for $2^s/g$ provided that $t \geqslant 4g$. If $o \leqslant t \leqslant 4g$, α_E may be obtained approximately from table 5.1.4.5. for $2^s/g$.

When the teeth are out-of-line and such that $t \geqslant (s+4g)$ the value of α_E is approximately the same as for the in-line condition. The approximation illustrated in Fig. 5.1.4.1.2. will thus provide the value of α_E for any position x. Hence the value of α for use with the equations of section 2 when $t \geqslant (s+4g)$ are :

$$\alpha_E = 0.70 + 0.06\,{}^s/g \quad ({}^s/g \leqslant 10),$$

$$\alpha_E = 1.30 \quad ({}^s/g \geqslant 10),$$

$$\alpha = 1.5\,\alpha_E\,(1 - e^{-1.9\,\alpha\, p/\pi}).$$

When $(s+4g) \geqslant t \geqslant o$ a better value of the exponent is $1.8\,\alpha\, p/\pi$.

5.3.3. Permeance of Approximate Trapezoids.

To obtain some fairly accurate results for comparative purposes the method set out in 4.7 is used. Two plots are given, Fig. 5.3.3.1.(a) taken from Schofield's paper [21] for $m/\ell = 3/4$ and Fig. 5.3.3.2.(b) as calculated from equations 4.7.12. to 4.7.15. for $m/\ell = 7/8$. Straight lines placed accurately on the equipotential lines produce a number of shapes approximating to trapezoids. Full details of the sections available from Fig. 5.3.3.1.(a) are given in Fig. 5.3.3.2. together with the permeance p for the complete single slot.

Calculations from plots (a) and (b) are given in tables 5.3.3.1 and 5.3.3.2. respectively.

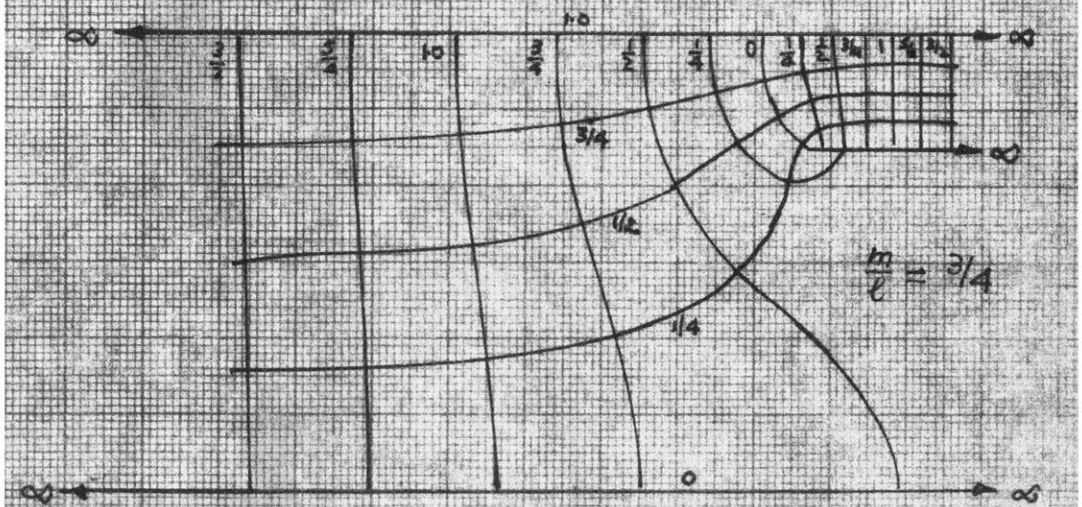

FIG 5.3.3.1.(a)

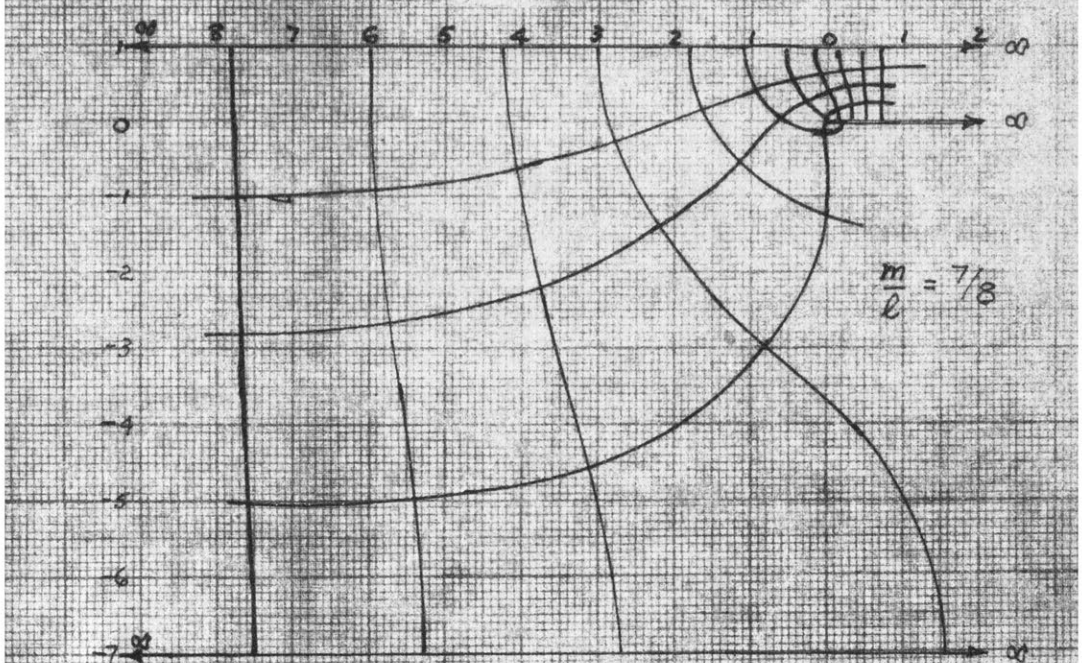

FIG. 5.3.3.1.(b)

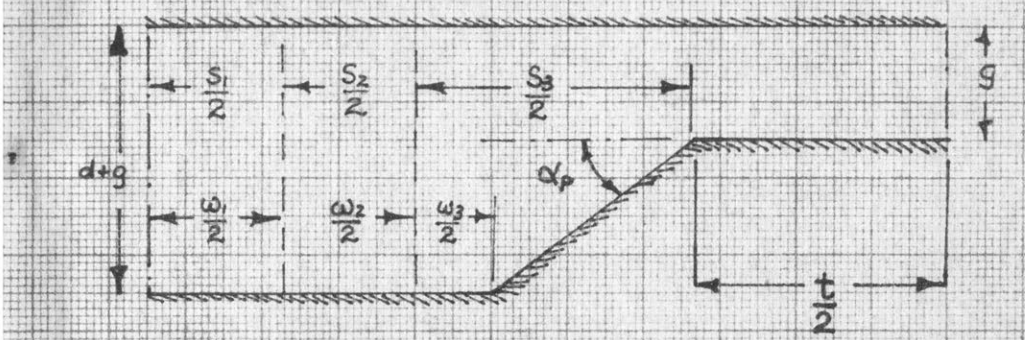

DETAILS FROM FIG. 5.3.3.1(a)

$\alpha_p = 13.5°$; $g = 7.0$; $d = 20.0$.												
S	$S_1 = 294$				$S_2 = 236$				$S_3 = 182$			
ω	$\omega_1 = 127$				$\omega_2 = 109$				$\omega_3 = 55$			
t	62	48	34	20	62	48	34	20	62	48	34	20
p	24	22	20	18	22	20	18	16	20	18	16	14
$\alpha_p = 31.5°$; $g = 14.0$; $d = 41.0$.												
S	$S_1 = 294$				$S_2 = 236$				$S_3 = 180$			
ω	$\omega_1 = 160$				$\omega_2 = 102$				$\omega_3 = 46$			
t	62	48	34	20	62	48	34	20	62	48	34	20
p	12	11	10	9	11	10	9	8	10	9	8	7
$\alpha_p = 56.3°$; $g = 22.0$; $d = 60.0$.												
S	$S_1 = 288$				$S_2 = 226$				$S_3 = 168$			
ω	$\omega_1 = 208$				$\omega_2 = 146$				$\omega_3 = 88$			
t	68	54	40	26	68	54	40	26	68	54	40	26
p	8	7.33	6.66	6.0	7.33	6.66	6.0	5.33	6.66	6.0	5.33	4.66

MEASUREMENTS IN 1/48'S INCHES

FIG. 5.3.3.2

Table 5.3.3.1.

s/g	42.0	33.7	26.0	21.0	16.9	12.9	13.1	10.3	7.6
w/s	0.432	0.462	0.302	0.544	0.432	0.255	0.723	0.646	0.523
t/g	8.86	8.86	8.86	4.43	4.43	4.43	3.09	3.09	3.09
p_s	15.14	13.14	11.14	7.57	6.57	5.57	4.91	4.25	3.57
α_p	0.235	0.235	0.235	0.549	0.549	0.549	0.982	0.982	0.982
α_E	0.235	0.253	0.270	0.465	0.502	0.554	0.702	0.740	0.770
C'	0.279	0.220	0.141	0.279	0.221	0.136	0.250	0.173	0.066
s/b									

Consider the first example in table 5.3.3.1, $s/g = 294/7 = 42.0$. The contribution by the t-region is $62/7 = 8.84$ so that the equivalent slot permeance, $p_s = 24 - 8.86 = 15.14$. From equation 1.4.1

$$p_s = \frac{2}{\alpha}\log_e(1 + \frac{\alpha s}{2g}); \quad C' = 1 - p_s/(s/2g); \quad \ldots\ldots \quad 5.3.3.1.$$

where C' is the equivalent Carter coefficient. For this example, $p_s = 15.16$, $\alpha_E = 0.235$ and $C' = 0.279$. Since the slot has some $\underline{w}$ at its base the previous results will underestimate the permeance, since from equation 5.2.1.1. with $\alpha_E = 1.31$ (for $s/g = 42.0$), $\alpha = 0.259$ or 0.249 with 1.8 in the exponent. This type of slot is outside the scope of this thesis and will not be considered further. A wide range of plots similar to Fig. 5.3.3.1.(a) and (b) is required to enable overall deductions to be made on the effect of $\underline{w}$. No doubt the equations of Section 2 could be varied to include $\underline{w}$ but the number of discontinuities would increase. A preferable method would be the determination of approximations similar to those given in this work for triangular slots. A suggested method is to determine a transfer constant k, where $k = \alpha_E'/\alpha_E$. A plot of this constant for the previous

Table 5.3.3.2.

s/g	62.4	48.0	34.0	22.0	29.4	22.3	15.4	20.8	15.1
w/s	0.397	0.217	0	0	0.510	0.354	0.062	0.600	0.449
t/g	9.6	9.6	9.6	9.6	5.0	5.0	5.0	3.07	3.07
p_s	14.4	12.4	10.4	8.4	7.0	6.0	5.0	7.13	5.33
α_p	0.334	0.334	0.334	0.350	0.690	0.690	0.690	0.977	0.977
α_E	0·334	0·362	0·386	0·400	0·690	0·750	0·773	0.522	0.690
C'	0.537	0.483	0.389	0.237	0.523	0.462	0.351	0.314	0.291

results is given in Fig. 5.3.3.3. The value α_E is the exact substitute angle for $\alpha_p = \pi/2$. Before commencing this it will be necessary to extend the results of Coe and Taylor[4] for shallow slots to obtain new values for α_E for large t.

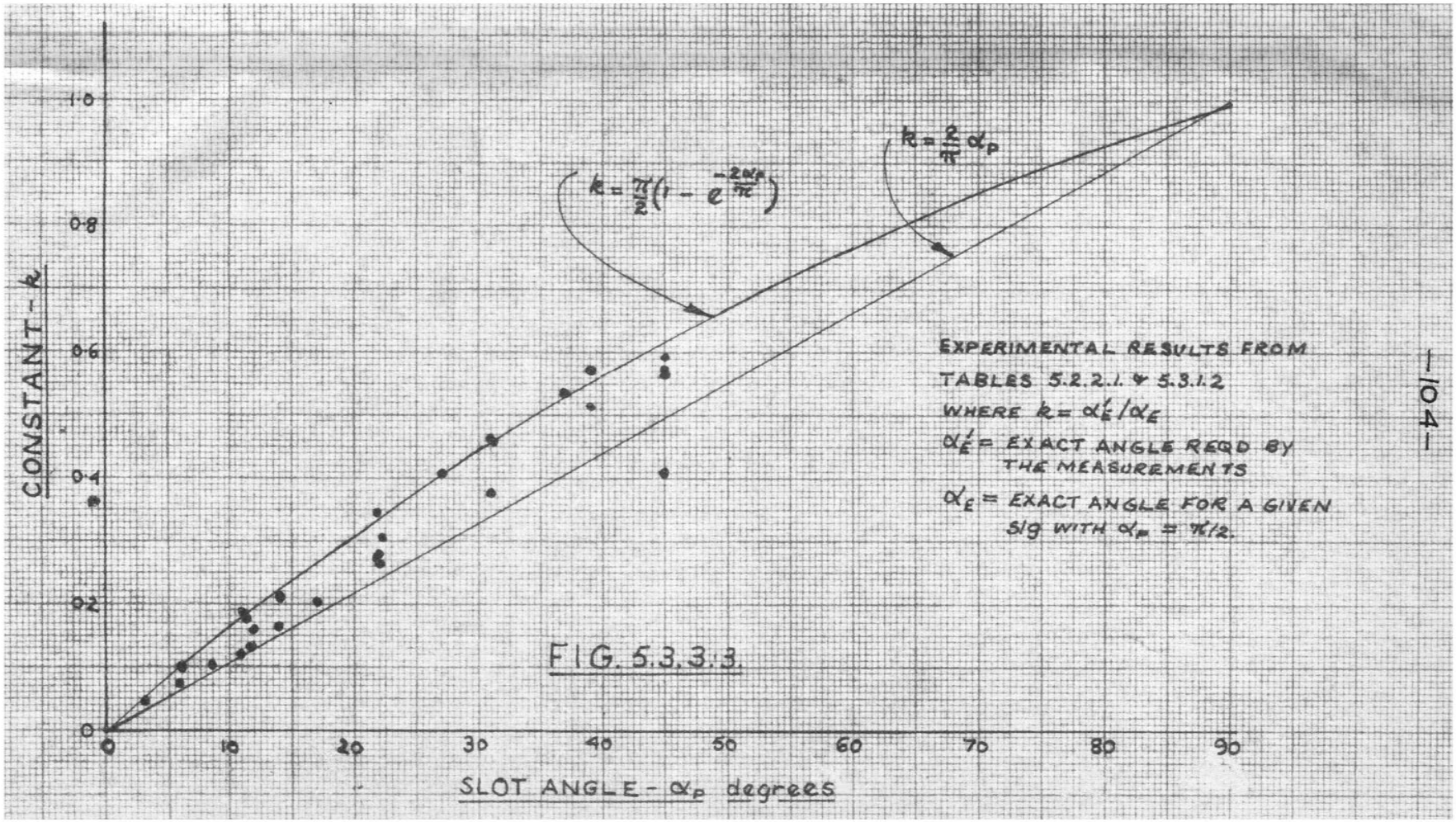
CONSTANT - k
1·0
0·8
0·6
0·4
0·2
0
0
10
20
30
40
50
60
70
80
90
SLOT ANGLE - α_p degrees
$k = \frac{\pi}{2}\left(1 - e^{\frac{-2\alpha_p}{\pi}}\right)$
$k = \frac{2}{\pi}\alpha_p$
EXPERIMENTAL RESULTS FROM
TABLES 5.2.2.1 & 5.3.1.2
WHERE $k = \alpha_E'/\alpha_E$
α_E' = EXACT ANGLE REQD BY
THE MEASUREMENTS
α_E = EXACT ANGLE FOR A GIVEN
S/G WITH $\alpha_p = \pi/2$.

FIG. 5.3.3.3.

SECTION 6.

PRACTICAL CONSIDERATIONS CIRCULAR TEETH.

6.1. General.

Any of the methods discussed in Section 3 may be applied to the circular tooth provided due allowance is made for any w which may exist at the base of the slot, particularly when $^{d}/_{s}$ is small. Only a few of the latter types of problem have been studied in Section 5 so confirmation of the methods used will be obtained from practical considerations.

Douglas' solution forms a limiting case for opposed circular teeth as well as providing an exact figure for the leakage permeance of circular poles. For example consider two parallel equipotential planes separated by a distance $(t + g)$ and extending to some large distance $(s + t)$. The permeance is $(s + t)/(t + g)$ due to the rectilineal distribution of flux. If we now interpose two opposed semicircular equipotential teeth of diameter t and separated by a distance g, the permeance is greater than $(s + t)/(t + g)$. The limiting condition occurs when potential is removed from the s portion so that flux originates on one semicircular tooth and terminates on the other, the limiting flux line being the parallel planes extending to infinity. The permeance in this latter case is obtained from Douglas' equation. It will be shown later how this result can be useful in estimating the accuracy of the experimental results.

A few cases only will be studied in this section, the first being the application of the substitute angle method to the leakage permeance of circular poles. Secondly some cases of opposed and displaced circular teeth will be studied in relation to the result for trapezoidal teeth from Section 5.

6.2. Circular Pole Leakage the Problem of Douglas and Hague.

Circular pole leakage does not fall into the same category of problems for which the substitue angle method was intended. However the equivalent trapezoid of 3.2.2. provides a simple solution to the problem. It will be shown that a substitute angle of 0.5 enables almost exact agreement to be obtained with Douglas' result when $t/(t + g) > 0.6$. Evidently equally good agreement could be obtained with a smaller value of α when $t/(t + g) < 0.6$. Considering the limiting condition of the evolute method (say) viz., $t/s = 1/(\pi/2-1)$ we obtain from 3.2.2.2.

$$t' = \frac{t}{4}\left(1 + \frac{2}{\sqrt{3}}\right),$$

$$t'' = t' \cos 30^{\circ} = \frac{t}{8}\left(\sqrt{3} + \frac{2}{\sqrt{3}}\right),$$

Hence,

$$g' = (t + g) - 2t'' = t\left[1 - \frac{\sqrt{3}}{4} - \frac{1}{2\sqrt{3}}\right] + g.$$

The equivalent permeance p_o is therefore

$$p_o = \frac{t'}{g'} + \frac{1}{\alpha}\log_e\left(1 + \frac{2\alpha t'}{g'}\right) \quad \ldots\ldots \quad 6.2.1.$$

A table (6.2.1) has been calculated for $t/(t + g)$ varying from 0.6 to 0.99 from equation 6.2.1. It will be appreciated that the normal ratio s/g has no meaning in this instance even though a value is implicit in equation 6.2.1..

Table 6.2.1.

$t/(t+g)$	0.6	0.8	0.9	0.94	0.97	0.98	0.99
t'	0.808	2.156	4.851	8.450	17.40	26.41	53.30
p_o	1.838	3.697	5.874	7.370	9.20	10.07	10.94

Table 6.2.2 has been calculated from Douglas' equation (1.3.6) and the results plotted in Fig. 6.2.1.1.

Table 6.2.2.

$t/(t+g)$	0.10	0.20	0.30	0.40	0.50	0.60	0.70
p_o	0.61742	0.84873	1.08735	1.36008	1.69344	2.12964	2.75190
$t/(t+g)$	0.80	0.85	0.90	0.91	0.92	0.93	0.94
p_o	3.75903	4.56144	5.77887	6.10346	6.46654	6.87555	7.33995
$t/(t+g)$	0.9461	0.95	0.96	0.97	0.9722	0.98	0.99
p_o	7.65555	7.87205	8.48803	9.20970	9.38543	10.0671	11.1030

Comparative results for the equivalent square with $\alpha = 1.0$ and for the equivalent trapezoid with $\alpha = \pi/3$ have been included in Fig. 6.2.1.1.. Both of these methods can be made accurate by reduction of α, but the author has chosen the second of these with $\alpha = 0.5$.

6.3. Opposed Teeth in Line.

Provided the results for trapezoidal teeth are accepted, the equivalent trapezoid of 32 will enable approximate values to be computed for opposed circular teeth in line. The author has compared these predictions with (a) resistance measurements on a scale model and (b) flux plotting on transformed models. The latter method was introduced because of marked variation between the results for the equivalent trapezoid and those for (a). The results for method (a)

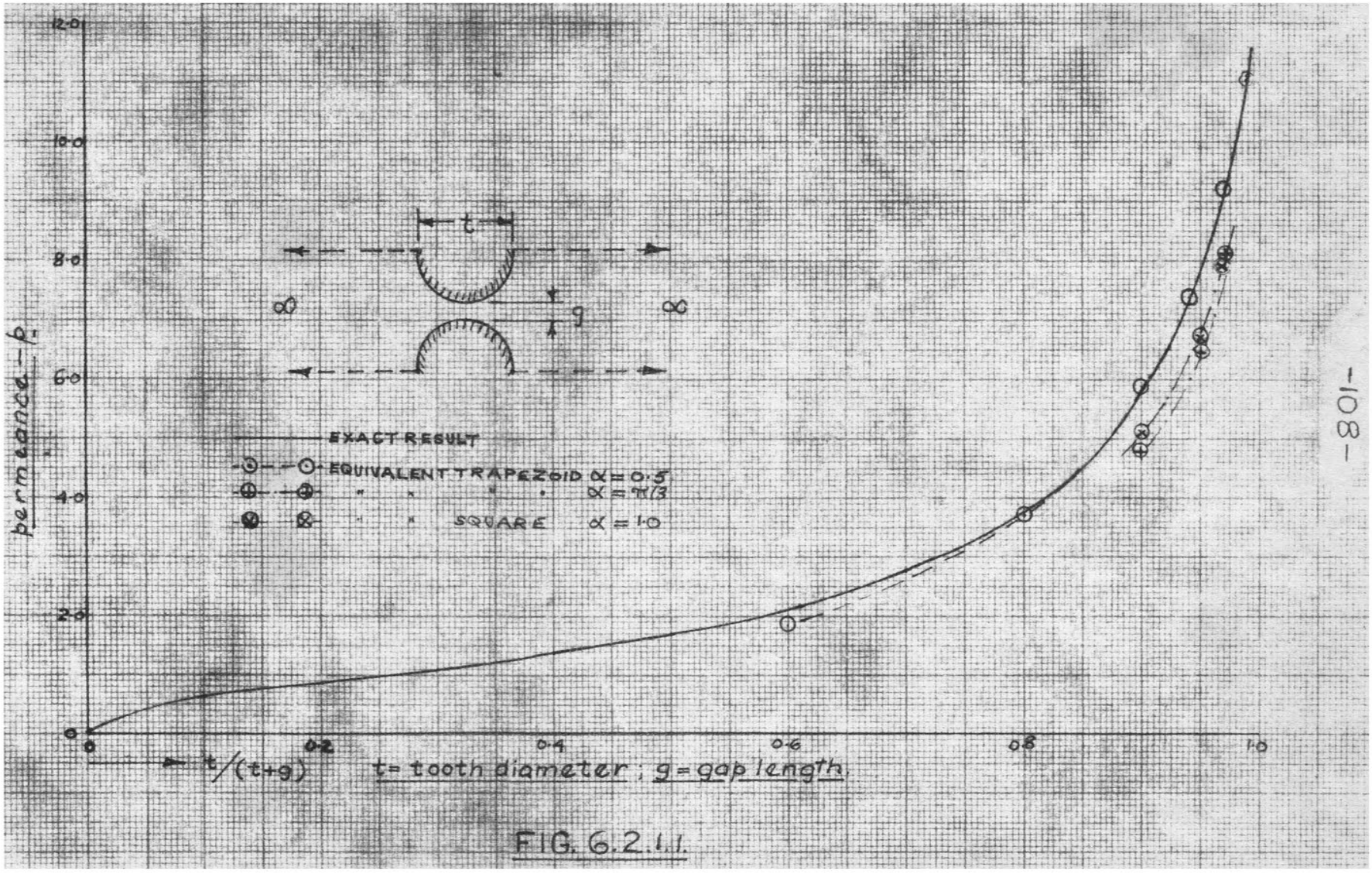
permeance - p.
12·0
10·0
8·0
6·0
4·0
2·0
0
0
0·2
0·4
0·6
0·8
1·0
t/(t+g)
t = tooth diameter ; g = gap length
t
g
∞
∞
EXACT RESULT
EQUIVALENT TRAPEZOID α = 0·5
" " " α = π/3
SQUARE α = 1·0

FIG. 6.2.1.1.

were assumed to be low for two main reasons, the first due to the thermal emf at the circular boundary causing a higher resistance than recorded, i.e., a smaller permeance, and the second due to the high current density near the centre-line of the opposing teeth. This latter effect is not expected to be large and could even cause a negative effect.

From 5.2.2., for trapezoidal teeth, the substitute angle for opposed teeth may be calculated approximately from

$$\alpha = 1.5\,\alpha_E\,(1 - e^{-1.8\,\alpha_p/\pi}) \qquad \ldots\ldots \quad 6.3.1.$$

where α_E is the exact substitute angle for rectangular teeth and α_p is the physical elevation of the tooth side. For the equivalent trapezoid $\alpha_p = \pi/3$, so that

$$\alpha = 1.5\,\alpha_E\,(1 - e^{-0.6}) = 0.677\,\alpha_E \qquad \ldots\ldots \quad 6.3.2.$$

The value of α_E corresponding to particular values of s'/g' (as defined for trapezoidal teeth) are obtained from Fig. 5.1.4.1.2, curve A. The approximate result for rectangular teeth taking account of out-of-line permeance will produce slightly different values for α_E (α_E') as follows :

$$\left.\begin{array}{l} \text{for } s'/g' < 10,\ \alpha_E' = 0.7 + 0.06\ s/g\,, \\ s'/g' > 10,\ \alpha_E' = 1.30\ . \end{array}\right\} \qquad 6.3.3.$$

The above values of α are recorded in table 6.3.1. where α_E is from Fig. 5.1.4.1.2.; α_E' from 6.3.3.; α from 6.3.2. for α_E and α' from α_E'.

Table 6.3.1.

s'/g'	5	10	15	20	25	> 25
α_E	1.13	1.24	1.29	1.31	1.31	1.31
α	0.764	0.839	0.872	0.887	0.887	0.887
$\alpha_{\frac{1}{E}}$	1.0	1.30	1.30	1.30	1.30	1.30
α'	0.677	0.880	0.880	0.880	0.880	0.880

The ratio s'/g' as given in table 6.3.1. must not be confused with the s/g ratio for circular teeth, which is defined with respect to the tooth diameter and the gap between the teeth. For the s/t ratio considered here variation of g or g' causes much smaller change in the s'/g' ratio than s/g.

Due to the finite slot depth inherent with this configuration the true permeance could be a little higher than that predicted by the equivalent trapezoid, but will almost certainly be compensated for by the variation from the true circular shape.

6.4. Practical Determination of Permeance.

Numerous methods were tried to determine the value of permeance. The method persevered with here was the measure of total resistance with fixed boundaries of brass on Teledeltos conducting paper.

The paper was calibrated using aluminium boundaries under a 7 lb. weight per 6" of boundary length. The measures of total resistance are given in Fig. 6.4.1. for a parallel strip 6" wide with various distances ℓ inches separating the boundaries. In drawing in the equivalent linear resistance there is seen to be considerable

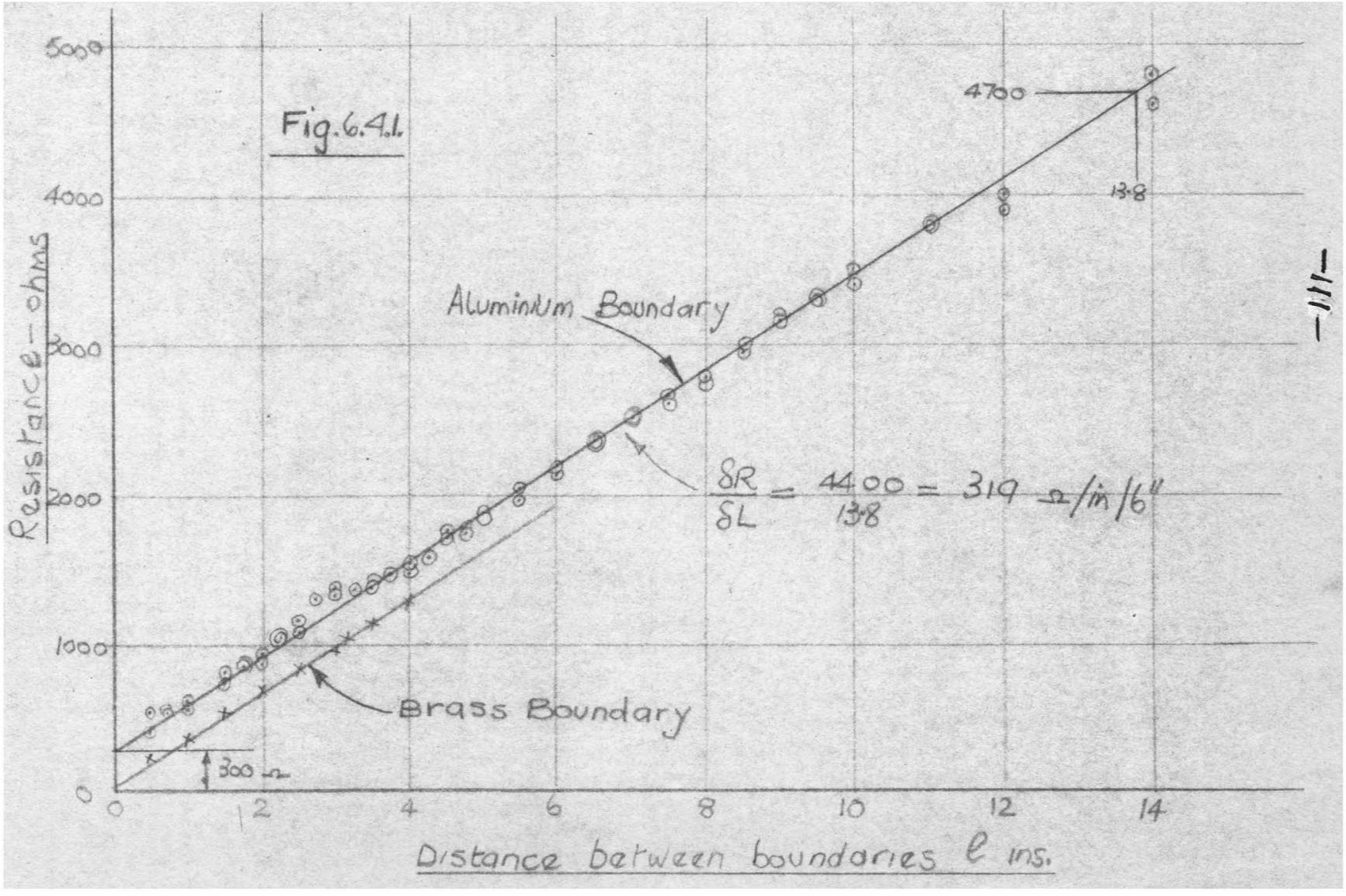
Fig. 6.4.1.
Resistance - ohms
5000
4000
3000
2000
1000
0
0
2
4
6
8
10
12
14
Distance between boundaries ℓ ins.
4700
13·8
Aluminium Boundary
Brass Boundary
300 Ω
δR/δL = 4400/13·8 = 319 Ω/in/16"

thermal e.m.f. at the boundaries corresponding to about 300 ohms. Numerous methods were tried to reduce this resistance; brass under considerable pressure was found to produce almost negligible e.m.f.. Incidentally, the graph for aluminium was taken with d.c. and the one for brass with a.c.. Resistance was measured on a comparative basis with a 1% decade box. Greater accuracy was not considered necessary since slight variations in boundary pressure could produce inaccuracies up to approximately ±3%.

6.4.1. Normally Shaped Models.

The results obtained from direct measurement on the models are given in table 6.4.1. for $t/s = 1.75$ (circular) and $t/s = 0.4$ (circular). The s/g ratio given in this table is the circular ratio; the ratio s'/g' is, as mentioned previously, the equivalent ratio for trapezoidal teeth. The results are plotted in Fig. 6.4.2.. Consider, for example, $s/g = 35.1$ and $t/s = 1.75$. The measured resistance was 221 ohms with no corrections for thermal e.m.f.. Hence, $P_o = 1914/221 = 8.7$ for the quarter section (as measured) which is the same as for the whole section. For this case t = 6.92" and s = 3.95", so that $t' = 0.539 \times 6.92 = 3.73$, $s' = 2 \times 3.73 = 7.46$ and $t'' = t' \cos \theta = 0.866 \times 3.73 = 3.23$. Therefore $g' = (t+g - 2t'')$ $= 7.032 - 6.46 = 0.57$ and $s'/g' = 7.46/057 = 13.05$. The remaining values are given in table 6.4.1. together with P_o' calculated from the equivalent value of α from table 6.3.1. or Fig. 6.3.1.

Table 6.4.1.

t/s = 1.75; t = 6.92"; s = 3.95"											
g	4.08	3.08	2.08	1.08	0.88	0.68	0.48	0.28	0.16	0.112	0.08
s/g	0.968	1.281	1.897	3.66	4.49	5.81	8.23	14.10	24.7	35.10	49.40
s'/g	1.64	2.10	2.93	4.83	5.57	6.53	7.93	10.1	12.0	13.0	13.8
R	1172	966	788	630	441	413	378	313	233	221	213
b_o	1.63	1.98	2.43	3.04	4.34	4.63	5.06	6.12	8.2	8.7	9.0
p_o'	-	-	-	4.45	4.94	5.66	6.79	7.72	8.89	9.44	9.47
t/s = 0.4; t = 6.72"; s = 16.92"											
g	5.08	3.08	2.08	1.08	-	0.68	-	0.28	-	-	-
s/g	3.33	5.49	8.13	15.65	-	24.85	-	60.3	-	-	-
s'/g	3.64	5.67	7.91	13.10	-	17.70	-	27.40	-	-	-
R	892	679	550	434	-	351	-	277	-	-	-
p_o	2.15	2.82	3.48	4.41	-	5.46	-	6.92	-	-	-

In all cases (for t/s = 1.75) p_o is seen to be both erratic and low, so a few transformed models will be studied to obtain greater accuracy.

6.4.2. Measurement on Transformed Models.

Using the method of 4.2. transformed areas are determined for various $t/(t+g)$. Models corresponding to different values of s/g can then be derived. The case for t = 20 and g = 1.0 is given in detail below.

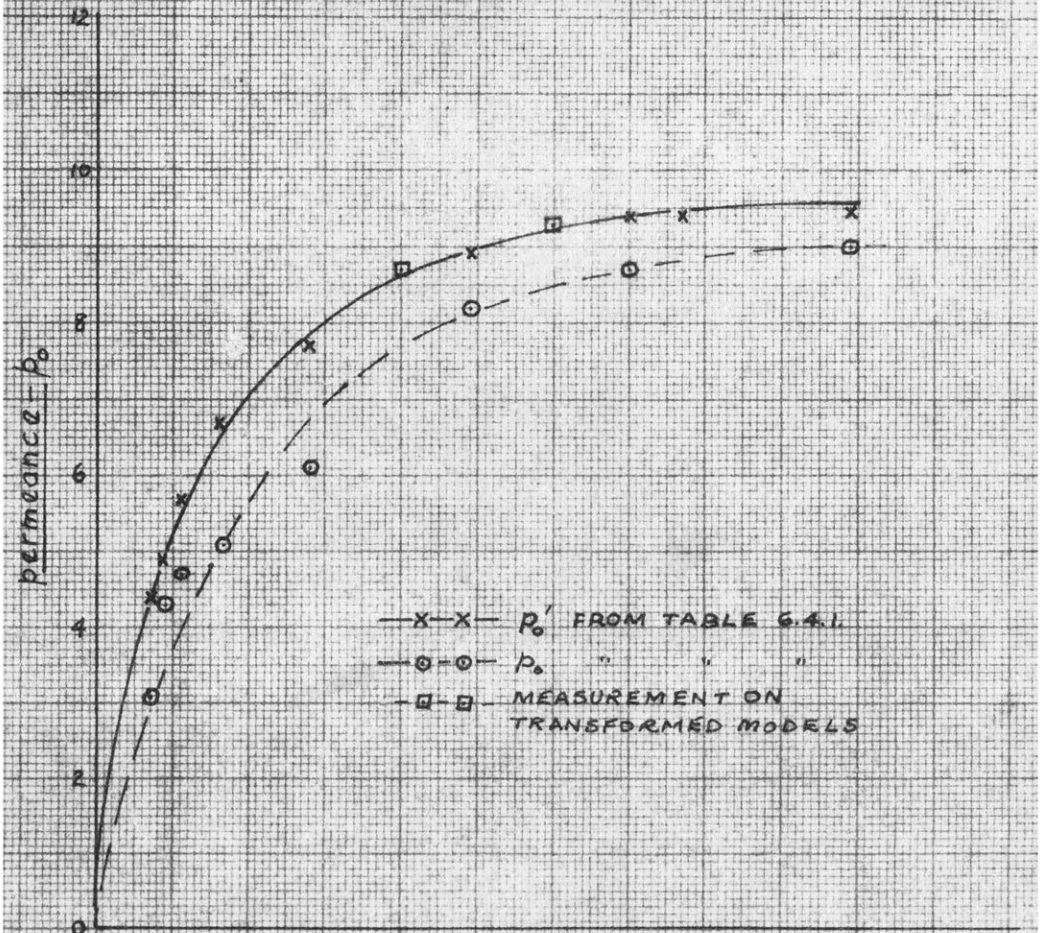
permeance = p_o
0
2
4
6
8
10
12
0
10
20
30
40
50
60
sig - (CIRCULAR)
—X—X— p_o' FROM TABLE 6.4.1.
—⊙—⊙— p_o " " "
—⊡—⊡— MEASUREMENT ON TRANSFORMED MODELS

FIG. 6.4.2.

From Fig. 6.4.2.1. and 4.2. the distance from the centre fitting a circle to the nearest pole is

$$b = \frac{H - \sqrt{H^2 - 4R^2}}{2} = 7.298435,$$

where $H = t+g = 21.0$ and $R = \frac{t}{2} = 10.0$. For the circle fitting the left tooth

$$u = \log_e \frac{r_1}{r_2} = \log_e \frac{H - R - b}{R - b}$$

$$= \log_e 1.370156 = 0.3149250.$$

In addition $a = (H-2b)/2 = 3.201562$. Dividing the semi-gap into nine equal parts we obtain

$$\delta u = \frac{0.314925}{9} = 0.0349917.$$

For the square network $\delta u = \delta v = (\theta_1 - \theta_2) = \alpha = 0.0349917$ radian = 2°.0'.17".6.. Hence values of x_k and R_k may now be calculated. Values of x_k are tabulated in Table 6.4.2.1., R_k may be constructed.

These results are plotted in Fig. 6.4.2.1. together with circles of radius $R_\alpha = \operatorname{cosec}\alpha$ and centre $y_\alpha = \operatorname{acot}\alpha$.

Preliminary resistance measurements taken on the transformed model (Fig. 6.4.2.2.) produced for $t/s = 1.75$, $\rho_o = 8.425$ and with the free edge method of Douglas, 8.36 for $t/s = 1.75$ and 8.06 for $t/s = 5.0$. A more precise measurement of the Douglas result with $t/s = 0$, produced the following for the transformed area :

$t = 20$; $g = 1.0$; $R = 2125$ ohms for the section of 6.4.2.2. from 0α to 19α. With the paper calibrated at 1914 ohm inches per inch $\rho_o' = 1914/2125 = 0.90$. For the remainder of the parallel strip $\rho_o'' = (89-19)/9 = 7.77$ and $\rho_o = \rho_o' + \rho_o'' = 8.67$. The value of

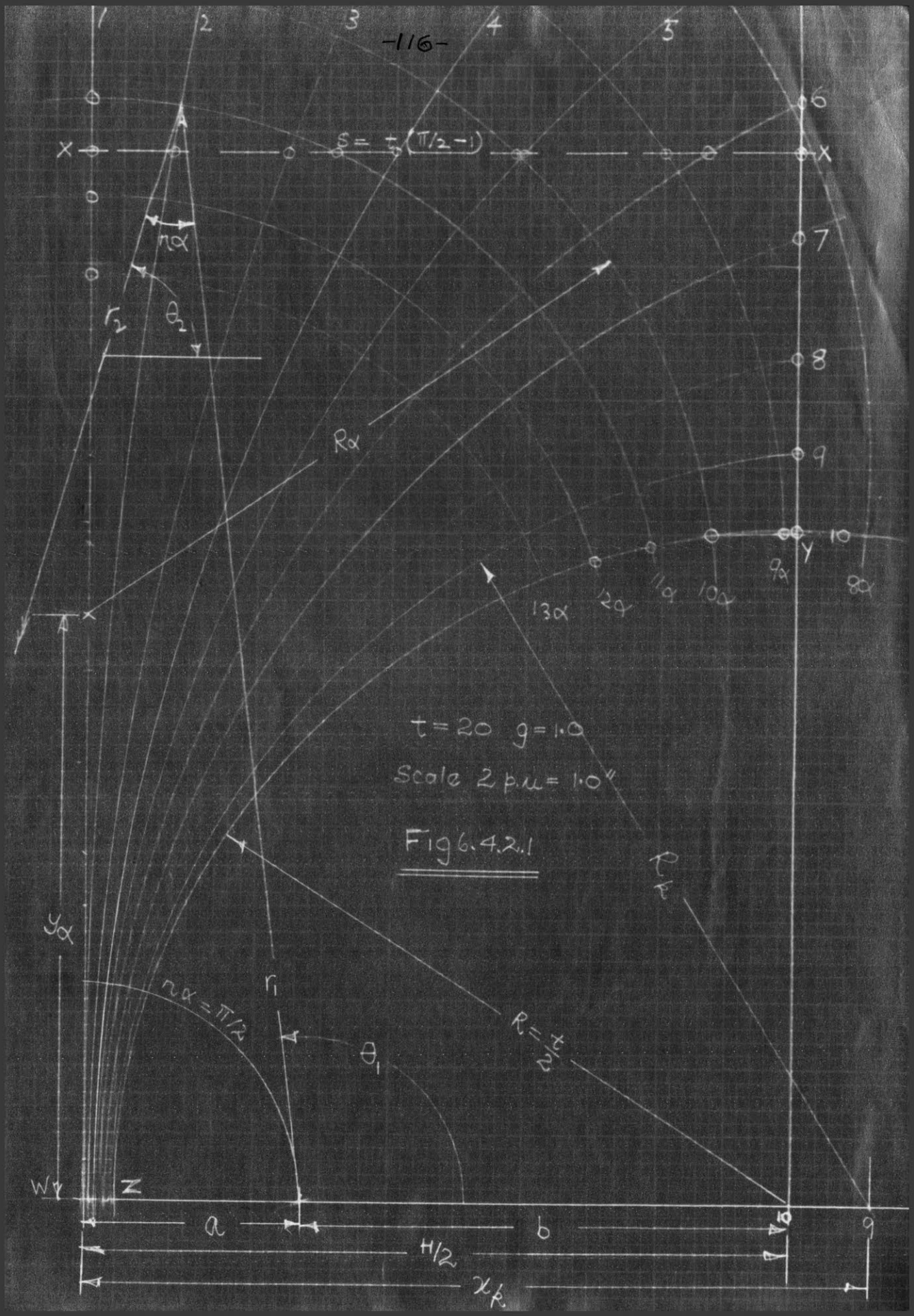
1
2
3
4
5
6
7
8
9
10
X
X
A
$S = \frac{1}{2}(\pi/2 - 1)$
$n\alpha$
r_2
θ_2
$R\alpha$
13α
12α
11α
10α
9α
8α
$t = 20$ $g = 1.0$
Scale 2 p.u = 1.0"
$y\alpha$
$n\alpha = \pi/2$
r_1
θ_1
$R = 2t$
r_E
W
Z
a
b
H/2
x_k

Fig 6.4.2.1

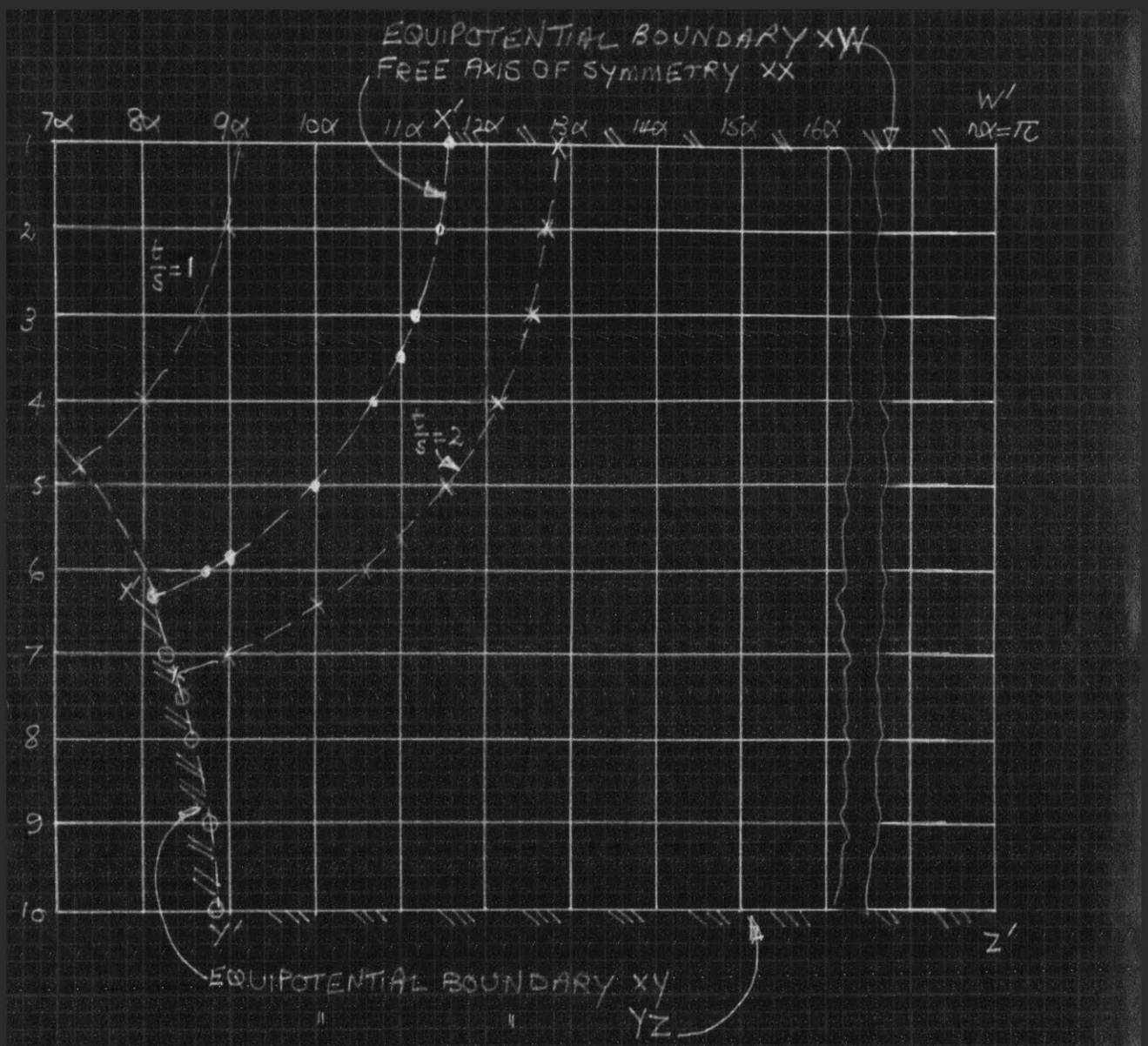

Fig 6.4.2.2. TRANSFORMED SHAPE OF FIG 6.4.2.1.

The line Y'X' continued to ∞α gives with no potential on Y'X' the true representation of the Douglas problem when g is small.

$t/(t+g)$ here is 20/21 = 0.9523 which from Fig. 6.2.1.1. gives Po = 8.4. The estimated maximum error from practical considerations is about 3% which agrees very well with Douglas' result.

Table 6.4.2.1.

Section	u	$e^u = k$	x_k
1	0	1.00	-
2	0.0349917	1.03561	91.837
3	0.0699833	1.07250	45.821
4	0.1049750	1.11100	30.610
5	0.1399667	1.15024	23.023
6	0.1749583	1.19120	18.485
7	0.2099500	1.233616	15.623
8	0.2449417	1.27754	13.331
9	0.2799333	1.32304	11.734
10	0.314925	1.370156	10.500

An additional model for larger $t/(t+g)$ has been calculated for a different number of sections. The details of the second model are given in Table 6.4.2.2..

Table 6.4.2.2.

t = 30.0; g = 1.0; b = 11.5948755; H = 31°0;
a = 3.9051245; α = 2°.27'.31".7

Section	u	$e^u = k$	k^2	x_k
1	0.0	1.00	1.00	-
2	0.0429144	1.043849	1.089620	91.055
3	0.0858288	1.089620	1.187272	45.611
4	0.1287432	1.127398	1.293675	30.430
5	0.1716577	1.187272	1.409613	22.970
6	0.2145721	1.239331	1.535942	18.478
7	0.2574865	1.293675	1.673594	15.500

The details were plotted similar to Fig. 6.4.2.1. and 6.4.2.2.. The transformed shapes were compared and found to agree. The results from these two models are recorded in Fig. 6.4.2. and agree very well with the results from the equivalent trapezoid.

6.5. Extension of Hague's Method.

It is possible (though not necessary here) to extend Hague's result as shown in 4.3.3..

An equipotential flow pattern is plotted in Fig. 6.5.1. from equation 4.3.3. for the case of $t/(t+g) = 0.5$. The pattern produced is within 1% of circularity and a few values extracted from this plot are given in Table 6.5.1.. These figures can be approximately extended by assuming linear flow beyond that shown in the figure.

Table 6.5.1.

t	1.5	1.5	1.5	1.5
$t/(t+g)$	0.5	0.5	0.61	0.61
s	1.5	2.28	1.5	2.28
t/s	1.0	0.658	1.0	0.658
s/g	1.0	0.76	0.782	1.19
Po	1.5	1.75	2.0	2.33

6.6. Out-of-Line Permeance.

In 6.4. good agreement was found between the in-line permeance and that predicted from the result for trapezoidal teeth. It is necessary to determine if the same assumptions apply to out-of-line teeth. By the method discussed in section 4, a bilinear transformation is applied to the case of $s/g = 20$; $t = 35.10$; which yields the

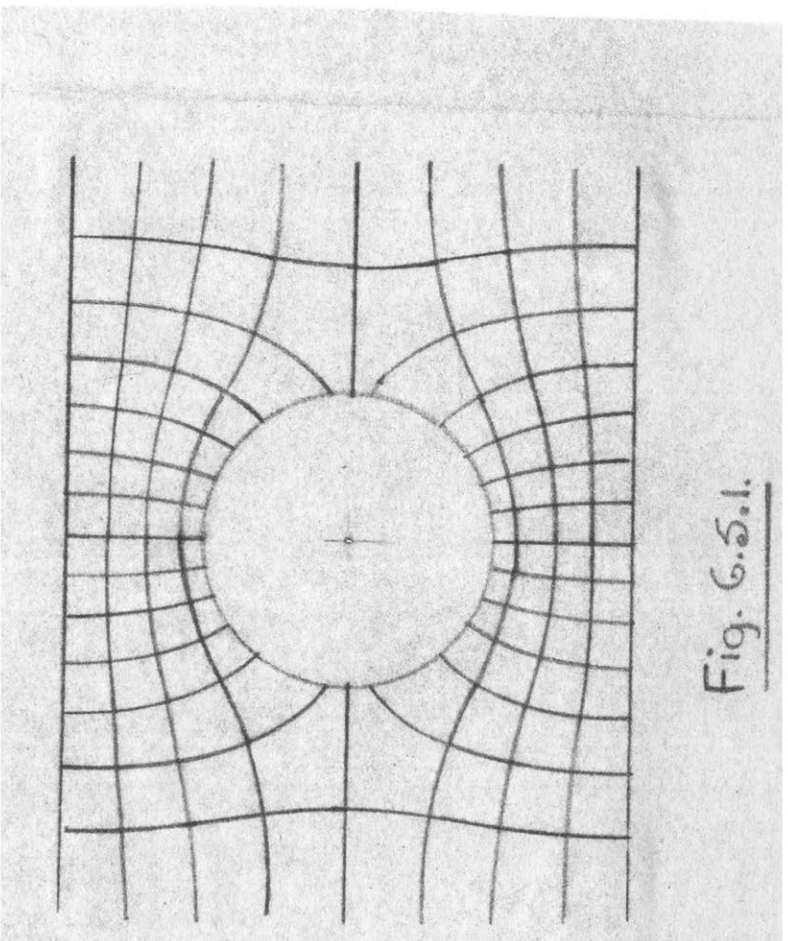

Fig. 6.5.1.

following :

$s = 20$; $g = 1.0$; $t = 35.10$; $g' = 10.311$;

$R = 17.55$; $b = 8.292$; $U = 0.7488$; $a = 14.413$;

$\delta u = \delta v = 0.14976^c = \alpha = 8°4'5"$.

Values of x_k are given in table 6.6.1. and the area plot in Fig. 6.6.2. The transformed area (Fig. 6.6.3) yields are approximate permeance of $(\pi/\delta v - 6)/10 = 1.5$ for each half. For both halves $p \doteq 3.0$. A resistance measurement on the transformed area of Fig. 6.6.3. produced a resistance of 2330 ohms or 0.825 for the quarter section, i.e., $p = 3.30$ which is close to the independent assessment above.

Table 6.6.1.

Section	u	k	k^2	x_k
1	0.0	1.00	1.00	-
2	0.14977	1.1616	1.3493	96.895
3	0.29955	1.3492	1.8204	49.530
4	0.44932	1.5672	2.4559	34.210
5	0.599096	1.8204	3.3139	26.870
6	0.74880	2.1145	4.4715	22.705

In comparing the results from the equivalent trapezoid the equations are

$$p = \frac{t' - s'}{g'} + \frac{4}{\alpha} \log_e \left(1 + \frac{\alpha\ s'}{2\ g'}\right)$$

for the equivalent square, and,

$$\frac{s' - t'}{g' + \alpha(s'-t')/2} + \frac{4}{\alpha} \log_e \frac{g' + \alpha s'/2}{g' + \alpha(s'-t')/2}$$

for the equivalent trapezoid. Figures for the equivalent square and the involute method are given in Table 6.6.2.

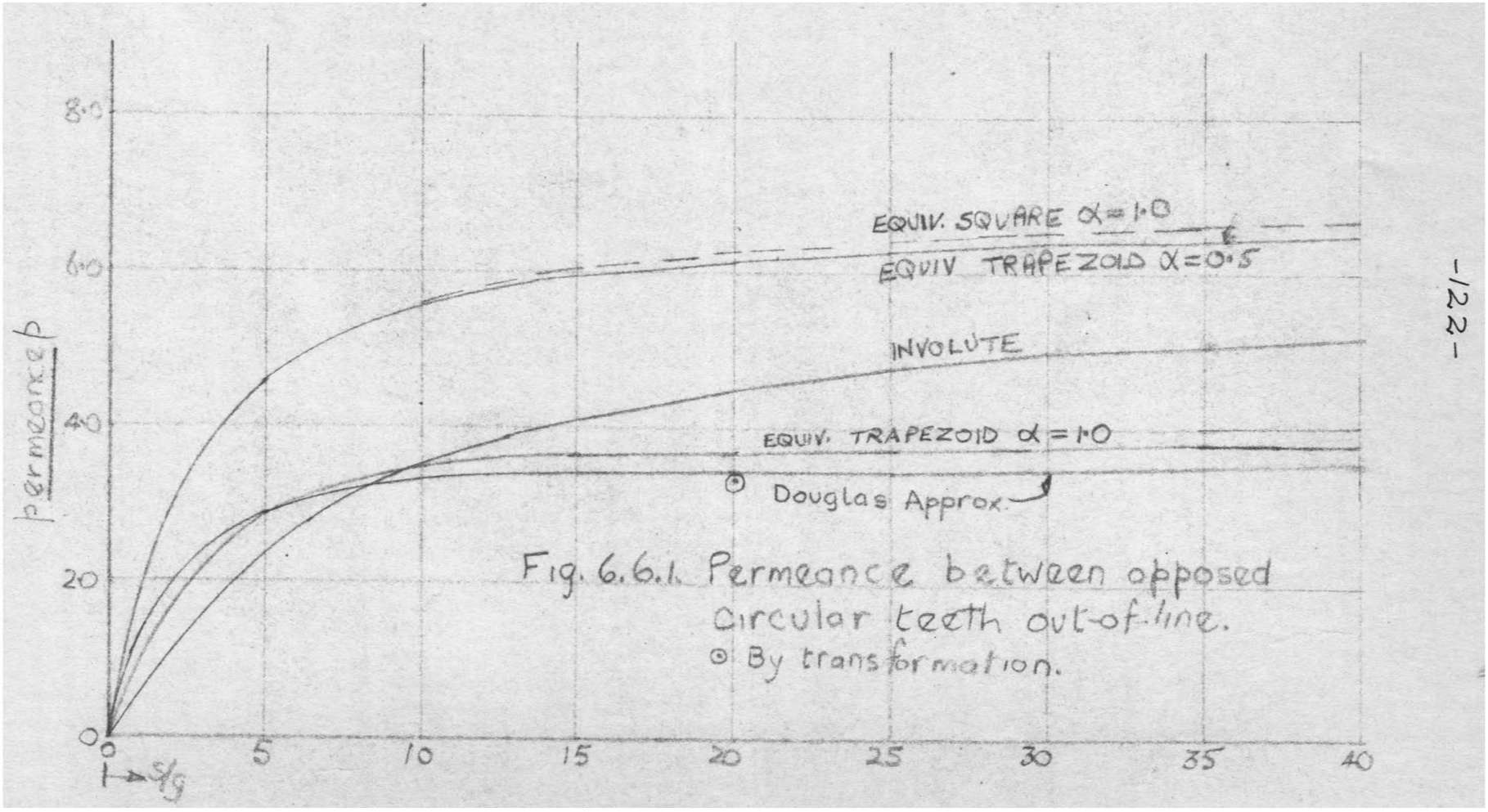

Fig. 6.6.1. Permeance between opposed circular teeth out-of-line.
⊙ By transformation.

Table 6.6.2.

Equivalent Square $g = 1.0$								
s/g	5	10	15	20	25	30	35	40
p $\alpha = 1.0$	4.48	5.57	5.95	6.25	6.39	6.57	6.66	6.80
	Involute							
p	2.42	3.48	4.07	4.46	4.73	4.93	5.06	5.19
	Douglas Approximation							
p	3.0	3.28	3.35	3.38	3.40	3.45	3.48	3.49

The Douglas approximation given in table 6.6.2. is a purely empirical result expressed in terms of s/g for a given ratio t/s. The permeance is obtained from Douglas' result for the corresponding ratio $t/(t+g)$.

For the equivalent trapezoid with $s/g = 20$; $t = 35.10$; $g = 1.0$, we obtain $t' = 0.539 \times 35.1 = 18.95$; $s' = 37.90$; $t'' = 0.866 \times 18.95 = 16.4$; $g' = 36.10 - 32.8 = 3.3$; $s'/g' = 11.48$. From Fig. 5.2.3.2. for $\alpha p = \pi/4$, α is approximately 0.75 from which for $\alpha p = \pi/3$, α is approximately 1.0. Hence $p = 3.693$, which compares favourably with the result obtained from the measurement on the transformed model.

Hence the equivalent trapezoid will give a good approximation to the permeance of opposed circular teeth, but further adjustment is necessary for the other methods. From table 6.3.1. $\alpha = 0.88$ is required for teeth in line when $s/g > 10$ and for teeth out-of-line $\alpha = 1.0$ throughout a wide range of s/g.

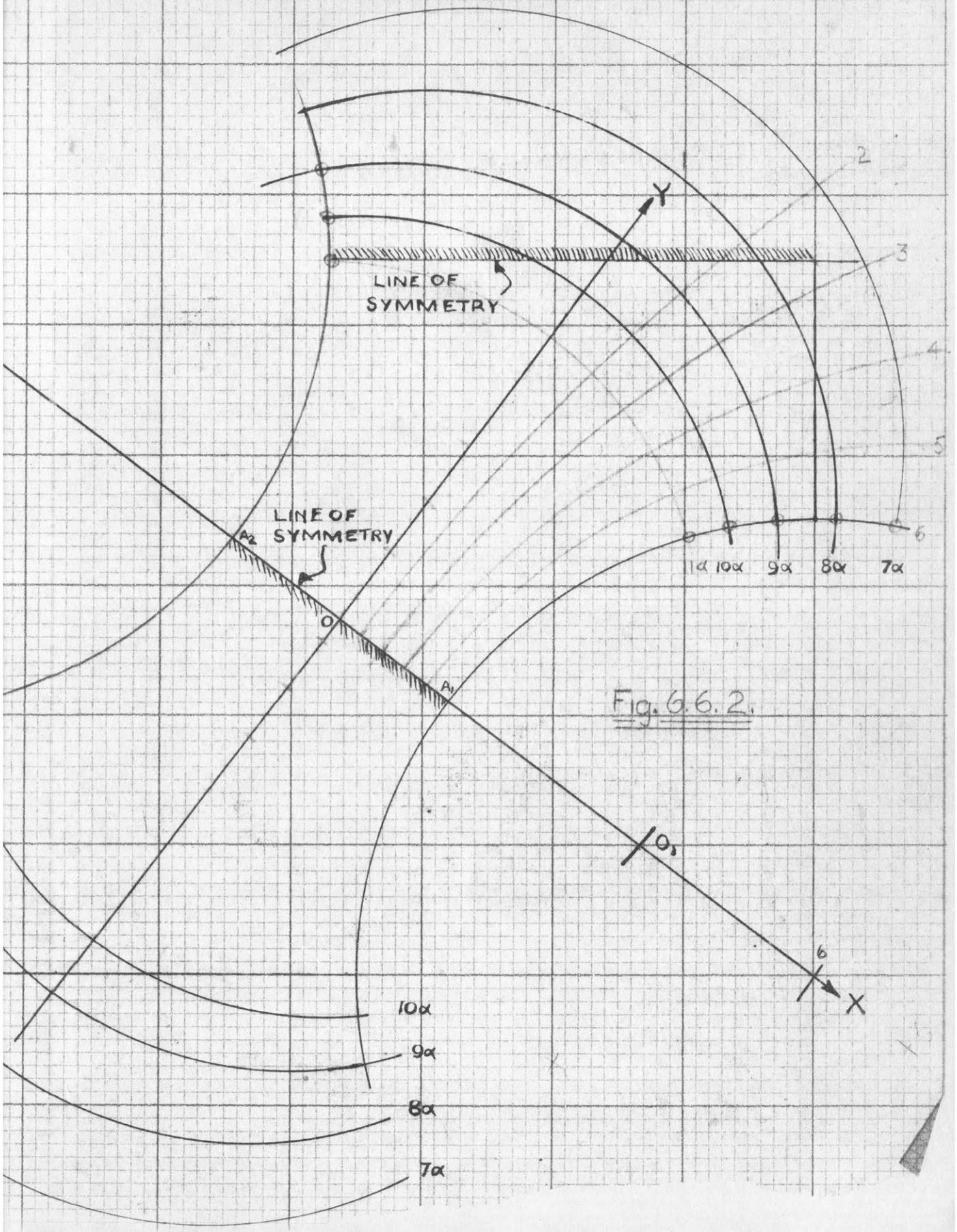
Y
2
3
4
5
6
LINE OF SYMMETRY
LINE OF SYMMETRY
A2
O
A1
1α 10α 9α 8α 7α
O1
6
X
10α
9α
8α
7α

Fig. 6.6.2.

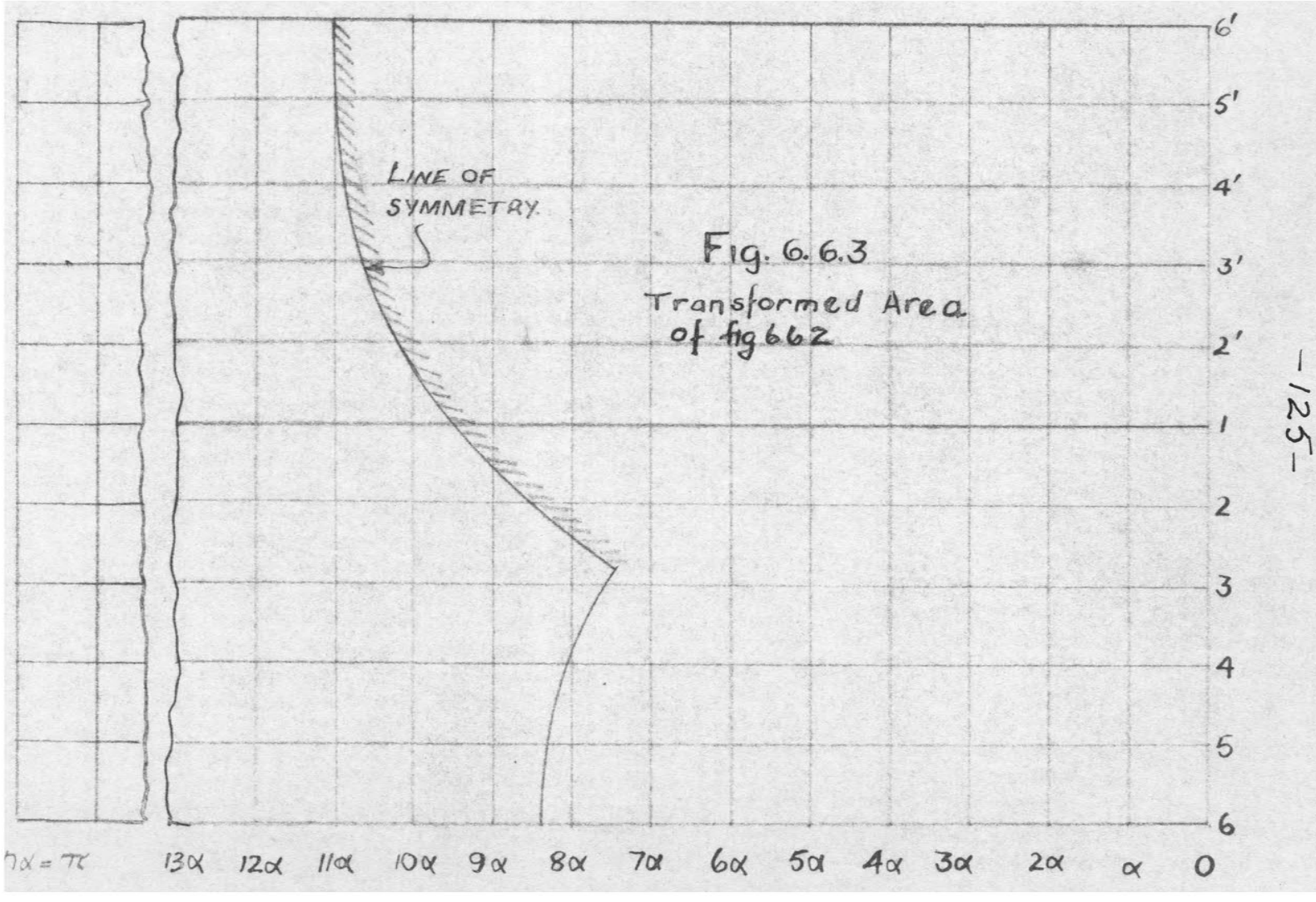

Fig. 6.6.3
Transformed Area of fig 662

SECTION 7.

BIBLIOGRAPHY.

7.1. References referred to in the text.

(1) University of London Thesis for Master of Science, 1925.

(2) Carter (a) J.I.E.E., p.925, Vol. 29.
(b) J.I.E.E., p.47, Vol. 34.
and, (c) Electrical World and Engineer, p.884, Vol. 38, November, 1901.

(3) Carter. J.I.E.E., p.1115, Vol. 64 and Electrician 1918, Vol. 81, p.400.

(4) Coe and Taylor. Some Problems in Electrical Machine Design involving Elliptic Functions. Philosoph. Mag. 1928, Vol. 6, p.120.

(4a) Also Hadamard. Finite Tooth Depth. Annales de Chemie et de Physique, 1909, Vol. 16, Ser. II, p.403.

(5) Clayton. Performance and Design of Direct Current Machines. Published by Pitman.

(6) Say. Design of Alternating Current Machines. Published by Pitman.

(7) Forbes. Journ. Soc. Telegr. Engs. (J.I.E.E.), p.551, Vol. 15, also Electrician, December, 1886.

(8) Cramp and Calderwood. J.I.E.E., p.1061, Vol. 61,

(9) Pohl. J.I.E.E., Vol. 93, pt. II, p.37.

(10) Arnold. Die Wechselstromtechnik, p.87, Vol. 4, 1913.

(11) Douglas. Trans. A.I.E.E., p.1067, Vol. 34, also Physical Review, p.391, Vol. 4, Series 2.

(12) Hague. J.I.E.E., p.1072, Vol. 61, [illegible].

(13) Pohl. J.I.E.E., p.1072, Vol. 93, Part II, 1946.

(14) Greig & Mukherji. J.I.E.E., Monograph 223S, 1957.

(15) Bondi & Mukherji. J.I.E.E., Monograph 225S, 1957.

(16) Chapman. "A Study of the Induction Motor"+ Published by Pitman, 1930, p.256.

(17) Walker, J.I.E.E., Part II, Vol. 89, 1943 and Vol. 93, 1946.

(18) Hancock. Production of a Sinusoidal Flux Distribution. J.I.E.E., Vol. 58, 1920, p.161.

(19) Liebmann. J.I.E.E., Monographs, Part C, March, 1957.

(20) Guy. British Patent Specn. 18027, 1901.

(21) Schofield. Philosophical Magazine Vol. 6, 1928, p.567. Also Vol. 10, 1930, p.480 and Vol. 12, 1931, p.329.

(22) Dixon. Elliptic Functions, publsihed by Macmillan, 1894, also Weber, Electromagnetic Fields, Vol. I, published by Wiley.

(23) Wieseman. Graphical Determination of Magnetic Fields. Jnl. A.I.E.E., Vol. 46, May, 1927, p.431.

(24) Gibbs. Conformal Transformations in Electrical Engineering. Published Chapman and Hall.

(25) Potier. For the first publication of a solution of a slotted armature and a plain surface in the study of the electrometer. Translation of Maxwell's Treatise, Vol. 2, 1889, p.563.

(26) Moore. Mapping Electric and Magnetic Fields Electric Journal, p.355, Vol. 23, July, 1926.

7.2. Electrolytic Analogue. Methods of Solving Field Problems.

(1) Ahmed. J.I.E.E., p.301, Vol. 62, 1924.

(2) Atkinson. Trans. A.I.E.E., p.971, Vol. 38, 1919 and p.966, Vol. 43, 1924.

(3) Baker. Plotting Electron Trajectories in Space - Charge Fields using the Electrolytic Tank. Proc. of the International Analogy Computation Meeting, 1955, p.314.

(4) Balachowsky and Tirroloy, Utilisation of the Electric Tank in Different Problems concerning High-Voltage Equipment. C.I.G.R.E., Paris, 1950, Paper No. 132, also Bulletin de la Societe Francaise des Electriciens, 1946, Vol. 6, p.181.

(5) Barkhausen and Bruck. Elect. Tech. Zeit., p.175, Vol. 54, 1933.

(6) Boothroyd. The Design of Electrolytic Wave Filters with the Aid of the Electrolytic Tank. J.I.E.E., p.65, Vol. 98, part IV, October, 1951.

(7) Bowman-Manifold and Nicholl. Nature, p.39, Vol. 142, July, 1938.

(8) Cheers, Raymer and Fowler. Preliminary Tests on Electric Potential Flow Apparatus. Aeronautical Tech. Report, NO2205, 1945. Dadda. The Electrolytic Tank of the Centre for the Study of Electrical Analogues.

(9) A survey of its Applications. L'Energia Elettrica, Vol. 28, 1951, p.23. (Contains an Exhaustive Bibliography), also Vol. 26, 1949, p.469.

(10) De Haller. Application of Electrical Anology to the Investigation of Cascades. Sulzer Technical Review, 1947, Vol. 3-4, p.11.

(11) Diggle and Hartill. Some Applications Electrolytic Tank to Engineering Design Problems. J.I.E.E., Vol. 101, Part II, p.349, 1954, also Metrop. Vickers Gazette, Vol. 26, No. 429, April, 1955, p.102.

(12) Douglas. Trans. A.I.E.E., p.982, Vol. 42, 1924.

(13) Einstein. Factors limiting the Accuracy of the Electrolytic Plotting Tanks. Brit. Journ. App. Phys., p.49, Vol. 2, February, 1951, also Journ. Scient. Inst., 1950, Vol. 27, p.27.

(14) Estorff. Electro. Tech. Zeit., p.60 and p.76, Vol. 37, 1916.

(15) Farr and Keen. Improving Field Analogues. Trans. A.I.E.E., Pt. 1, p.395, July, 1955.

(16) Farr and Wilson. Some Engineering Applications of the Electrolytic Field Analysed. Trans. A.I.E.E., 1951, Vol. 70, part II, p.1301.

(17) Fortescue and Farnsworth. The Electrolytic Trough. Trans. A.I.E.E., p.893, Vol. 32.

(18) Gelfard, Shinn and Tuteur. An Automatic Field Plotter. Trans. A.I.E.E., p.73, Pt. I, March, 1955.

(19) Green. Automatic Plotting of Electrostatic Fields. Review of Scientific Instruments, 1948, Vol. 19, p.646.

(20) Guébhard. Comptes Rendus de l'Académie des Sciences, 1880, Vol. 90, p.984; 1881, Vol. 93, pp.582 and 792; 1882, Vol. 94, pp.437 and 851; 1883, Vol. 96, p.1427. Journal de Physique, 1882, Vol. 1, p.205; 1883, Vol. 2, pp.87 and 335.

(21) Hartill. The Electrolytic Tank and its application to Engineering Design. Met. Vicks. Gaz., Vol. 24, April, 1942 and No. 10, July, 1953, also Bull. of Elect. Eng. Education No. 8, May, 1952.

(22) Hartill, McQueen and Robson. A Deep Electrolytic Tank for the Solution of 2 and 3. Dimensional Field Problems in Engineering. J.I.E.E., 1957, Vol. 104, pp.401 and 459.

(23) Hele-Shaw, Hay and Powell. Hydrodynamical and Electromagnetic Investigations Regarding the Magnetic Flux Distribution in Toothed-Core Armatures. J.I.E.E., p.21, Vol. 34, 1904.

(24) Holloway. An Electrolytic Tank Equipment for the Determination of Electron Trajectories, Potential (Vol. 103, p.155) and Gradients. Proc. IEE, Paper No. 1837M, May, 1955.

(25) Hubbard. Application of the Electrical Analogy in Fluid Mechanics Research. Review of Scient. Instruments, Vol. 20, No. 11, November, 1949, p.802.

(26) Kuhlmann. Hockspannungisolatoren. Archiv. fur Elektrotechnik, 1915, Vol. 3, p.203.

(27) Kusenose. Proc. I.R.E., p.1726, Vol. 17, 1929.

(28) McDonald. The Electrolytic Analogue in the Dewign of High Voltage Transformers. J.I.E.E., Vol. 100, Pt. II, p.145, 1953 paper No. S 1363, also C.I.G.R.E., Paris, 1950, Vol. 1, p.265.

(29) Mach. Annalen der Physik und Chemie. 1882, Vol. 17, p.257.

(30) McNall and Janssen. An Electrolytic Analogue Applied to the Solution of a Thermal Conduction Problem. ASME Preprint No. 54-SA-45, June, 1954.

(31) Mahar, Boothroyd and Cherry. An Electrolytic Tank for Exploring Potential Field Distribution. Nature, p.845, Vol. 161, 1948, also J.I.E.E., 1949, Vol. 96, Pt. I, p.163.

(32) Malavard. Use of Rheo-Electrical Analogies in Certain Aerodynamical Problems. Journal Royal Aeronautical Society, Vol. 51, 1947.

(33) Malavard and Miroux. Electrical Analogies for Heat Transfer Problems. The Engineers Digest, Vol. 13, December, 1952, p.416.

(34) Michall and Janssen. An Electrolytic Analogue Applied to the Solution of a Thermal Conduction Problem. A.S.M.E., print No. 54-SA-LS, June, 1954.

(35) Mickelson. Automatic Equipment and Techniques for Field Mapping. General Electric Review, Vol. 52, 1949, p.19.

(36) Moore. Fields from fluid flow mappers. Journ. App. Phys. p.790, No.8, Vol. 20, August, 1949. Trans. A.I.E.E., Vol. 71, 1952, Vol. 71, 1952 Journ. App. Mechs. A.S.M.E. Vol. 72, September, 1950 p.291.

(37) Nobite. Annalen der Physik und Chemie, 1827, Vol. 9, p.183; 1827, Vol. 10, p.392.

(38) Pères and Malavard. La Méthode d'Analogies Reographiques et Rhéometriques. Bulletin de la Société Francaise des Electriciens, Vol. 8, 1939, p.715.

(39) Relf. An Electrical Method for Tracing Lines in the Two-Dimensional Motion of a Perfect Fluid. Philosoph. Mag., Vol. 48, September, 1924.

(40) Sander. A new Form of Electrolytic Tank. J.I.E.E. Monographs Part C, March, 1957.

(41) Sander, Oatlay and Yates. Factors the Design of an Automatic Electron-Trajectory Tracer, J.I.E.E., 1952, Vol. 99, Pt. III, P.169.

(42) Sander and Yates. Accurate Mapping of Electric Fields in an Electrolytic Tank. J.I.E.E., p.167, part II, Vol. 100, 1953, also Vol. 104, Part C, p.81, 1956.

(43) Simpson. Scanning Device for Electrolytic Tank Field Plotting, Rev. Scient. Inst., p.37, Vol. 12.

(44) Some applications of the Electrolytic Field Analyser. Trans. A.I.E.E., p.416, Vol. 70(2), 1951.

(45) Sunatani, Matuyama and Hatamura. The solution of torsion problems by means of a liquid surface. Tech. Reports of Tokohu Imperial University, p.374, Vol. 12, 1938.

(46) Theile and Himpan. Die Auswahl des Elektroden - Material fur die Feldbildaufnahme im elektrolytisehen Trog. Die Telefunkenrohre, 1940, Vol. 18, p.50.

(47) Voigt. Annalen der Physik und Chemie. 1882, Vol. 17, p.257.

(48) Wedmore. J.I.E.E., p.568, Vol.61, 1923.

(49) Willoughby. Some Applications of Field Plotting. J.I.E.E., 1946, Vol. 93, Pt. III, p.275.

(50) Zschadge. Elect. Tech. Zeit., p.1215, Vol. 46, 1925.

7.3. References to Numerical and Graphical Methods of Solution of Field Problems.

(1) Allen. Relaxation Methods. New York, McGraw-Hill, 1954.

(2) Analogue Calculating Machine for Functions of a Complex Variable. Nature p.687, Vol. 163, 1949.

(3) Battistini. Lehman's Method for Graphical Determination of Magnetic Fields. Electrotechnico, p.267, Vol. 36, 1949.

(4) Bewley. Two-Dimensional Fields in Electrical Engineering. New York. The Macmillan Co., 1948.

(5) Bickley. Experiments in Approximating to the Solution of Partial Differential Equations. Phil. Mag., p.50, Vol. 32, July, 1941.

(6) Bickley. Finite Difference Formulae for the Square Lattice. Quart. Journ. Mech. App. Maths. p.35, Vol. I, March, 1948.

(7) Cheers, Raynor and Fowler. Preliminary Tests on Electric Potential Flow Apparatus. Aero. Res. Council Tech. Report, No. 2205, 1945.

(8) Christopherson and Southwell. Relaxation Methods Applied to Engineering Problems. Proc. Roy. Soc., p.317, Vol. A.168, 1938.

(9) Crowley-Milling. An analogue Computer for Sowing the Equations of Motion in Particle Accelerators. Journal Internationales de Calcul. Analogique, 1956, p.257.

(10) Dellenbaugh. Direct Recording Method of Measuring Magnetic Flux Distribution. Journ. A.I.E.E., p.583, Vol. 39, 1920.

(11) Djang. A Modified Method of Iteration of the Picard Type in the Solution of Differential Equations. Journ. Franklin Inst., p.453, December, 1948.

(12) Domb. On the Iterative Solutions of Equations. Proc. Camb. Philosoph. Soc., p.237, Part II, Vol. 45, 1949.

(13) Douglas and Kane. Potential Gradient and Flux Density. Trans. A.I.E.E., p.982, 1924.

(14) Drisinberre. Numerical Analysis of Heat Flow. New York, McGraw-Hill, 1949. Also Trans. ASME, Vol. 67, No. 8, 1949, p.703.

(15) Eddy. Stability in the Numerical Solution of Initial Value Problems in Partial Differential Equations. U.S. Naval

(15) Contd.
Ordnance Lab. Memo. 10232, October, 1949.

(16) Ell. New Method to Illustrate Direction and Density in an Electric Field by means of Sensitized Paper or Plates. Tekn. Tidskr. (Elektr.), p.49, Vol. 51, April, 1952.

(17) Ellerbrock, Schum and Nachtigall. Use of Electric Analogs for Calculation of Temperative Distribution. NACA TN No. 3060, December, 1953.

(18) Emmons. The Numerical Solution of Heat Conduction Problems. Trans. ASME, Vol. 65, No. 6, 1943, p.607. Also Partial Differential Equations. Quart of Applied Maths Vol. II, No. 2, 1944, p.173.

(19) Factors Influencing the Design of a Rubber Model. Discussion and Demonstration of Other Methods of Solving the Laplace Equation J.I.E.E., p.439, Part II, Vol. 97, August, 1950.

(20) Fox. A Short Account of Relaxation Methods. Quarterly Journal of Applied Mathematics, p.253, September, 1948.

(21) Fowler. Analysis of Numerical Solutions of Transient Heat Flow Problems. Quart. of App. Maths., Vol. 3, No. 4, 1945, p.361.

(22) Freeman. Relaxation Methods in Electrical Engineering, Electrical Times, p.751 and p.799. Vol. 116, 1949.

(23) Fremlin, Hall and Shafford. Triode Amplification Factors, Elect. Commun., Vol. 23, No. 4, p.426, 1946.

(24) Frocht. "Photoelasticity". Published by Wiley, Vol. II, 1948.

(25) Frocht and Lenin. A rational Approach to the Numerical

(25) Contd.
Solution of Laplace's Equation, Journ. Appl. Physics, Vol. 12, p.596, August, 1941.

(26) Gonarko. Calculation of Electric and Magnetic Fields by Potential Networks. Electrichestvo, p.52, No. 3, March, 1949.

(27) Hartree. Notes on the Iterative Processes. Proc. Camb. Phil. Soc., p.230, Vol. 45, Part II, 1949.

(28) Kormes. Numerical Solution of the Potential Equation by means of Punched Cards. Rev. Sci, Instrum Vol. 14, 1943, p.248.

(29) Kayan also Refrigeration Engineering, Vol. 51, June, 1946, pp.533, 568, 574 and 582.

(30) Kayan. An Electrical Geometrical Analogue for Complex Heat Flow. Trans. ASME, Vol. 67, No. 8, November, 1945, p.713 also Vol. 71, 1949, p.9.

(31) Lehmann. Graphical Method for Determining Path of Lines of Force in Air. E.T.Z., p.995 and p.1019, Vol. 30, 1909, also La Lumiere Electrique, Vol. 8, October-November, 1909, La Revue Generale de l'Electricite, Vol. 14, September, 15 and 22, 1923 and January, 9 and 16, 1926.

(32) Liebman. Precise Solution of Partial Differential Equations by Resistance Networks. Nature, p.149, Vol. 164, 1949.

(33) Liebmann. Solution of Partial Differential Equations with a Resistance Network Analogue. Brit. Journ. App. Phys., p.92, Vol. 1, 1950, also, Sitzungsberichte der Math. Phys. Klasse der Bayer. Akad., Munchen, p.385, 1918.

(34) Lutz. Graphical Determination of Wall Temperatures for Heat Transfer Through Walls of Arbitrary Shape. NACA TM No. 1280 Washington 1950, also R.T.P. Translation No. 2500 Calif. Inst. of Tech.

(35) McGivern and Supper. A membrane Analogy Supplementing Photo-elasticity. Trans. ASME, Vol. 56, 1934, p.601.

(36) Malavard. L'Analogie électrique comme méthode auxiliare de la photo-élasticité. Compt. rend., Paris, Vol. 206, p.38, 1938.

(37) Maheal. An Assymetrical Finite Difference Network. J.I.E.E., p.295, Part II, 1953.

(38) Mises, Vieweg and Sohn. "Differential and Integral Gleichungen der Mechanik und Physik", Berlin, 1950.

(39) Moore. Mapping Electric and Magnetic Fields. Electric Journal, p.355, Vol. 23, July, 1926.

(40) Moore. Fundamentals of Electrical Design. Published by McGraw-Hill Book Co., Inc., New York, 1927.

(41) Morse and Feshbach. Methods of Theoretical Physics Mass. Inst. of Tech., 1946, p.139.

(42) Moskovitz. The Numerical Solution of Laplace's and Poisson's Equations. Quart. Journ. App. Math., p.148, Vol. II, 1944.

(43) Motz and Worthy. Calculation by Southwell's Relaxation Method. J.I.E.E., p.522, Vol. 92, part II, 1945.

(44) Numerical Methods of Analysis in Engineering. Published by the Macmillan Company, New York, 1949.

(45) O'Brien, Hyman and Kaplam. Study of Numerical Solution of Partial-Differential Equations. U.S. Naval Ordnance Laboratory Memo., 10433, January, 1949.

(46) Ollendarff. Potential Feeder der Elektrotechnik Springer, Berlin, 1932.

(47) Packh. A Resistor Network for the Approximate Solution of the Laplace Equation. Rev. Scient. Instrum., p.788, Vol. 18, October, 1947.

(48) Prioroggia. Approximate Numerical Determination of Electrostatic and Analogous Harmonic Fields. Energia Elett., p.533, Vol. 25, October, 1948.

(49) Puchstein. Calculation of Slot Constants. Trans. A.I.E.E., p.1315, Vol. 66, 1947.

(50) Relf. An Electrical Method for Tracing Lines in the Two-Dimensional Flow of a Perfect Fluid. Philosophical Magazine, Vol. 48, September, 1924.

(51) Richardson. Free Hand Flux Plotting. Philosoph. Mag., p.237, Vol. 15, No. 96, February, 1908.

(52) Richardson. Solution of Partial Differential Equations. Phil. Trans., p.307, 1910.

(53) Rogowaki. Mitterleingen über Forschungsarbeiten, No. 71, 1909.

(54) Roters. "Electromagnetic Devices". Published by Wiley.

(55) Scarborough. Numerical Mathematical Analysis. Published by John Hopkins Press, Baltimore, 1930.

(56) Schmidt. On the Numerical Solution of Linear Simultaneous Equations by an Iterative Process. Phil. Mag., p.369, Vol. 32, November, 1941.

(57) Schneider. Numerical Solution of Laplace's Equation in Composite Rectangular Areas. Journal of App. Physics, September, 1946

(58) Schneider. Conduction Heat Transfer. Published by Addison-Wesley, Cambridge, Mass., 1955.

(59) Shaw. Introduction to Relaxation Methods. Dover Publications Inc., 1953.

(60) Shortley and Weller. The Numerical Solution of Laplace's Equation. Journal of Applied Physics, p.334, Vol. 9, 1938.

(61) Southwell. Relaxation. Methods Proc. Roy. Soc., p.56, 1935, also p.41, 1935.

(62) Southwell. Relaxation Methods in Engineering Science. Oxford University Press, 1940.

(63) Southwell. Relaxation Methods in Theoretical Physics. Oxford University Press, 1946.

(64) Spangenburg and Walters. An Electrical Network for the Study of Electromagnetic Fields. Techn. Report, No. 1, Stanford University, 1947.

(65) Still. Flux Distribution in Air Gap of Teeth of Dynamos. Electrician London, p.152 and p.187, Vol. 88, 1922.

(66) Stevenson. Fundamental Theory of Flux Plotting. Gen. Elect. Rev., p.797, Vol. 29, No. 11, November, 1926.

(67) Stevenson and Park. Graphical Determination of Magnetic Fields. Trans. A.I.E.E., Vol. XLVI, 1927.

(68) Strutt. Approximate Solution of Field of Rectangular Iron Conductor. Archiv. fur Elektrontechnik, April, 1927.

(69) Symposium at Illinois Institute of Technology on "Numerical Methods of Analysis in Engineering", published by Macmillan, 1949.

(70) Synge. Geometrical Interpretation of the Relaxation Method. Quart. Journ. App. Maths., p.87, Vol. 2, April, 1948.

(71) Tasny-Tschiassny. Network Analysis by the Chain Relaxation Method. J.I.E.E., p.177, Part III, Vol. 95, May, 1948.

(72) Tasny-Tschiassny. The Triangulation of a Two-Dimensional Continuum for the Purpose of the Approx. Solution of Second Order Partial Differential Equations. Journ. App. Phys., p.419, Vol. 20, 1949.

(73) Tasny-Tschiassny. Assymetrical Finite Difference Network for Tensor Conductivities. Quart. Journ. App. Maths., p.417, Vol. 12, 1955.

(74) Tasny-Tschiassny. Nets composed of Parts of Circles for the Approx. Solution of Field Problems. Aust. Journ. Physics, p.8, Vol. 8, 1955.

(75) Tasny-Tschiassny. The Approximate Solution of Electric Field Problems with the Aid of Curvilinear Nets. J.I.E.E., Part C, March, 1957.

(76) Thornton. Distribution of Magnetic Induction and Hysteresis Loss in Armatures. Journ. IEE, p.125, Vol. 17, 1906.

(77) Tranter. The Combined Use of Relaxation Methods and Fourier Transforms in the Solution of some Three-Dimensional Boundary Value Problems. Quart. Journ. Mech. App. Maths., p.281, Vol. 1, September, 1948.

(78) Unger. Field Distribution in Synch. Machines. E.T.Z., p.306, Vol. 41, 1920.

(79) Waddicor. Resistance-Model for the Solution of Thermal Resistance Problems. J.I.E.E., p.568, Vol. 61, 1923.

(80) Weber. Two-Dimensional Relaxation. "Electro-Magnetic Fields", Published by Wiley, p.259, 1950.

(81) Weller, Shortley and Freed. Numerical Integration of Porisson's Equation. Journ. of App. Physics Vol. II, No.4, p.283, 1940.

(82) Wieseman. Graphical Determination of Magnetic Fields, J.I.E.E., May, 1927.

(83) Wilson and Miles. Application of Membrane Analogy to the Solution of Heat Conduction Problems. Journ. Applied Physics, Vol. 21, June, 1950, p.532.

(84) Zworykin. The Liebmann Procedure. "Electron Optics and the Electron Microscope", p.386, published by Wiley, 1945.

7.4. Some Analytical Methods of Solution of Field Problems.

(1) Cramp and Calderwood. Calculation of Air-Space Flux. J.I.E.E., p.1061, Vol. 61, 1923.

(2) Pohl. The Magnetic Leakage of Salient Poles. J.I.E.E., p.170, Vol. 52, 1914.

(3) Douglas. Reluctance of Irregular Magnetic Fields. Trans. A.I.E.E., p.1067, Vol. 34, 1915, also Phys. Rev. p.391, Vol. 4, Ser. 2, 1914.

(4) Bewley. Two-Dimensional Magnetic Fields. Published by Macmillan, New York, 1948.

(5) Heller. Effect of Slots on the Magnetic Field of Squirrel Cage Induction Motors. Electrotech. Obs., p.277, Vol. 36, August, 1947.

(6) Davy. The Field between Equal Semi-Infinite Rectangular Electrodes or Magnetic Pole Pieces. Phil. Mag., p.819, Vol. 35, 1944.

(7) Pöllot. Slot Leakage with Closed Slots. Arch. Electrotechn., p.220, Vol. 37, 1943.

(8) Nakamura. Application of Conformal Representation to Flux,

(8) Contd.
Distribution in the Iron Cores of Electrical Machines. E.T.J., p.6, Vol. 3, January, 1939.

(9) Mitchell. The Theory of Free Stream Lines. Phil. Trabs., p.389, Ser. A, 1890.

(10) Atwood. Electric and Magnetic Fields. Published by Chapman and Hall, London.

(11) Carter. Theory of Pole Face Losses. J.I.E.E., p.168, Vol. 54, 1916.

(12) Neville. Calculation of Tooth Reluctance. J.I.E.E., p.161, Vol. 58, 1920.

(13) Hancock. Production of a Sinusoidal Flux Wave, with Particular Reference to the Inductor Alternator. J.I.E.E., Part C, 1957.

(14) Carter. Magnetic Centering of Dynamo-Electric Machinery. Proc. I.C.E., p.311, Vol. 187, 1912.

(15) Ollendorff. Potential Felder der Elektrotechnik. Published by Springer, Berlin, 1932.

(16) Cockcroft. The Effect of Curved Boundaries on the Distribution of Electrical Stress Around Conductors. J.I.E.E., p.385, Vol. 66, 1928.

(17) Darwin. Some Conformal Transformations Involving Elliptic Functions. Phil. Mag., p.1, Vol. 41, January, 1950.

(18) Okubo. Similarity of the Stress Distribution in a Circular Disc and a Square Plate. Journ. App. Phys., p.720, Vol. 11, November, 1940.

(19) Cristoffel. Annali di Matematica, p.89, Vol. 1, 1867.

(20) Schwartz. Crelle's Journal, p.105, Vol. 70, 1869.

(21) The Calculation of the Magnetic Field of Rectangular Conductors in a Closed Slot and its Application to the Reactance of Transformer Windings. J.I.E.E., p.55, October, 1951.

(22) Electromagnetic Problems in Electrical Engineering. Published by the Oxford University Press, 1929.

(23) Kucera. Elektrot und Masch., p.329, Vol. 58, 1940.

(24) Coggleshall. Journ. App. Phys., p.855, Vol. 18, 1947.

(25) Herzog. Arch. fur Elektrot., p.790, Vol. 29, 1935.

(26) Dreyfus. Arch. fur Elektrot., p.123, Vol. 13, 1924.

(27) Mie. Elektrot. Zeit., p.1, Vol. 26, 1905.

(28) Lewent. "Konforme Abbildung". Published by Teubner, Leipzig, 1912.

(29) Hague. "Electromagnetic Problems in Electrical Engineering". Published by Oxford University Press, London, 1929.

(30) Walker. "Conjugate Functions for Engineers". Published by Oxford University Press, 1933.

(31) Gibb. "Conformal Transformation in Electrical Engineering.

7.5. <u>References to Small Motors and Machines</u>.

(1) Model of a Radio Frequency Electric Motor. J. Tech. Phys., p.1258, U.S.S.R., Vol. 18, October, 1948.

(2) Pre-Determination of the Shaded-Pole Induction Motor Performance. Selsk. Skr., p.3, Vol. 5, 1947.

(3) Theory of an Oscillating Motor. Arch. f. Electrot., p.269, Vol. 33, April, 1939.

(4) Applications of Small Motors. Westinghouse Engineering, p.52, Vol. 9, March, 1949.

(5) Comparison of Small and Medium Sized Power Servomotors. Instrum. Pract., p.57, Vol. 3, December, 1948.

(6) Performance Calculations on Shaded-Pole Motors. Trans. A.I.E.E., p.1431, Vol. 66, 1947, also p.1007, Vol. 55, 1936.

(7) Unexcited Synchronous Motors. Electrotechnica, p.184, Vol. 36, April, 1949.

(8) Gramophone Motors. Elect. Rev., p.535, Vol. 122, April, 1938.

(9) Theory of Hysteresis Motor Torque. Trans. A.I.E.E., p.907, Vol. 59, 1940.

(10) Synchronous Motors. Electrotechnik und Maschinbau, p.82, Vol. 58, February, 1940.

(11) Synchronous Motor for Servograph Recorders. Bull, Seism. Soc. Amer., p.129, Vol. 31, April, 1941.

(12) Generators for Tachometers. Arch. Tech. Messen., Issue 174, J162-6, T81-2, July, 1950.

(13) Design of a Small 2-pole d.c. Motor. Electrotechnik, Berlin, p.278, Vol. 4, August, 1950.

(14) Analysis of Shaded Pole Motor by Symmetrical Components. Electrotechnics, p.104, Vol. 22, March, 1950.

(15) Instrument Motor as Integrator and Counter. Electrotek Zeit., p.113, Vol. 72, February, 1950.

(16) Homopolar Alternator. Elektrotekh. Obs., p.516, Vol. 39, No. 24, 1950.

(17) A Reluctance Motor Design Method. Elect. Eng., N.Y., p.618, Vol. 70, July, 1951, also, Trans. A.I.E.E., p.177, Vol. 51.

(18) Hysteresis Forces and the Hysteresis Motor. Zeit. Ver. desch. Mg., p.219, Vol. 86, April, 1942.

(19) Constant Speed Impulse Motor. P.O. Office Elect. Engs. J., p.109, Vol. 37, January, 1945.

(20) Electric Motors for Instruments and Control Apparatus. Instruments, p.216, p.310 and p.314, Vol. 18, May, 1945.

(21) Selsyn Design and Applications. Trans. A.I.E.E., p.703, Vol. 64, October, 1945.

(22) Small Two-Phase Motor. Electrician, p.599, Vol. 135, No. 30, 1945, also Engineering, p.81, Vol. 161, January, 1946.

(23) Damping and Synchronising Torques of Power Selsyns. Trans. A.I.E.E., p.366, Vol. 64, Supp. June, 1945.

(24) Theory of Pulsating Field Machines. J.I.E.E., p.37, Vol. 93, February, 1946.

(25) Performance Calculations on Polyphase Reluctance Motors Trans. A.I.E.E., p.191, Vol. 65, April, 1946.

(26) The Shaded-Pole, 1-Phase, Asynchronous Motor. Elektrotech. Obz. p.33, Vol. 35, 1946.

(27) Electrical Accuracy of Selsyn Generator Control System. Trans. A.I.E.E., p.570, Vol. 65, 1946.

(28) D.C. Impulse Type Motors by Siemens Schukert Zachlerwerk, Nurnberg BIOS, Report No. 409, H.M.S.O., 1946.

(29) The Electrotor. Electrical Review, p.663, Vol. 140, April, 1947. Electronic Engineering, p.160, Vol. 19, May, 1947. Electrician, p.1157, Vol. 138, May, 1947. Engineer, p.183, May, 1947.

(30) Principle Dimensions of d.c. Midget Machines. Electrotech., Zeit., p.297, Vol. 65, September, 1944.

(31) Standardisation Problems and Technical Peculiarities of Small Motors. Elektrotechnik, Berlin, p.41, Vol. 2, February, 1948.

(32) A Counter Motor. Naturforsch., p.573, Vol. 2(a), October, 1947.

(33) The Hysteresis Motor. Electr. Engineering N.Y., p.241, Vol. 67, March, 1948.

(34) High Frequency Induction a.c. Generator, G.E.C. Journal, p.190, Vol. 14, August, 1947.

(35) A Phase Sensitive Synchronous Motor. A.W.A. Technical Review, p.355, Vol. 7, No. 4, 1947.

(36) Tests on Speed Transients of Small Control Motors. Gen. Elect. Rev., p.18, Vol. 51, March, 1948.

(37) Special Types of Fractional Horsepower Motors. Electrotech. Und Maschinenbau, p.317, Vol. 62, July, 1944.

(38) Fractional Horsepower Motors. Teknisk Tidskift, Stockholm, p.545, Vol. 78, September, 1948.

(39) Motor Design for an Electrically Driven Gyroscope. Elect. Eng. N.Y., p.446, Vol. 69, May, 1950.

(40) Source of Torque in an Electrical Machine. Electrotech. Zeit., p311, Vol. 71, June, 1950.

(41) Calculation of Working Characteristics of Miniature Induction Motors. Electrichestvo, p.64, No. 11, November, 1949.

(42) Application of Special Heteropolar Inductor Alternators. Electrotechnica, p.518, Vol. 36, November, 1949.

(43) High Frequency Alternators. Journ. Gen. Elect. Co., p.190, Vol. 14, August, 1947.

(44) Dry Shaving Apparatus. Philips Tech. Rev., p.350, Vol. 4, December, 1939.

(45) Investigation on Synchronous Motors with Permanent Magnets

(45) Contd.
for the Pole System. Arch. fur Electrot., p.385, Vol. 33, June, 1939.

(46) The Phonic Chronometer. Journ. Scient. Inst., p.161, Vol. 1, 1924.

(47) Short Circuit Characteristics and Load Performance of Inductor Type Alternators. J.I.E.E., Vol. 94, Part II, 1947.

(48) Hysteresis Motor. J.I.E.E., p.379, Vol. 77.

SECTION 8.

SUMMARY AND CONCLUSIONS.

8.1. General.

In writing conclusions to the task that has occupied the author for several years it is comforting to know that the subject matter is still alive after about 80 years of contributions.

The general theme of the thesis was to obtain values of permeance as teeth of various trapezoidal shapes were moved with respect to each other. In order to apply a uniform method to all shapes which did not involve frequent recourse to higher mathematics, the substitute angle method invented by Dr. Pohl.was adopted. Basically, the method assumes that all slots are of triangular section and the flux lines idealised into straight lines and circular arcs. The substitute angle is the angle that the side of the fictitious triangular slot makes with the plane of the air-gap. Every different type of slot and tooth shape requires a different value of the substitute angle to produce the same permeance; furthermore this value of angle is also a function of both the (slot opening)/(gap length) and the degree of displacement. Hence, though a uniform method of treatment can be adopted, it is not possible to express the results in terms of a unique substitute angle. However it has been shown that most shapes met with in practical applications are amenable to approximate treatment by means of a substitute angle determined from the shape and the ratio of the opening to the gap length, this value being held constant throughout the range of movement of the opposed teeth.

This thesis has been largely devoted to determining the values of this substitute angle.

8.2. Discussion of the Sections.

Section 1 contains a comprehensive survey of existing knowledge related to the present study and in particular to the permeance of air-gaps.

The survey reveals that the subject virtually begins with the lemmas of Forbes in 1886 and followed nearly 20 years later by the work of Carter. Carter probably took his lead from Potier's solution of a slotted armature problem in 1889. Carter's work has never really been superceded though many distinguished men, for example, Hadamard 1909, Douglas 1915 and 1924, Coe and Taylor 1928, Cockcroft 1928, Miles Walker 1915, have added a few refinements throughout the years. All results published to date apply only to rectangular teeth and slots, plus a few special configurations. Dr. Pohl is the only person who has suggested a method for the empirical solution of problems of other than rectangular shape, but gives no details of any investigation into this subject. No analytical results exist for slots or teeth of trapezoidal section, due mainly to the difficulty of solving the complex elliptic integrals that arise. Even the solution of the integrals would only be the first stage of a problem involving much laborious algebra and arithmetic. A work published in recent years (Handbook of Elliptic Integrals for Engineers and Physicists, published by Springer, New York, 1954) will certainly assist with the solution of some of the foregoing problems since it contains tabulated solutions to about 3000 elliptic integrals. However a study of this work reveals that only a few special cases of interest to this work have been covered.

Little use has been made by the author of the many numerical methods available for the solution of problems associated with trapezoidal

teeth. The author is aware of a method, developed by Mr. G. F. Freeman, of using relaxation in the vicinity of a corner of any angle. This method is, as yet, unpublished, is not used by the author and has not been seen anywhere else in print.

Section 2 contains an orderly development of the equations for use with the substitute angle method as applied to slots of triangular section. From these equations a number of tables have been calculated for a number of values of s, t and g, and for 6 values of the substitute angle. Due to the amount of computational work associated with the calculation of these tables only a limited range has been provided. This range may easily be extended by direct calculation from the equations in Section 2. An example of the use of the tables is included in the summary of Section 2.

In Section 3 a number of empirical methods have been suggested by the author for the application of the substitute angle method to teeth and slots of circular or elliptic shape. No scientific reasoning has been applied in developing these methods, only simplicity, since if an empirical method becomes complicated, its value is lost. The value of some of them is discussed in Section 6.

Section 4 contains a collection of solutions to miscellaneous problems associated with this work, some of which have been used in other sections. Among these solutions is a method that the author considered may be an alternative to the substitute angle method, but it proved neither more accurate nor simpler. An empirical method is suggested for the solution of the problem of the leakage flux associated with the ends of the core. The pulsating permeance from this cause can become significant when the core is short and there is no reason why a substitute angle should not be used.

Section 5 is devoted to a special study of the permeance of teeth of rectangular, triangular and trapezoidal section and the determination of the appropriate values of the substitute angle.

As the rectangular tooth represents the limiting shape for the other two they have been studied as separate entities. The first part of Section 5 includes a comparison of some accurate results published by Dr. Liebmann with a number of other methods, including the substitute angle method in the form suggested by Dr. Pohl. This comparison provided full justification for further investigation of the substitute angle method. On comparing the substitute angle method directly with Carter's result an error in Dr. Pohl's assumptions was immediately apparent. The value of the substitute angle determined by Dr. Pohl was to obtain approximate equality with Carter's coefficient for a single slot and, when the same substitute angle is used for opposed teeth, it applies to the permeance of twice s/g. The author has suggested a new value for the substitute angle approximation and has extended the study to examine the limits of its application to successive slots with varying t and d. A special study has been made of the case where t is zero with both small and infinite slot depth; formulae have been given for each case. No analytical study has been made of the teeth out-of-line position except where the tooth width is greater than the slot width plus four times the gap length. Values of the exact substitute angle have been determined for each case studied here.

With triangular teeth, analytical results were available for the limiting values of slot angle, intermediate values being obtained by means of graphical flux plotting. Practical resistance measurement was used to

determine intermediate values of permeance with the teeth-out-of-line position, for one value of the slot angle.

Curves have been calculated relating the exact value of the substitute angle to the (slot opening)/(gap length) for both the in and out-of-line positions. An empirical formula is given which enables a substitute angle to be calculated for any value of slot angle. No results have been studied for other than a triangular slot, but provided the slot depth is a little greater than the slot width the error, with some w present, is not significant.

It was expected that results for trapezoidal teeth would be similar to those for triangular teeth, so a few curves were determined by means of graphical flux plotting. Within the limits of accuracy of the experimental method used, it was not found possible to completely separate the results for triangular and trapezoidal teeth, but the error is not serious and becomes much less as t increases.

To obtain some independent results for approximate trapezoids a conformal transformation of a rectilineal shape was used. Values of the substitute angle were determined for each case and where appropriate the results have been compared with the previous results. That they are not all compatible is due to the fact that some w exists at the base of these approximate shapes, which has not been catered for in the assumptions made.

Section 6 deals with two aspects of circular shapes, the flux leakage between isolated opposed circular poles (or teeth) and the permeance of opposed circular teeth, successive teeth being connected by equipotential planes. An analytical result available for the former case enabled an exact comparison to be made with the substitute angle method.

A sufficient range of values of the parameter $t/(t+g)$ was studied to show that good agreement is obtainable. For opposed circular teeth, two methods were used to determine the permeance; the first, giving doubtful results, was the direct measure of resistance from the normal boundary configuration, the second made use of a transformation and flux plotting. The results were compared with those predicted from the equivalent shapes suggested in Section 4, but the equivalent trapezoid is favoured by the author. The transformation method was extended to the case of teeth out-of-line and reasonable agreement was obtained between the measured results and those obtained from the equivalent trapezoid. Differences here are attributable to experimental errors for both results, due to the existence of some $\underline{w}$ in the equivalent trapezoid and to the variation from the circular shape. No separate empirical relationship has been stated for the application of the substitute angle method to circular teeth, since, having shown that the equivalent trapezoid is compatible (approximately) with the result predicted from the trapezoidal tooth, then the result for the latter type of tooth will be applicable. A plot has been calculated for the circular shape using a modification of Hague's method, but they apply to only low values of s/g and do not have much bearing on the range of interest to this work.

A fairly comprehensive bibliography, though not large by modern standards, has been included in Section 7.

8.3. Results of the Substitute Angle Approximation.

The title of the author's thesis stated specifically that the study was to be directed towards the determination of permeance when teeth of a specified boundary configuration were displaced with respect to each

other. A number of other related results have been determined which do not fall into the above category, these will not be mentioned here.

Stated explicitly, the substitute angle method means that wherever a permeance has to be determined, the flux lines may be assumed to follow straight lines crossing the air-gap and circular arcs within the slot. The extent of penetration of these flux lines into the slot is generally smaller than if they were continued to the tooth wall, in fact they penetrate to an angular extent of α , where α is the substitute angle.

The substitute angle for a given trapezoidal shape is a function of numerous parameters which prevents the specification of a unique value for a given slot. The variation of the substitute angle with some of these parameters is so small, however, that it can be determined from a few simple formulae, which are easy to remember and sufficiently accurate for most practical purposes. Alternatively more precise results may be obtained from the graphs included in the work.

To simplify the results the author has taken the exact substitute angle α_E, for rectangular teeth, as the transfer constant for teeth of other shape.

Opposed Rectangular Teeth

$$\alpha_E = 0.70 + 0.06\ s/g, \text{ for } s/g \leqslant 10.$$

$$\alpha_E = 1.30, \quad \text{for } s/g \geqslant 10.$$

Where α_p, the slot angle, is $\pi/2$ and α_E is the substitute angle. These results apply particularly to the cases where $d > s$ and $t \geqslant (s+4g)$, but where precise accuracy is not required, provided $d > s$, t may be any value.

Opposed Trapezoidal Teeth.

$$\alpha = 1.5 \times \alpha_E (1 - e^{-1.8\alpha_p/\pi}).$$

Where α_p, the slot angle, $< \pi/2$ and α_E is the angle corresponding to $\alpha_p = \pi/2$, for a given s/g.

For greater accuracy a better value of α_E may be obtained from the equations discussed in Section 5 for particular slot configurations.

8.4. Suggestions for Further Work.

The aim of this work was to provide simple formulae that could be applied to teeth of any shape. The generality of the method adopted by the author is restricted mainly by the shape of the fictitious slot. If this were trapezoidal the equations required to express a particular permeance would be more numerous, though if tedium is not a factor, no more difficult. As indicated in 8.3. the author has achieved a reasonably uniform method for all shapes but the results indicate that there may be a more general method. To amplify this, all results obtained by the author have been plotted in Fig. 5.3.3.3. in terms of α_p, the physical slot angle, and k a transfer constant. This constant is defined such that $k = \alpha_E' / \alpha_E$, where α_E' is the exact substitute angle required to agree with the measurements and α_E is the exact substitute angle required for a given s/g when $\alpha_p = \pi/2$. The results are seen to be almost wholly within the field given by

$$k = \frac{\pi}{2}(1 - e^{-2\alpha_p/\pi})$$

and $$k = \frac{2}{\pi} \cdot \alpha_p.$$

The spread of this field could be due to the experimental methods used, in which case a unique curve might be obtainable.

It would seem from the author's reading that experimental results, no matter how good, are eventually replaced by an analytical result. In

this subject there are a wealth of problems requiring an analytical solution. Some years ago the thought occurred to the author that opposed teeth of any shape could be represented by two Fourier Series F_1 and F_2, where F_1 represents the upper boundary and F_2 the lower boundary. The field between the two boundaries would be determinable as some function of F_1 and F_2. Now it has been shown in recent years that a Fourier series is summable to its constant term by a matrix transformation. Hence the original configuration could be transformed to a series of parallel lines representing an orthogonal distribution. Provided then that the matrix was reversible the lines of equipotential (say) in the transformed plane could be transformed back to the original plane and would be expressed as a Fourier series. This method was discussed with Dr. Jackson, a specialist in infinite matrices, and he indicated that a k or γ infinite skew matrix might be applicable, but would contain, in any case, an infinite number of series with complex terms. To take this subject further is beyond the capacity of the author.

No study has been made of the cases, which are numerous in practice, where the number of rotor teeth differ from the number of stator teeth. The substitute angle method can be applied exactly as indicated in Section 2, but more discontinuities will be introduced. No doubt the substitute angle for a given α_p will be the same as obtained in this thesis.

8.5. Acknowledgements.

Thanks are due to Mr. G. F. Freeman for suggesting the topic originally, for much useful encouragement and suggestions subsequently, and to Professor R. E. Vowels for much time spent in reading my very rough notes. Thanks are also due to Mr. R. Smart and M. G. Bell for a great amount of help in producing the tables in Appendix 3.

APPENDIX 1.

HARMONIC ANALYSIS BY SELECTED ORDINATES.

APPENDIX 1.

Harmonic Analysis by Selected Ordinates.

The method of harmonic analysis used in Appendix 3 was based on the method of selected ordinates using ordinates at 1/10th intervals of pole pitch. The tables mentioned were calculated on Utecom, but the following is the general method.

A1.1. Consider a complex wave of periodic interval 2π radians. Erect k ordinates at intervals of $2\pi/k$ radians and measure the heights of these ordinates as y_o, y_1, y_2 —— y_{k-1}. These figures enable an approximate analysis of the wave shape to be determined, the larger the value of k the more accurate the analysis.

The order n of the highest harmonic that can be determined with reasonable accuracy by means of a k-ordinate analysis is given by $n = (k-2)/2$.

A1.2. The general expansion of a periodic function (single-valued) $y = f(t)$ having a period 2π, may be expressed in the form :

$$y = a_o + a_1'\sin(wt + \phi_1) + a_2'\sin(2wt + \phi_2) + a_3'\sin(3wt + \phi_3) ——$$

$$= a_o + a_1\sin wt + a_2\sin 2wt + a_3\sin 3wt ——$$

$$+ b_1\cos wt + b_2\cos 2wt + b_3\cos 3wt ——\ .$$

By integration,

$$a_o = \frac{1}{2\pi}\int_o^{2\pi} y\,d(wt) \qquad ——— \quad A1.1$$

$$a_n = \frac{1}{\pi}\int_o^{2\pi} y\sin(nwt)\,d(wt) ——— \quad A1.2$$

$$b_n = \frac{1}{\pi}\int_o^{2\pi} y\cos(nwt)\,d(wt) ——— \quad A1.3$$

The coefficient a_o is seen to be the mean value between 0 and 2π of the curve, therefore -

$$a_o = \frac{1}{k}\ (y_o + y_1 + y_2 + \text{——} y_{k-1}\ )$$

$$= \frac{1}{k} \sum_{m=o}^{m=k-1} y \qquad \text{——————} \quad \text{Al.4.}$$

The coefficient a_n is twice the mean value between 0 and 2π therefore -

a_n = 2x average ordinate of ysin(nwt)

$= \frac{2}{k}$ x sum of k ordinates

$$= \frac{2}{k}\left(y_o \sin\frac{2\pi\, 0n}{k} + y_1 \sin\frac{2\pi\, 1n}{k} + y_2 \sin\frac{2\pi\, 2n}{k} + \text{——} y_{k-1} \sin\frac{2\pi(k-1)n}{k}\right)$$

$$= \frac{2}{k} \sum_{m=o}^{m=k-1} y_m \sin\left(mn\frac{2\pi}{k}\right) \qquad \text{————} \quad \text{Al.5.}$$

Similarly,

$$b_n = \frac{2}{k} \sum_{m=o}^{m=k-1} y_m \cos\left(mn\frac{2\pi}{k}\right) \qquad \text{————} \quad \text{Al.6.}$$

APPENDIX 2.

CURVES FOR RECTANGULAR

SLOTS.

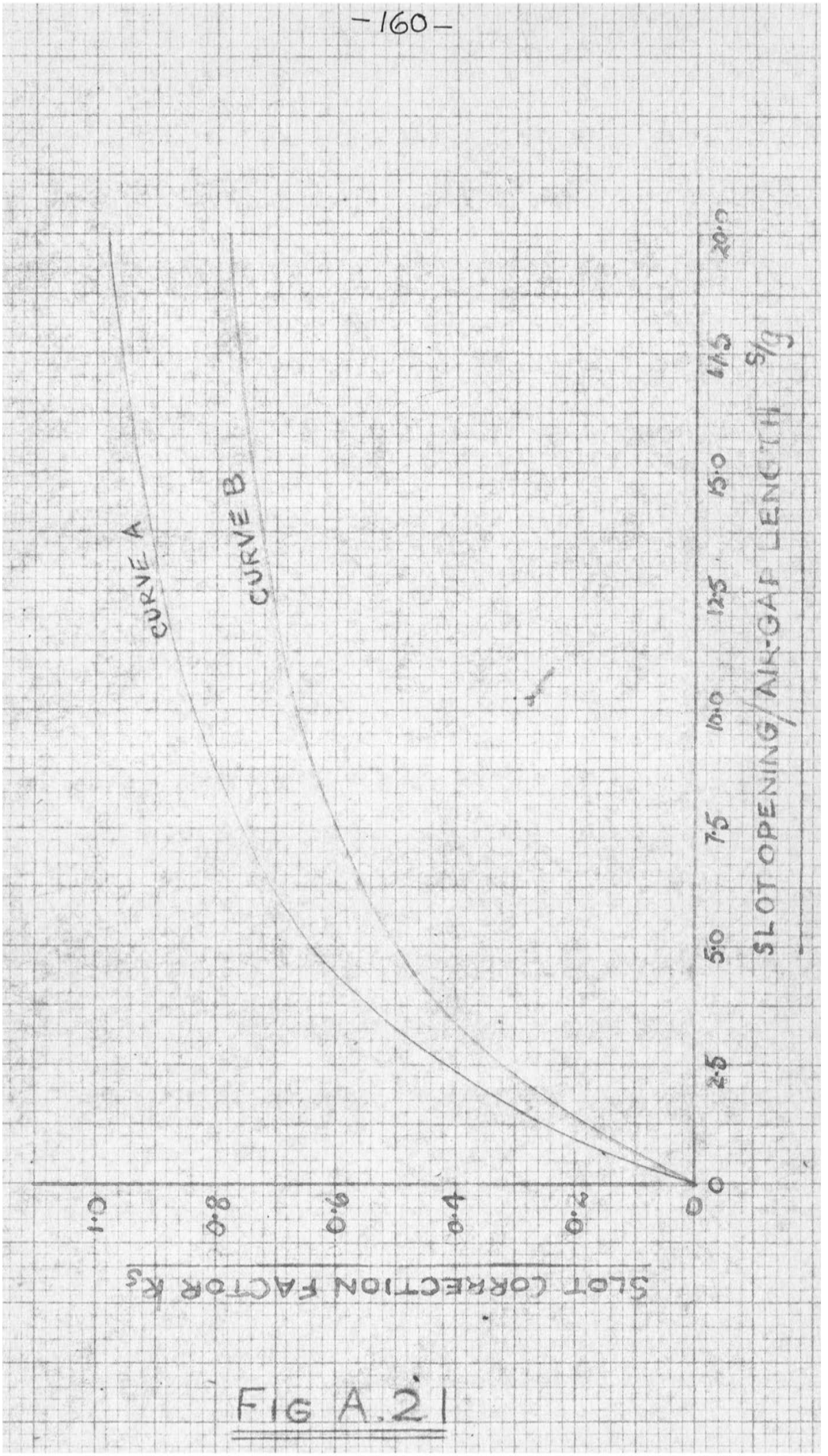
CURVE A
CURVE B
SLOT CORRECTION FACTOR K_s
1.0
0.8
0.6
0.4
0.2
0
0
2.5
5.0
7.5
10.0
12.5
15.0
17.5
20.0
SLOT OPENING/AIR-GAP LENGTH s/g

FIG A.21

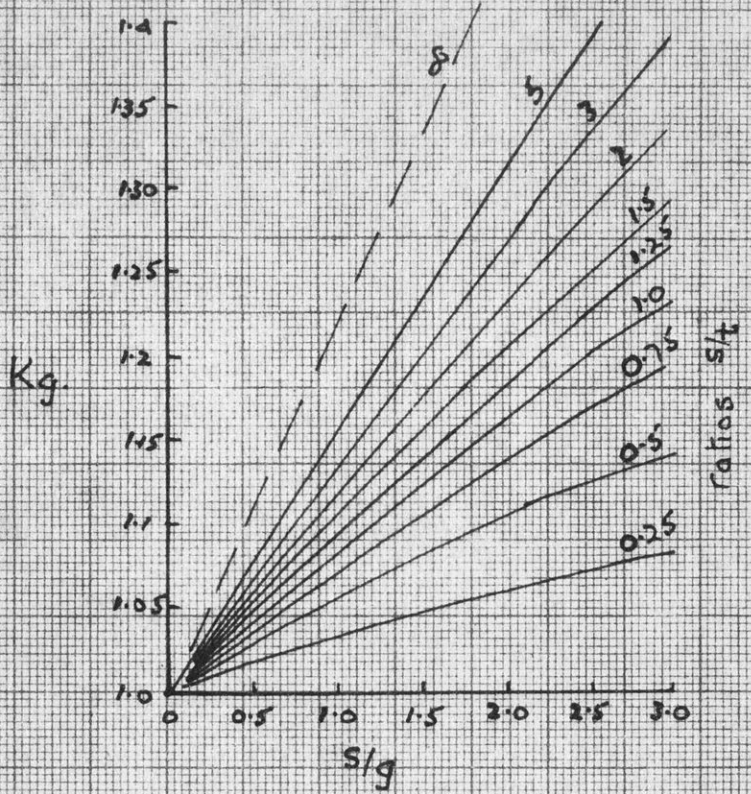

$$K_g = \frac{g'}{g}$$

g' is the length of the equivalent unslotted gap

s = slot width, t = tooth width, g = gap length

Ref. 4. Coe & Taylor p. 114.

FIG. A 2.2

APPENDIX 3.

TABLE OF PERMEANCE VARIATION

AND

ITS HARMONIC CONTENT

APPENDIX 3.

Tables of Permeance Variation and the Harmonic Content.

A.3. General.

The equations developed in Section 2 and summarised in 2.4. provide permeance values for a range of trapezoidal shapes. The calculated permeance from these equations represents the true permeance of that shape if the exact value α_E is used for every position. It has been shown that good approximation to the true permeance may be obtained by assuming that α is constant throughout the range of movement of one member with respect to the other but whose value is determined by the configuration of the teeth.

A number of empirical methods have been suggested for obtaining an approximate value for α in most cases met with in practice and are summarised in Section 8.

From the equations in Section 2.4. numeric permeance values for a number of values of s and t have been calculated. These values have been calculated for displacements in multiples of $^1/_{10}$th the tooth pitch (s+t), i.e., 6 values of x, representing the total variation from maximum to minimum permeance. Six constant values of α have been chosen, from 0.25 to 1.5 in intervals of 0.25. The chart given below indicates the table number in which the permeance calculation may be found for a given s and t, g being, of course, unity. Where the table does not cover the range of s and t required additional values may be computed from the equations in Section 2.

An additional set of tables has been computed from the permeance tables in A.3.1. and given an harmonic analysis of the wave

up to the fifth harmonic, such that

$$p = a_o + b_1\cos\theta + b_2\cos 2\theta + b_3 \cos 3\theta + b_4 \cos 4\theta + b_5 \cos 5\theta$$

These are given the same table number as the permeance values but are set out in A.3.2. Hence, the chart below applies to both permeance variation (A.3.1) and harmonic analysis (A.3.2.).

CHART OF TABLE NUMBERS.

S \ T	0	1	2	3	4	6	8	9	10	12	15	20
5	1	8	13	24	-	-	-	-	-	-	-	-
10	2	9	14	18	19	25	-	-	-	-	-	-
15	-	-	-	-	-	-	-	26				
20	3	10	15	-	20	21	22	-	23	27	-	-
30	4	11	16	-	-	-	-	-	-	-	28	
40	-	-	-	-	-	-	-	-	-	-	-	29
50	5	12	17	-	-	-	-	-	-	-	-	-
75	6	-	-	-	-	-	-	-	-	-	-	-
100	7	-	-	-	-	-	-	-	-	-	-	-

A.3.1. Permeance Variation.

S = 5; g = 1.0; t = o						1
x	0	0.1(s+t)	0.2(s+t)	0.3(s+t)	0.4(s+t)	0.5(s+t)
α = 0.25	3.2437	3.2237	3.1800	3.1315	3.0928	3.0769
0.50	2.5055	2.4649	2.3863	2.3066	2.2463	2.2222
0.75	2.0775	2.0212	1.9237	1.8318	1.7652	1.7391
1.00	1.7918	1.7235	1.6163	1.5211	1.4543	1.4286
1.25	1.5848	1.5074	1.3958	1.3014	1.2368	1.2121
1.50	1.4267	1.3423	1.2293	1.1375	1.0759	1.0526
S = 10; g = 1.0; t = 0						2
α = 0.25	5.0111	4.9297	4.7726	4.6131	4.4926	4.4444
0.50	3.5835	3.4471	3.2326	3.0422	2.9087	2.8571
0.75	2.8534	2.6846	2.4586	2.2750	2.1519	2.1053
1.00	2.3979	2.2094	1.9875	1.8181	1.7079	1.6667
1.25	2.0822	1.8818	1.6694	1.5146	1.4159	1.3793
1.50	1.8484	1.6409	1.4396	1.2981	1.2092	1.1765
S = 20; g = 1.0; t = 0						3
α = 0.25	7.1670	6.8941	6.4652	6.0845	5.8174	5.7143
0.50	4.7958	4.4189	3.9750	3.6363	3.4158	3.3333
0.75	3.6968	3.2817	2.8792	2.5961	2.4184	2.3529
1.00	3.0445	2.6178	2.2591	2.0193	1.8720	1.8182
1.25	2.6065	2.1799	1.8594	1.6524	1.5270	1.4815
1.50	2.2893	1.8687	1.5801	1.3984	1.2894	1.2500
S = 30; g = 1.0; t = 0						4
α = 0.25	8.5603	8.0537	7.3756	6.8249	6.4556	6.3158
0.50	5.5452	4.9226	4.3188	3.8942	3.6276	3.5294
0.75	4.2093	3.5679	3.0596	2.7262	2.5230	2.4490
1.00	3.4340	2.8031	2.3701	2.0975	1.9341	1.8750
1.25	2.9205	2.3099	1.9346	1.7046	1.5682	1.5190
1.50	2.5524	1.9650	1.6344	1.4357	1.3187	1.2766
S = 50; g = 1.0; t = 0						5
α = 0.25	10.4108	9.4088	8.3468	7.5728	7.0795	6.8966
0.50	6.5162	5.4498	4.6484	4.1309	3.8176	3.7037
0.75	4.8675	3.8499	3.2243	2.8410	2.6136	2.5316
1.00	3.9318	2.9789	2.4687	2.1651	1.9870	1.9231
1.25	3.3208	2.4301	2.0001	1.7490	1.6028	1.5504
1.50	2.8872	2.0524	1.6811	1.4671	1.3430	1.2987
S = 75; g = 1.0; t = 0						6
α = 0.25	11.9326	10.3377	8.9532	8.0175	7.4402	7.2289
0.50	7.3013	5.7748	4.8364	4.2615	3.9204	3.7925
0.75	5.3966	4.0149	3.3147	2.9024	2.6615	2.5751
1.00	4.3307	3.0786	2.5217	2.2007	2.0146	1.9481
1.25	3.6410	2.4969	2.0349	1.7722	1.6207	1.5666
1.50	3.1545	2.1002	1.7057	1.4834	1.3556	1.3100

S = 100; g = 1.0; t = o						7
X	0	0.1(s+t)	0.2(s+t)	0.3(s+t)	0.4(s+t)	0.5(s+t)
α = 0.25	13.0324	10.8996	9.2968	8.2619	7.6351	7.4074
0.50	7.8636	5.9578	4.9373	4.3302	3.9740	3.8462
0.75	5.7743	4.1048	3.3622	2.9343	2.6861	2.5974
1.00	4.6151	3.1319	2.5492	2.2190	2.0286	1.9608
1.25	3.8690	2.5321	2.0529	1.7841	1.6298	1.5748
1.50	3.3449	2.1252	1.7183	1.4917	1.3620	1.3158
S = 5; g = 1.0; t = 1.0						8
α = 0.25	4.2437	4.2125	4.1363	4.0455	3.9739	3.9473
0.50	3.5055	3.4385	3.2838	3.1126	2.9872	2.9423
0.75	3.0775	2.9798	2.7661	2.5470	2.3975	2.3454
1.00	2.7918	2.6675	2.4091	2.1621	2.0038	1.9499
1.25	2.5848	2.4374	2.1441	1.8814	1.7218	1.6686
1.50	2.4267	2.2589	1.9376	1.6668	1.5097	1.4583
S = 10; g = 1.0; t = 1.0						9
α = 0.25	6.0111	5.8966	5.6502	5.4020	5.2193	5.1498
0.50	4.5835	4.3697	3.9813	3.6560	3.4404	3.3621
0.75	3.8534	3.5629	3.1062	2.7738	2.5684	2.4957
1.00	3.3979	3.0459	2.5564	2.2375	2.0496	1.9844
1.25	3.0822	2.6794	2.1759	1.8760	1.7054	1.6470
1.50	2.8484	2.4028	1.8958	1.6155	1.4603	1.4076
S = 20; g = 1.0; t = 1.0						10
α = 0.25	8.1670	7.7915	7.1929	6.6860	6.3413	6.2115
0.50	5.7958	5.1985	4.5155	4.0429	3.7507	3.6448
0.75	4.6968	3.9639	3.3066	2.9022	2.6638	2.5791
1.00	4.0445	3.2216	2.6118	2.2645	2.0656	1.9956
1.25	3.6065	2.7206	2.1594	1.8568	1.6868	1.6274
1.50	3.2893	2.3577	1.8411	1.5736	1.4254	1.3739
S = 30; g = 1.0; t = 1.0						11
α = 0.25	9.5603	8.8754	7.9890	7.3067	6.8623	6.6970
0.50	6.5452	5.5811	4.7378	4.1968	3.8713	3.7540
0.75	5.2093	4.1121	3.3764	2.9464	2.6967	2.6079
1.00	4.4340	3.2653	2.6245	2.2705	2.0690	1.9980
1.25	3.9205	2.7112	2.1471	1.8470	1.6784	1.6192
1.50	3.5524	2.3193	1.8168	1.5567	1.4119	1.3612
S = 50; g = 1.0; t = 1.0						12
α = 0.25	11.4108	10.0992	8.8092	7.9156	7.3594	7.1555
0.50	7.5162	5.9448	4.9359	4.3307	3.9751	3.8477
0.75	5.8675	4.2333	3.4325	2.9818	2.7232	2.6313
1.00	4.9318	3.2913	2.6318	2.2738	2.0790	1.9992
1.25	4.3208	2.6935	2.1342	1.8380	1.6708	1.6120
1.50	3.8871	2.2800	1.7949	1.5418	1.4003	1.3505

S = 5; g = 1.0; t = 2.0						13
x	0	0.1(s+t)	0.2(s+t)	0.3(s+t)	0.4(s+t)	0.5(s+t)
α = 0.25	5.2437	5.2023	5.1047	4.9863	4.8895	4.8547
0.50	4.5055	4.4172	4.2205	3.9851	3.7929	3.7248
0.75	4.0775	3.9497	3.6799	3.3631	3.1103	3.0239
1.00	3.7918	3.6304	3.3059	2.9311	2.6411	2.5459
1.25	3.5848	3.3946	3.0276	2.6100	2.2974	2.1987
1.50	3.4267	3.2113	2.8105	2.3599	20.342	1.9350
S = 10; g = 1.0; t = 2.0						14
α = 0.25	7.0111	6.8771	6.5676	6.2252	5.9745	6.8845
0.50	5.5835	5.3350	4.8182	4.3243	4.0075	3.8999
0.75	4.8534	4.5179	3.8752	3.3337	3.0195	2.9165
1.00	4.3979	3.9933	3.2674	2.7184	2.4234	2.3293
1.25	4.0821	3.6210	2.8366	2.2971	2.0243	1.9389
1.50	3.8484	3.3397	2.5127	1.9899	1.7383	1.6606
S = 20; g = 1.0; t = 2.0						15
α = 0.25	9.1670	8.7393	7.9626	7.31197	6.8809	6.7242
0.50	6.7958	6.0917	5.1129	4.4751	4.0993	3.9688
0.75	5.6968	4.8056	3.7916	3.2310	2.9206	2.8152
1.00	5.0445	4.0161	3.0192	2.5296	2.2687	2.1812
1.25	4.6065	3.4720	2.5103	2.0789	1.8547	1.7803
1.50	4.2893	3.0701	2.1491	1.7646	1.5686	1.5039
S = 30; g = 1.0; t = 2.0						16
α = 0.25	10.5603	9.7558	8.6354	7.8050	7.2785	7.0873
0.50	7.5452	6.3377	5.1915	4.5136	4.1221	3.9850
0.75	6.2093	4.7690	3.7244	3.1781	2.8759	2.7717
1.00	5.4340	3.8438	2.9064	2.4530	2.2084	2.1248
1.25	4.9205	3.2270	2.3838	1.9975	1.7925	1.7227
1.50	4.5524	2.7843	2.0209	1.6848	1.5084	1.4486
S = 50; g = 1.0; t = 20						17
α = 0.25	12.4108	10.8391	9.2914	8.2671	7.6438	7.4186
0.50	8.5162	6.4983	5.2398	4.5366	4.1356	3.9942
0.75	6.8675	4.6722	3.6538	3.1273	2.8349	2.7328
1.00	5.9318	3.6541	2.8057	2.3863	2.1566	2.0769
1.25	5.3208	3.0025	2.2774	1.9292	1.7403	1.6749
1.50	4.8872	2.5490	1.9167	1.6191	1.4597	1.4033
S = 10; g = 1.0; t = 3.0						18
α = 0.25	8.0111	7.8563	7.5047	7.0830	6.7624	6.6505
0.50	6.5835	6.2987	5.7141	5.0584	4.6186	4.4748
0.75	5.8534	5.4712	4.7453	3.9756	3.5155	3.3726
1.00	5.3979	4.9391	4.1187	3.2886	2.8401	2.7063
1.25	5.0822	4.5611	3.6730	2.8100	2.3833	2.2599
1.50	4.8484	4.2755	3.3365	2.4558	2.0535	1.9400

S = 10; g = 1.0; t = 4.0						19
x	0	0.1(s+t)	0.2(s+t)	0.3(s+t)	0.4(s+t)	0.5(s+t)
α = 0.25	9.0111	8.8345	8.4410	7.9702	7.5857	7.4496
0.50	7.5835	7.2608	6.6117	5.8623	5.2822	5.0918
0.75	6.8534	6.4227	5.6211	4.7199	4.0684	3.8701
1.00	6.3979	5.8831	4.9806	3.9853	3.3134	3.1219
1.25	6.0822	5.4995	4.5253	3.4663	2.7968	2.6163
1.50	5.8484	5.2096	4.1818	3.0770	2.4205	2.2518
S = 20; g = 1.0; t = 4.0						20
α = 0.25	11.1670	10.6701	9.6364	8.6386	8.0151	7.7997
0.50	8.7958	7.9866	6.5348	5.4368	4.8469	4.6586
0.75	7.6968	6.6795	5.0254	3.9799	3.4766	3.3212
1.00	7.0445	5.8760	4.1080	3.1423	2.7109	2.5805
1.25	6.6065	5.3218	3.4843	2.5971	2.2218	2.1099
1.50	6.2893	4.9120	3.0299	2.2135	1.8823	1.7845
S = 20; g = 1.0: t = 6.0						21
α = 0.25	13.1670	12.5975	11.4283	10.1169	9.2373	8.9495
0.50	10.7958	9.8781	8.2374	6.5772	5.6802	5.4126
0.75	9.6968	8.5510	6.6730	4.9116	4.1070	3.8799
1.00	9.0445	7.7346	5.7137	3.9295	3.2176	3.0238
1.25	8.6065	7.1715	5.0550	3.2784	2.6452	2.4772
1.50	8.2893	6.7551	4.5701	2.8140	2.2459	2.0980
S = 20; g = 1.0; t = 8.0						22
α = 0.25	15.1670	14.5216	13.2235	11.7245	10.5645	10.1836
0.50	12.7958	11.7661	9.9612	7.9705	6.6268	6.2437
0.75	11.6968	10.4192	8.3636	6.1540	4.8410	4.5035
1.00	11.0445	9.5903	7.3851	5.0538	3.8165	3.5222
1.25	10.6065	9.0185	6.7138	4.3064	3.1510	2.8922
1.50	10.2893	8.5958	6.1533	3.7616	2.6835	2.4533
S = 20; g = 1.0; t = 10.0						23
α = 0.25	17.1670	16.4428	15.0148	13.4016	12.0116	11.5138
0.50	14.7958	13.6510	11.6815	9.5377	7.7237	7.1691
0.75	13.6968	12.2844	10.0512	7.6694	5.7240	5.2088
1.00	13.0445	11.4433	9.0540	6.5375	4.5555	4.0912
1.25	12.6065	10.8632	8.3706	5.7676	3.7863	3.3687
1.50	12.2893	10.4345	7.8685	5.2052	3.2406	2.8632
S = 5; g = 1.0; t = 3.0						24
α = 0.25	6.2437	6.1909	6.0715	5.9377	5.8371	5.7978
0.50	5.5055	5.3938	5.1547	4.8862	4.6680	4.5771
0.75	5.0775	4.9169	4.5912	4.2288	3.9210	3.7905
1.00	4.7918	4.5903	4.2008	3.7714	3.3967	3.2385
1.25	4.5848	4.3486	3.9102	3.4313	3.0056	2.8285
1.50	4.4267	4.1605	3.6837	3.1666	2.7011	2.5116

S = 10; g = 1.0; t = 6.0						25
x	o	0.1(s+t)	0.2(s+t)	0.3(s+t)	0.4(s+t)	0.5(s+t)
α = 0.25	11.0111	10.7876	10.3093	9.7724	9.3360	9.1541
0.50	9.5835	9.1806	8.4015	7.5428	6.7934	6.4770
0.75	8.8534	8.3210	7.3673	6.3333	5.4022	5.0232
1.00	8.3979	7.7664	6.6995	5.5566	4.5103	4.1059
1.25	8.0822	7.3719	6.2254	5.0086	3.8841	3.4732
1.50	7.8484	7.0735	5.8682	4.5980	3.4176	3.0101
S = 15; g = 1.0; t = 9.0						26
α = 0.25	15.2326	14.7508	13.7737	12.6864	11.7630	11.3716
0.50	13.2801	12.4814	11.0510	9.5000	8.1034	7.5348
0.75	12.3407	11.3313	9.6664	7.8918	6.2584	5.6445
1.00	11.7726	10.6103	8.8023	6.8971	5.1264	4.5151
1.25	11.3865	10.1070	8.2026	6.2118	4.3540	3.7632
1.50	11.1047	9.7318	7.7580	5.7067	3.7904	3.2263
S = 20; g = 1.0; t = 12.0						27
α = 0.25	19.1670	18.3612	16.8030	15.0855	13.5868	12.9539
0.50	16.7958	15.5329	13.3989	11.1132	9.0206	8.2118
0.75	15.6968	14.1471	11.7365	9.1961	6.8352	6.0201
1.00	15.0445	13.2941	10.7209	8.0366	5.5302	4.7538
1.25	14.6065	12.7058	10.0256	7.2489	4.6554	3.9283
1.50	14.2893	12.2712	9.5152	6.6742	4.0253	3.3473
S = 30; g = 1.0; t = 15.0						28
α = 0.25	23.5603	22.1176	19.4849	16.5743	14.0773	13.2509
0.50	20.5452	18.4267	15.0768	11.5041	8.5860	7.8133
0.75	19.2093	16.6941	13.0254	9.1795	6.2026	5.5424
1.00	18.4340	15.6517	11.8027	7.8078	4.8609	4.2948
1.25	17.9205	14.9437	10.9787	6.8901	3.9985	3.5058
1.50	17.5524	14.4264	10.3805	6.2275	3.3968	2.9618
S = 40; g = 1.0; t = 20.0						29
α = 0.25	29.5916	27.3019	23.3629	19.0754	15.4475	14.3382
0.50	26.0890	22.8867	18.1079	13.0750	9.1109	8.1824
0.75	24.5786	20.8689	15.7370	10.4104	6.4813	5.7264
1.00	23.7136	19.6727	14.3460	8.8625	5.0340	4.4047
1.25	23.1455	18.8682	13.4182	7.8371	4.1164	3.5788
1.50	22.7406	18.2846	12.7495	7.1018	3.4823	3.0137

A.32 Harmonic Content of Permeance.

S = 5; g = 10; t = o						1
α	a_o	b_1	b_2	b_3	b_4	b_5
0.25	3.1576	0.0817	0.0024	0.0015	0.0003	0.0001
0.50	2.3535	0.1372	0.0093	0.0039	0.0011	0.0006
0.75	1.8899	0.1618	0.0161	0.0063	0.0022	0.0010
1.00	1.5850	0.1715	0.0216	0.0086	0.0035	0.0015
1.25	1.3670	0.1738	0.0258	0.0105	0.0048	0.0020
1.50	1.2048	0.1723	0.0289	0.0122	0.0059	0.0025
S = 10; g = 1.0; t = o						2
0.25	4.7071	0.2745	0.0185	0.0077	0.00021	0.0010
0.50	3.1701	0.3430	0.0432	0.0172	0.0070	0.0030
0.75	2.4099	0.3430	0.0560	0.0242	0.0116	0.0050
1.00	1.9510	0.3294	0.0656	0.0294	0.0156	0.0067
1.25	1.6424	0.3104	0.0696	0.0329	0.0187	0.0081
1.50	1.4200	0.2915	0.0713	0.0352	0.0210	0.0092
S = 20; g = 1.0; t = o						3
0.25	6.3403	0.6860	0.0864	0.0343	0.0139	0.0060
0.50	3.9020	0.6580	0.1312	0.0589	0.0313	0.0134
0.75	2.8400	0.5831	0.1425	0.0704	0.0421	0.0183
1.00	2.2398	0.5162	0.1430	0.0755	0.0484	0.0214
1.25	1.8525	0.4618	0.1394	0.0773	0.0521	0.0233
1.50	1.5812	0.4178	0.1344	0.0774	0.0540	0.0244
S = 30; g = 1.0; t = o						4
0.25	7.2295	1.0341	0.1732	0.0731	0.0352	0.0150
0.50	4.2600	0.8747	0.2140	0.1057	0.0632	0.0275
0.75	3.0411	0.7314	0.2122	0.1151	0.0758	0.0337
1.00	2.3718	0.6266	0.2016	0.1162	0.0810	0.0366
1.25	1.9473	0.5488	0.1896	0.1142	0.0827	0.0381
S = 50; g = 1.0; t = o						5
0.25	8.2122	1.5522	0.3479	0.1645	0.0935	0.0403
0.50	4.6312	1.1546	0.3485	0.1933	0.1302	0.0582
0.75	3.2456	0.9146	0.3160	0.1903	0.1379	0.0630
1.00	2.5054	0.7603	0.2853	0.1809	0.1367	0.0632
1.25	2.0435	0.6529	0.2594	0.1706	0.1326	0.0618
1.50	1.7273	0.5737	0.2381	0.1607	0.1276	0.0597

S = 75; g = 1.0; t = o						6
α	a_o	b_1	b_2	b_3	b_4	b_5
0.25	8.8658	1.9939	0.5380	0.2798	0.1770	0.0780
0.50	4.8685	1.3719	0.4740	0.2855	0.2069	0.0945
0.75	3.3758	1.0532	0.4076	0.2635	0.2023	0.0939
1.00	2.5909	0.8605	0.3572	0.2411	0.1913	0.0896
1.25	2.1056	0.7308	0.3184	0.2216	0.1796	0.0847
1.50	1.7754	0.6373	0.2880	0.2049	0.1688	0.0800
S = 100; g = 1.0; t = o						7
0.25	9.2626	2.3093	0.6960	0.3866	0.2604	0.1165
0.50	5.0107	1.5205	0.5706	0.3618	0.2735	0.1264
0.75	3.4546	1.1474	0.4762	0.3215	0.2551	0.1195
1.00	2.6433	0.9287	0.4100	0.2876	0.2346	0.1108
1.25	2.1441	0.7841	0.3615	0.2603	0.2162	0.1027
1.50	1.8054	0.6808	0.3243	0.2381	0.2004	0.0956
S = 5; g = 1.0; t = 1.0						8
0.25	4.0926	0.1477	0.0024	0.0004	0.0004	0.0000
0.50	3.0091	0.6798	0.3860	0.4014	0.3993	0.2003
0.75	2.6803	0.3619	0.0299	0.0035	0.0012	0.0006
1.00	2.3226	0.4137	0.0465	0.0064	0.0017	0.0008
1.25	2.0622	0.4472	0.0621	0.0028	0.0023	0.0010
1.50	1.7631	0.6696	0.1236	0.2134	0.1970	0.1011
S = 10; g = 1.0; t = 1.0						9
0.25	5.5497	0.4220	0.0296	0.0082	0.0011	0.0002
0.50	3.8839	0.5852	0.0830	0.0241	0.0057	0.0014
0.75	3.0371	0.6344	0.1249	0.0411	0.0125	0.0033
1.00	2.5161	0.6444	0.1549	0.0564	0.0201	0.0059
1.25	2.1602	0.6392	0.1766	0.0696	0.0278	0.0087
1.50	1.9004	0.6278	0.1925	0.0810	0.0350	0.0116
S = 20; g = 1.0; t = 1.0						10
0.25	7.0401	0.9230	0.1313	0.0478	0.0178	0.0069
0.50	4.4455	0.9572	0.2247	0.0983	0.0500	0.0200
0.75	3.2948	0.8942	0.2652	0.1319	0.0779	0.0326
1.00	2.6366	0.8268	0.2836	0.1545	0.0998	0.0431
1.25	2.2080	0.7678	0.2919	0.1701	0.1170	0.0516
1.50	1.9058	0.7178	0.2953	0.1813	0.1305	0.0586

S = 30; g = 1.0; t = 1.0						11
α	a_0	b_1	b_2	b_3	b_4	b_5
0.25	7.8323	1.3084	0.2469	0.1030	0.0493	0.0201
0.50	4.7072	1.1785	0.3369	0.1718	0.1053	0.0453
0.75	3.4080	1.0314	0.3590	0.2061	0.1417	0.0630
1.00	2.6890	0.9181	0.3617	0.2247	0.1651	0.0751
1.25	2.2306	0.8315	0.3581	0.2355	0.1811	0.0835
1.50	1.9122	0.7640	0.3523	0.2419	0.1923	0.0896
S = 50; g = 1.0; t = 1.0						12
0.25	8.6932	1.8481	0.4590	0.2233	0.1308	0.0562
0.50	4.9736	1.4459	0.5002	0.2944	0.2080	0.0939
0.75	3.5240	1.1917	0.4839	0.3148	0.2415	0.1117
1.00	2.7466	1.0257	0.4615	0.3199	0.2573	0.1207
1.25	2.2604	0.9093	0.4408	0.3194	0.2652	0.1256
1.50	1.9271	0.8233	0.4227	0.3167	0.2690	0.1283
S = 5; g = 1.0; t = 2.0						13
0.25	5.0463	0.1936	0.0016	0.0009	0.0012	0.0000
0.50	4.1061	0.3873	0.0055	0.0028	0.0035	0.0002
0.75	3.5307	0.5215	0.0138	0.0044	0.0062	0.0008
1.00	3.1354	0.6156	0.0244	0.0056	0.0089	0.0016
1.25	2.8442	0.6838	0.0359	0.0064	0.0116	0.0027
1.50	2.6193	0.7349	0.0475	0.0070	0.0140	0.0039
S = 10; g = 1.0; t = 2.0						14
0.25	6.0183	1.3597	0.7721	0.8029	0.7985	0.4006
0.50	4.6453	0.8274	0.0929	0.0128	0.0034	0.0016
0.75	3.5262	1.3392	0.2472	0.4269	0.3941	0.2023
1.00	3.1531	0.9895	0.2016	0.0420	0.0088	0.0027
1.25	2.7578	1.0120	0.2407	0.0567	0.0119	0.0029
1.50	2.4670	1.0204	0.2724	0.0704	0.0151	0.0030
S = 20; g = 1.0; t = 2.0						15
0.25	7.7680	1.1704	0.1660	0.0483	0.0114	0.0027
0.50	5.0322	1.2889	0.3099	0.1127	0.0401	0.0117
0.75	3.8009	1.2556	0.3849	0.1619	0.0701	0.0232
1.00	3.0892	1.1986	0.4263	0.1982	0.0973	0.0347
1.25	2.6218	1.1419	0.4507	0.2257	0.1208	0.0454
1.50	2.2897	1.0905	0.4655	0.2471	0.1412	0.0551

S = 30; g = 1.0; t = 1.0						16
α	a_o	b_1	b_2	b_3	b_4	b_5
0.25	8.4597	1.5988	0.3148	0.1197	0.0493	0.0179
0.50	5.1859	1.5128	0.4583	0.2188	0.1207	0.0484
0.75	3.8075	1.3677	0.5075	0.2767	0.1754	0.0744
1.00	3.0381	1.2470	0.5255	0.3129	0.2157	0.0945
1.25	2.5445	1.1516	0.5312	0.3372	0.2459	0.1101
1.50	2.1997	1.0752	0.5317	0.3543	0.2691	0.1224
S = 50; g = 1.0; t = 2.0						17
0.25	9.1911	2.1590	0.5685	0.2720	0.1551	0.0650
0.50	5.3330	1.7559	0.6528	0.3848	0.2693	0.1203
0.75	3.8176	1.4866	0.6536	0.4294	0.3289	0.1513
1.00	3.0014	1.3074	0.6398	0.4501	0.3631	0.1698
1.25	2.4894	1.1806	0.6241	0.4605	0.3844	0.1818
1.50	2.1377	1.0863	0.6093	0.4657	0.3983	0.1898
S = 10; g = 1.0; t = 3.0						18
0.25	7.3073	0.6783	0.0186	0.0004	0.0047	0.0016
0.50	5.4438	1.0465	0.0751	0.0019	0.0103	0.0060
0.75	4.4640	1.2242	0.1338	0.0053	0.0150	0.0109
1.00	3.8476	1.3201	0.1853	0.0103	0.0190	0.0154
1.25	3.4196	1.3758	0.2288	0.0159	0.0223	0.0193
1.50	3.1030	1.4095	0.2655	0.0220	0.0255	0.0226
S = 10; g = 1.0; t = 4.0						19
0.25	8.2123	0.7745	0.0110	0.0056	0.0070	0.0005
0.50	6.2709	1.2313	0.0488	0.0113	0.0179	0.0033
0.75	5.2387	1.4699	0.0951	0.0141	0.0279	0.0077
1.00	4.5844	1.6098	0.1393	0.0155	0.0361	0.0127
1.25	4.1274	1.6987	0.1790	0.0164	0.0428	0.0178
1.50	3.7877	1.7584	0.2141	0.0171	0.0481	0.0227
S = 20; g = 1.0; t = 4.0						20
0.25	9.2906	1.6547	0.1858	0.0256	0.0069	0.0032
0.50	6.3064	1.9792	0.4031	0.0840	0.0176	0.0053
0.75	4.9340	2.0408	0.5448	0.1408	0.0302	0.0061
1.00	4.1298	2.0364	0.6402	0.1891	0.0424	0.0066
1.25	3.5965	2.0121	0.7078	0.2291	0.0538	0.0071
1.50	3.2149	1.9823	0.7577	0.2623	0.0642	0.0078

S = 20; g = 1.0; t = 6.0						21
α	a_o	b_1	b_2	b_3	b_4	b_5
0.25	10.8875	2.0929	0.1501	0.0038	0.0206	0.0120
0.50	7.6953	2.6403	0.3707	0.0206	0.0381	0.0308
0.75	6.2061	2.8191	0.5311	0.0441	0.0511	0.0452
1.00	5.3258	2.8864	0.6469	0.0684	0.0615	0.0555
1.25	4.7382	2.9102	0.7334	0.0914	0.0700	0.0629
1.50	4.3157	2.9145	0.8006	0.1126	0.0774	0.0685
S = 20; g = 1.0; t = 8.0						22
0.25	12.5418	2.4625	0.0976	0.0223	0.0358	0.0066
0.50	9.1688	3.2196	0.2786	0.0310	0.0723	0.0254
0.75	7.5755	3.5169	0.4283	0.0341	0.0963	0.0455
1.00	6.6257	3.6610	0.5452	0.0364	0.1123	0.0637
1.25	5.9877	3.7392	0.6377	0.0385	0.1237	0.0793
1.50	5.5131	3.7800	0.7140	0.0403	0.1340	0.0915
S = 20; g = 1.0; t = 10.0						23
0.25	14.2410	2.7640	0.0580	0.0610	0.0410	0.0010
0.50	10.7152	3.7084	0.1684	0.0990	0.0988	0.0060
0.75	9.0363	4.1150	0.2726	0.1159	0.1438	0.0131
1.00	8.0316	4.3307	0.3592	0.1249	0.1770	0.0210
1.25	7.3550	4.4594	0.4306	0.1304	0.2019	0.0289
1.50	6.8649	4.5424	0.4901	0.1342	0.2211	0.0365
S = 5; g = 1.0; t = 3.0						24
0.25	6.0115	0.2202	0.0088	0.0021	0.0004	0.0006
0.50	5.0287	0.4538	0.0109	0.0091	0.0016	0.0013
0.75	4.4183	0.6245	0.0118	0.0170	0.0038	0.0020
1.00	4.4183	0.6245	0.0118	0.0241	0.0068	0.0025
1.25	3.6804	0.8451	0.0159	0.0303	0.0103	0.0028
1.50	3.4361	0.9191	0.0190	0.0353	0.0140	0.0031
S = 10; g = 1.0; t = 6.0						25
0.25	10.0575	0.9075	0.0218	0.0182	0.0031	0.0027
0.50	7.9895	1.5000	0.0269	0.0483	0.0136	0.0050
0.75	6.8724	1.8384	0.0380	0.0707	0.0279	0.0061
1.00	6.1569	2.0534	0.0521	0.0861	0.0428	0.0065
1.25	5.6534	2.2008	0.0669	0.0969	0.0572	0.0067
1.50	5.2773	2.3077	0.0815	0.1047	0.0704	0.0067

S = 15; g = 1.0; t = 9.0						26
α	a_o	b_1	b_2	b_3	b_4	b_5
0.25	13.2551	1.8734	0.0354	0.0510	0.0114	0.0060
0.50	10.3086	2.7575	0.0570	0.1060	0.0419	0.0091
0.75	8.8281	3.2001	0.0893	0.1379	0.0752	0.0099
1.00	7.9159	3.4616	0.1223	0.1571	0.1055	0.0100
1.25	7.2900	3.6325	0.1528	0.1693	0.1319	0.0099
1.50	6.8304	3.7519	0.1803	0.1774	0.1547	0.0098
S = 20; g = 1.0; t = 12.0						27
0.25	15.9790	3.0000	0.0540	0.0960	0.0270	0.0100
0.50	12.3130	4.1060	0.1040	0.1730	0.0860	0.0130
0.75	10.5546	4.6154	0.1630	0.2094	0.1408	0.0134
1.00	9.4961	4.9024	0.2165	0.2298	0.1865	0.0132
1.25	8.7806	5.0840	0.2627	0.2420	0.2240	0.0131
1.50	8.2608	5.2080	0.3027	0.2498	0.2548	0.0132
S = 30; g = 1.0; t = 15.0						28
0.25	18.1310	5.0230	0.1670	0.1260	0.1060	0.0050
0.50	13.5540	6.1720	0.4090	0.1740	0.2160	0.0190
0.75	11.4950	6.6040	0.5950	0.1920	0.2860	0.0380
1.00	10.2970	6.8140	0.7350	0.2010	0.3320	0.0540
1.25	9.5040	6.9300	0.8440	0.2070	0.3640	0.0700
1.50	8.9370	7.0010	0.9310	0.2110	0.3880	0.0830
S = 40; g = 1.0; t = 20.0						29
0.25	21.4300	7.4160	0.3370	0.1980	0.1980	0.0120
0.50	16.0620	8.6610	0.7190	0.2500	0.3540	0.0420
0.75	13.7290	9.0840	0.9800	0.2680	0.4430	0.0730
1.00	12.3940	9.2770	1.1670	0.2780	0.4970	0.1000
1.25	11.5200	9.3770	1.3070	0.284	0.5340	0.1220
1.50	10.8980	9.4330	1.4180	0.2880	0.5600	0.1420